論文 / 著書情報
Article / Book Information

題目(和文)	
Title(English)	Investigation of Utilising Coriolis Effect for Attenuating Long-Period Vibration of Tall Flexible and Rolling Structures
著者(和文)	WALKERMarioPatrick
Author(English)	Mario Walker
出典(和文)	学位:博士(学術), 学位授与機関:東京工業大学, 報告番号:甲第10888号, 授与年月日:2018年3月26日, 学位の種別:課程博士, 審査員:大熊 政明,坂本 啓,鈴森 康一,髙原 弘樹,山浦 弘
Citation(English)	Degree:Doctor (Academic), Conferring organization: Tokyo Institute of Technology, Report number:甲第10888号, Conferred date:2018/3/26, Degree Type:Course doctor, Examiner:,,,,
学位種別(和文)	博士論文
Type(English)	Doctoral Thesis

TOKYO INSTITUTE OF TECHNOLOGY

DOCTORAL THESIS

Investigation of Utilising Coriolis Effect for Attenuating Long-period Vibration of Tall Flexible and Rolling Structures

Author:
Mario P. WALKER

Supervisor:
Prof. Masaaki OKUMA

A thesis submitted in fulfillment of the requirements for the degree of Doctor of Engineering

in the

Department of Mechanical and Aerospace Engineering
Graduate School of Science and Engineering

January 10, 2018

Declaration of Authorship

I, Mario P. WALKER, declare that this thesis titled, "Investigation of Utilising Coriolis Effect for Attenuating Long-period Vibration of Tall Flexible and Rolling Structures" and the work presented in it are my own. I confirm that:

- This work was done wholly or mainly while in candidature for a research degree at this University.
- Where any part of this thesis has previously been submitted for a degree or any other qualification at this University or any other institution, this has been clearly stated.
- Where I have consulted the published work of others, this is always clearly attributed.
- Where I have quoted from the work of others, the source is always given. With the exception of such quotations, this thesis is entirely my own work.
- I have acknowledged all main sources of help.
- Where the thesis is based on work done by myself jointly with others, I have made clear exactly what was done by others and what I have contributed myself.

Signed:

Date:

"All intelligent people know that ones nationality has nothing to do with great ideals and great principles."

Marcus Garvey

TOKYO INSTITUTE OF TECHNOLOGY

Abstract

Department of Mechanical and Aerospace Engineering
Graduate School of Science and Engineering

Doctor of Engineering

Investigation of Utilising Coriolis Effect for Attenuating Long-period Vibration of Tall Flexible and Rolling Structures

by Mario P. WALKER

This thesis proposes a new method to attenuate the dynamic response of long-period structures using Coriolis effect. The effect of vibration control of the Coriolis inducing dampers is investigated numerically and analytically. Two methods are proposed, one consisting of a moving mass with cyclic motion which is applied to tall building structures and he other consisting of unidirectional water-flow which is applied to ship rolling. Furthermore, the first method requires carefully synchronised control as well as larger angular motion for effective damping. An enhanced Coriolis effect damping system is proposed using Fuzzy logic controllers. The newly proposed method incorporates a traditional mass damper coupled with the Coriolis effect inducing system which allows for better performance. The results presented open the door for alternative approaches to vibration control of flexible and rolling structures with low inherent damping.

Acknowledgements

I would like to first of all thank my supervisor, Professor Masaaki Okuma, for his support and guidance throughout the whole process of the study. I would also like to say thank you to Professor Hiraku Sakamoto for his invaluable input in seminars and whenever we talk. A special thanks to the Japanese Government (MEXT) for their financial support in my studies. To the members of Okuma Sakamoto Laboratory, I would like to express my gratitude for your feedback and input, and for making my time in the lab a memorable experience. My sincerest thanks to Atsuko Ishii for always ensuring that all the proper administrative procedures are taken concerning my studies. Finally, I would like to express my gratitude to friends and family both here and overseas for their words of encouragement, motivation and for pushing me to continue.

Contents

List of Figures

List of Tables

List of Abbreviations

DOF	**D**egree **O**f **F**reedom
FEM	**F**inite **E**lement **M**ethod
FLC	**F**uzzy **L**ogic **C**ontroller
TMD	**T**uned **M**ass **D**amper

Physical Constants

gravity $\quad g = 9.81\,\mathrm{m\,s^{-2}}$

Nomenclature

$[C]$	Damping matrix of structure
$[c]$	Damping matrix of moving finite element
$[K]$	Stiffness matrix of structure
$[k]$	Stiffness matrix of moving finite element
$[M]$	Mass matrix of structure
$[m]$	Mass matrix of moving finite element
β	Dimensionless stroke length
Δ	Displacement (ship weight)
$[\hat{C}]$	Overall damping matrix of system
$[F(\hat{t})]$	Overall external force vector at any time t
$[\hat{K}]$	Overall stiffness matrix of system
$[\hat{M}]$	Overall mass matrix of system
μ	Mass ratio
ω_e	wave encounter frequency
ω_r	Natural frequency of structure ($r =$ mode of vibration)
ϕ	Roll angle
ψ	Phase angle
ρ	Material density of the structure
ρ_f	Density of fluid
τ	Natural time period of structure
ζ_r	Damping ratio of structure ($r =$ mode of vibration)
A	Cross-section of structure
A_f	Cross-section of pipe
a_i	Rayleigh damping constants ($i = 0, 1$)

A_{44} Added mass

b Average displacement of moving mass

B_{44} Damping in the rolling direction

C_{44} Restoring moment

E Modulus of elasticity of the structure

$f_B(y,t)$ Force per unit length applied to the structure

$f_s(t)$ Force applied to moving mass

f_{si} Equivalent nodal forces of the s_e^{th} element ($i = 1-6$)

H Height of the structure

h Height of elements

I Moment of inertia of the structure

I_{44} Ship inertia

M Mass of structure

m Moving mass

n Number of elements

N_i Shape functions of beam element ($i = 1-6$)

q_i global horizontal displacement ($i = 0-3, \quad g$)

$r(t)$ Distance from pivot to the centre of gravity of water-flow

$s(t)$ Curvilinear coordinate of moving mass along the structure

s_0 Height from ground to moving mass at time $t = 0$

s_e^{th} Element on which moving mass is located at time t

T Total kinetic energy of the system

t Time

T_B Kinetic energy of the structure

T_m Kinetic energy of the moving mass

$u(y,t)$ Horizontal deflection of the structure

V Potential energy of the system

w_i relative horizontal displacement from neutral axis of primary structure ($i = 0-3$)

x	Transverse coordinate
y	Longitudinal coordinate
$y_m(t)$	Position of moving mass on the s_e^{th} element
$(\dot{})$	Derivative with respect to time t
$()'$	Derivative with respect to y-coordinate

Dedicated to my parents.

Chapter 1

Introduction

1.1 Background and Motivation

As the name indicates, long-period structures are susceptible to long-period vibrations when subjected to excitations. These vibrations are hazardous to the structures, unpleasant for occupants and may even pose serious serviceability issues (Kareem, Kijewski, and Tamura, 1991). This has been, and remain a great concern for researchers.

There are several types of long-period structures existing in society. Popular among these are flexible structures, as in the case for structural systems, and rolling structures, as in the case for ocean-going vessels. For the case of tall structures, the direction of evolution is towards lightness (Ali and Moon, 2007) and are often featured with increased flexibility and lack of sufficient inherent damping making them vulnerable to excitation (Kareem, Kijewski, and Tamura, 1991). Additionally, urbanisation and population increase create the need to maximise space, forcing mankind to continue building upwards. As a result structures are being built taller and more flexible, and this trend is not likely to be reversed in the future. Following this trend we will most likely see a significant amount of tall or super tall structures, in particular in metropolitan areas in the future.

Similarly, rolling structures in the form of ocean going vessels are faced with low inherent damping conditions and as such are subjected to motions which can disrupt on-board operations and equipment, damage machinery and can also reduce the efficiency of the propulsion system. Roll motion is of particular interest for researchers, as it is a major contributing factor to capsizing. The low damping conditions during rolling makes it important to address for ship safety and operation and this motion can become severe even in relatively moderate weather conditions without any apparent pre-warning for the crew onboard (Söder et al., 2013). In (Perez, 2010) it was highlighted that transverse accelerations from roll motion interrupts the on-board crew performance and in severe cases will completely prevent performance. Roll motion can cause sea sickness, cargo damage and limit the capability to handle equipment on-board which can be detrimental to naval vessels performing weapon operations, launching or recovering systems, landing airborne systems and sonar operations (Monk, 1988; Perez and Blanke, 2012).

There are several measures in existence to reduce the dynamic response of long-period structures (tall flexible and rolling), which common practice

involves generating counteractive force through some motion and generally in the direction of the vibration. For example in the case of tall flexible structures, a common auxiliary damping measure implemented is mass damper. Likewise for ship structures, researchers have developed several methods over the years to minimise motions. These systems are generally classified into two categories: internal and external systems, and can be of a passive or active nature (Townsend, Murphy, and Shenoi, 2007). Furthermore these systems operate in one of two ways, either the system manipulates the centre of gravity of the ship in order to provide some restoring moment or the system generates the restoring force itself and apply directly to the unstable vessel. Common internal systems include anti-roll tanks and gyroscopic systems whereas common external systems include bilge keels, fin stabilisers and rudder control. These systems will be discussed in more details in the next chapter (See Chapter 2).

However, these type of measures face several challenges. One of which is needing space in the lateral direction for effective motion, and often times this space is very limited. For the case of tall structures, conventional systems make use of the lateral space and (based on the current trend) as structures become taller and thinner, conventional systems will not have adequate space for effective motion. For the case of ship structures, not only is space an issue (particularly in the case of internal systems) but there are other challenges that present themselves. For example water flow in anti-roll tanks creates complications. Additionally for most internal systems there are issues of weight and volume (Townsend, Murphy, and Shenoi, 2007). For external systems like bilge keels and fin stabilisers, an extremely large size is required to produce significant damping creating operational challenges. They are also ineffective at zero forward speed (Lewis, 1989; Lloyd, 1998).

An alternative approach could be to use the longitudinal or radial space which offers more usable space. When tall flexible structures vibrate they undergo a certain amount of rotational motion as is the case for rolling structures. As such, any motion in the longitudinal or radial direction will induce Coriolis effect which may be used to attenuate the dynamic response of these structures. And this is the principle behind the proposed research. The basic idea is to develop an innovative alternative approach to damping tall flexible and rolling structures by using motion in the longitudinal/radial direction which the coupling effect of the translation and the rotation will create internal forces within the system. If carefully manoeuvred this concept could produce effective restoring force on the primary structure. Conceptually, this provides solution to space requirements in the lateral direction. Additionally for rolling structures, this offers an alternative approach that is independent of the forward speed of the vessel and if properly conceptualise should provide no weight or volume issues.

1.2 Objectives

The primary objective of this research is to investigate the effectiveness of the Coriolis effect induced by longitudinal/radial motion through flexible and

rolling structures. The performance of the proposed concept will be quantitatively assessed by studying the degree of reduction of response compared to cases without the proposed concept. Additionally comparisons will be made to traditional damping measures. The investigations will be studied under different cases of excitations which include seismic excitation (for tall flexible structures), beam wave excitations (for rolling structures) and free response. This research focuses on dynamic response dominated by the first natural frequencies of tall building structures and ships. The objectives of this research can be summarised as follow:

1. Theoretical investigations of tall flexible structures under free response has been carried out on a benchmark model. The correlations between the Coriolis effect, the inertial properties and characteristics of motion have been investigated. Following this, ways to realise this effect are proposed and explored.

2. From proposals in the previous investigation, investigation of the performance in the case of rolling structures using benchmark model has been done. These studies have been carried out for a ship benchmark model and the efficacy of the system is studied.

3. From another proposal in the first investigation, development of a hybrid enhanced effect damper has been done for the case of super tall structures. The extent to which the effect can be enhanced has been studied.

4. Development of a fuzzy logic controller (FLC) for the hybrid enhanced effect system and developing optimal parameters to be used for fuzzy logic control are secondary goals of this research.

1.3 Scope of the Research

The objective of the present study is to develop an active control strategy to attenuate long-period structures. The study focuses on tall building structures and ships. These structures are assumed to be dominated by the first mode of vibration and as such investigations focuses on reducing the dynamic response in the first mode. Effects of the longitudinal or radial components of the excitations (seismic for tall structures and beam waves for ships) are ignored. The present study focuses on studying the effects of the proposed concept and does not focus on developing a working model of the actual damping device. The research problem is approached from the viewpoint of mechanics and control. For the case of tall flexible structures, these were investigated as continuous systems. For the case of rolling ships, the hydrodynamic nonlinearities were not considered.

Even though the research focuses on specific structures mentioned above, the concept can be extended to any long period structure that have similar behavioural characteristics. Especially for cases where there is low structural damping and where lateral space is insufficient for adequate damping motion.

1.4 Preface

This dissertation is organised into seven main chapters. The contents of this dissertation are summarised as follow:

- Chapter 2 presents a review of the literature that contributed to the present work. Review of the state-of-the-art currently in the field of structural control and stabilising systems in marine engineering will be presented. Key concepts and prevailing concepts in the field of study will be highlighted. Theoretical analysis approaches in particular the approach of Finite Element Method will be discussed. Gaps in findings and where further research is needed will be given. Finally, how this present study fits into the status quo and how it attempts to address the issue will be described.

- Chapter 3 presents the approach taken to address the research problem. The research question, hypothesis and their rationales will be presented and the design of the research will be discussed in detail. The procedure taken to get the results of the investigations are listed and how the results are analysed in order to achieve the goals of the research is described.

- The attenuation of tall flexible structures using moving mass in the longitudinal direction is investigated in Chapter 4. The analysis is done using the approach of moving finite element method (MFEM). Details of the formulation of the MFEM model specifically for the case of a flexible beam structure is given in order to analyse the dynamic response. The performance of the proposed concept using the Shinjuku Mitsui Building as the benchmark model is analysed. Vital parameters are identified and based on the results proposal for further investigations are made.

- Inspired by proposal made in the previous chapter, Chapter 5 proposes and investigates a method to reduce the rolling of ships by inducing Coriolis effect using water-flow in the radial direction of the vessel. Performance and robustness of such a system is studied using a Ro-Ro vessel as the benchmark model. The primary structure is modelled as a single degree of freedom (SDOF) system with water-flow having another degree of freedom (DOF). Numerical investigations and analytical investigations based on linearising the system are conducted. A comparison of performance of the proposed concept with the analytical results and without the stabilising system is done.

- Also inspired by proposal made in Chapter 4, a multi-degree-of-freedom hybrid enhanced effect damper is proposed and investigated in Chapter 6. A benchmark super tall structure based on a proposed structure for Melbourne is investigated. The system is studied under seismic excitations based on recordings from the Loma Prieta earthquake in California in 1989. Additionally, the system is studied under free response. Control algorithm based on the theory of fuzzy logic is designed for the hybrid enhanced effect damping system. Stability of the

fuzzy logic controllers are verified using Lyapunov's direct method and phase plane method. The performance of the proposed system is investigated. Finally, comparison of the results from the investigation is done for system without control, with an optimal tuned mass damper (TMD) optimised based on Hartog's method, a Fuzzy logic controlled active tuned mass damper and the proposed hybrid enhanced effect damper.

- Chapter 7 highlights conclusions drawn from the research. Furthermore, recommendations and further extension of the research are given.

Chapter 2

Literature Review

2.1 Overview

The concerns of engineers are safety and comfort when designing structures. Human structures are exposed to elements which makes them susceptible to excitations. Long-period structures are those most vulnerable to long-period excitations such as seismic ground motion, wind excitation, etc. Population and societal demands lead to a rapid increase in the number of long-period structures. There are many types of long-period human structures which could be in the form of tall/long flexible structures (such as tall buildings, bridges, towers, etc.) or rolling structures (such as ships, ocean-going vessels, etc.). Not only are these structures vulnerable to excitations, but a common feature associated with these are low inherent damping. For example in the case of tall building structures they usually have damping in the range of 0.5% - 1%, especially for those greater than 250 m (Smith and Willford, 2007). For the case of ships and other ocean-going vessels, the hydrodynamic damping is very nonlinear but what is certain is the roll motion is the least damped and has largest amplitude of all the unwanted motions for these vessels (Moaleji and Greig, 2007).

Reducing the response of these structures is of utmost importance and years of research have gone into developing strategies to control unwanted vibrations in these structures. Structural control have been in development for more than 40 years (Korkmaz, 2011). Since then there have been several measures developed to achieve this either through structural design or some auxiliary damping measure added to the structure. For the case of ocean-going vessels, measures to reduce roll have been suggested as early as 1906 (Moaleji and Greig, 2007). These can either be internal or external mechanisms added to the structure.

These will be discussed within this chapter. Discussion about the state-of-the-art currently in existence, their gap in findings and where further research is needed is done. In addition, an overview of the working principle behind the proposed concept will be given as well as modelling techniques used within this research.

2.2 Tall Structures

2.2.1 Classification of Tall Structures

For tall structures, there are several ways in which they can be classified. However, in terms of height, there is no universal classification by which they are separated into groups. For the purpose of this research tall structures are clearly classified into categories based on their height using the criteria developed by the Council on Tall Buildings and Urban Habitat (CTBUH) shown in Figure 2.1.

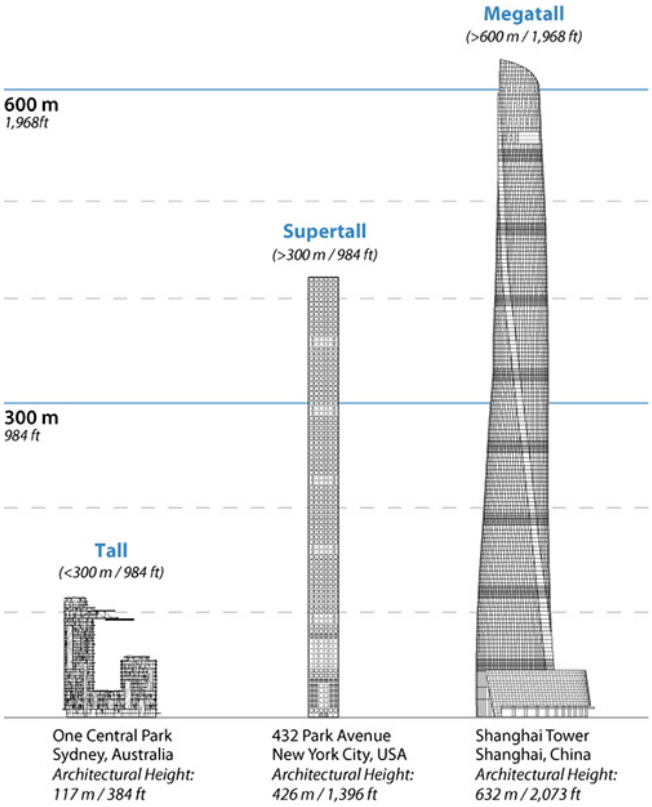

FIGURE 2.1: Height criteria of buildings according to the CTBUH

Following the figure above, any mentioning of tall structures refer to any structure over the height of 100 m, supertall structures are any structure over the height of 300 m and megatall any over the height of 600 m.

2.2.2 Structural Control

Structural control is done either through design or auxiliary measures and is generally classified into two categories, active and passive control (Nishitani and Inoue, 2001). Passive systems are those that require no energy source in order to function which means they have fixed properties and are only effective over a narrow range of loading conditions (Ali and Moon, 2007). Active systems on the other hand require external energy source making the

system more adaptable to varying conditions, making them more effective than passive systems. According to (Nishitani and Inoue, 2001), these can operate on the following principles :

- Reducing motion by transferring energy from the primary structure to an auxiliary oscillator system.
- Reduction of the excitation being transferred to the primary structure from the source.
- Energy-dissipating-material-based damping.
- Alter the characteristics of the primary structure to prevent resonance.
- Generate computer-controllable forces to counteract motion of the primary structure.

Passive Control

Passive systems generally operate under the first three principles mentioned above. As they do not require external energy source, they instead utilise the motion of the primary structure to generate control forces to mitigate the structure (Mahajan and Raijiwala, 2011). The various categories of passive control system are listed as follow taken from (Ali and Moon, 2007):

- Tuned Mass Dampers (TMDs) - Operate on the first principle by using an auxiliary oscillatory mass to generate counteractive inertial forces.
- Tuned Liquid Dampers (TLDs) - Similar to TMD, operate on the first principle, but instead of an oscillatory mass uses the motion of water (or some liquid) as the counteractive inertial force.
- Viscous Dampers (VDs) - Primarily function on the third principle, create damping force through deformation. When deformation occurs due to the vibration of the primary structure, motion within the damping device causes viscous fluid to flow within creating damping forces which dissipates the vibration input to the device therefore mitigating the vibration of the primary structure.
- Viscoelastic Dampers (VEDs) - Also operate on the third principle and also create damping force through deformation. As the name suggests, these devices contain viscoelastic materials that deform due to the vibration of the primary structure, when this occurs the vibration energy input is converted to some other source such as heat energy thus reducing the kinetic energy of the primary structure.
- Friction Dampers (FDs) - another damper that operate on the third principle, they operate in a similar manner to VEDs by translating the kinetic energy of the primary structure into heat through friction and as such dissipate the energy of the structure.

- Electro-Magnetic Dampers (EMDs) - EMDs function by using magnetic repulsion to dissipate vibration energy input.
- Base Isolation - These types of system primarily function on the second principle and as the name suggests is a method by which the primary structure is isolated from the base as such reducing the kinetic energy being transferred from ground motion to the structure.

Active Control

Active control devices are more versatile than passive systems and can operate on all the principles mentioned in Section 2.2.2. These require external energy source and have some feedback system that is used to determine the action needed by the system in order to provide the desired response of the primary structure. The general setup of an active control system is illustrated in Figure 2.2.

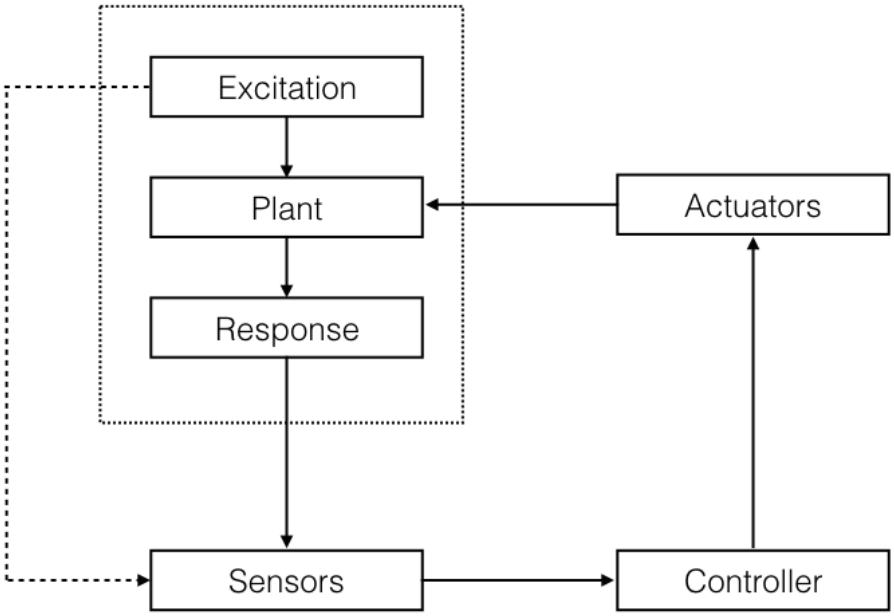

FIGURE 2.2: The general setup of an active control system

The typical active control system consists of sensors, controllers and actuators. The sensors are used to measure either the response of the structure (this is called feedback control), or measure the excitations (called feedforward control), or measure both (called feedback-feedforward (Suhardjo, Spencer, and Sain, 1990)). The controllers process the information from the sensors to determine the necessary action to be taken for a desired response of the plant (the primary structure) which the controller outputs to actuators which then carry out this action. Following (Ali and Moon, 2007) active control can be in the form of:

- Active Mass Dampers (AMDs) - These are similar to TMDs except as the name suggests the sliding mass is fitted with controller and actuators that move the mass when excitation is picked up by the sensors.
- Active Various Stiffness Devices (AVSDs) - AVSDs operate primarily on the fourth principle mentioned in Section 2.2.2 by altering the stiffness of the building thereby altering the frequency of the structure to prevent resonance when experiencing excitation.

Semi-Active and Hybrid Control

While structural control is generally categorised into two main categories, there are special categories which could consist of a combination of the two main categories. These are semi-active controllers and hybrid controllers. Semi-active controllers are damping systems which do not require external energy throughout it's whole operation, only on special occasions (Nishitani and Inoue, 2001). Whereas hybrid control systems are those that are a combination of passive and active control system. A general setup of semi-active control and hybrid control are shown in Figures 2.3 and 2.4.

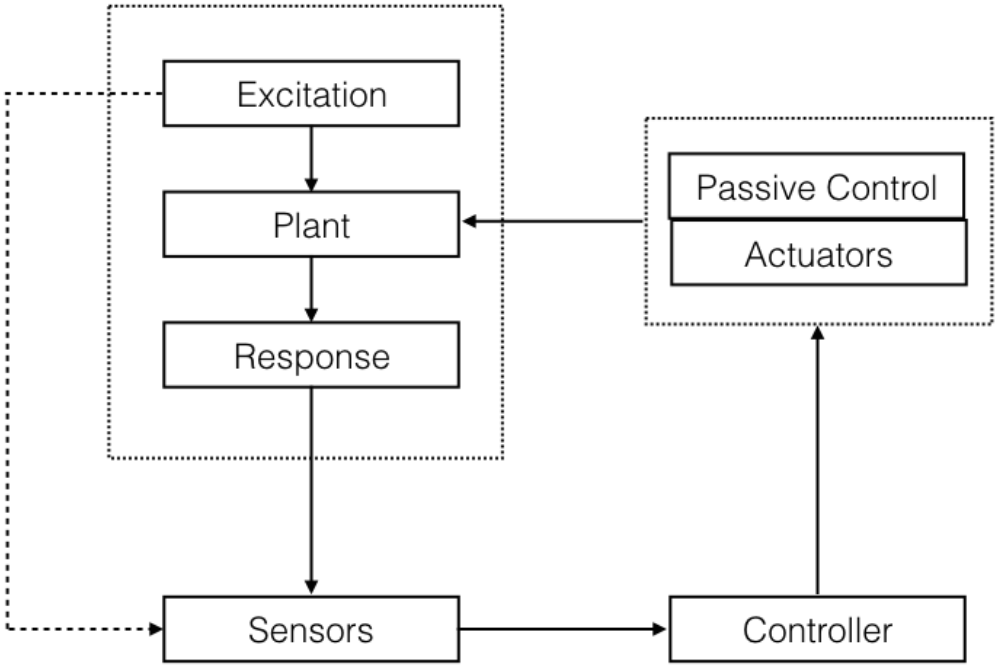

FIGURE 2.3: The general setup of an semi-active control system

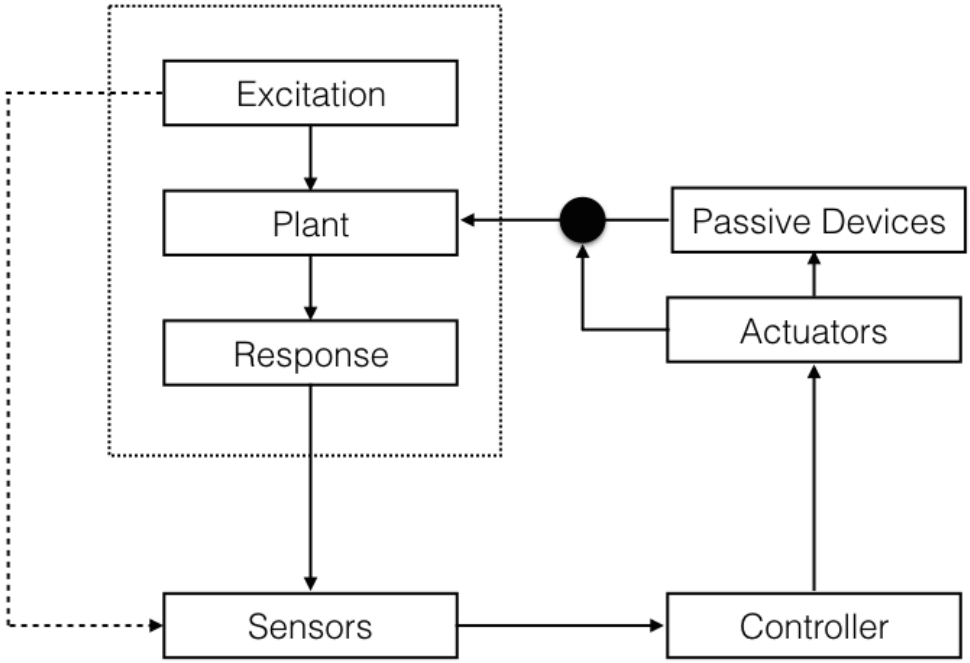

FIGURE 2.4: The general setup of an hybrid control system

2.3 Control Methods

In Chapter 6 a simple control strategy is proposed for the case of active control of tall flexible structures. As such several control methods will be discussed namely Proportional-Integral-Derivative (PID), Linear Quadratic Regulator (LQR) and Fuzzy Logic Controller (FLC). Their pros and cons will be highlighted.

2.3.1 PID Controller

The PID controller is the most commonly used form of feedback control. The theory behind the PID controller is illustrated in the equation (Bobál et al., 2009):

$$u(t) = K\left[e(t) + \frac{1}{T_I}\int_0^t e(\tau)d\tau + T_D\frac{de(t)}{dt}\right] \tag{2.1}$$

where K is the proportional gain, e is the control error, T_I is the integral time and T_D is the derivative time. Therefore the control signal of this "three-term" controller is the sum of the error of the three terms (Ang, Chong, and Li, 2005):

- P - proportional to the error.
- I - proportional to the integral of the error.
- D - proportional to the derivative of the error.

The advantages of PID controllers were presented in (Kozak, 2016) and are summarised as follow:

- For most cases not much knowledge about the control process is required and parameter tuning does not require mathematical model.
- Numerous research has led to numerous well-established tuning rules optimisation of the controller parameters.
- Simple, efficient and provides good performance and stability.
- Versatile and robust.

However, as stated in (Kozak, 2016) PID controllers have the following disadvantages:

- The controller will never provide perfect control as the controller can only act after the excitation is detected.
- There is no exact science to tuning and as such the PID control structure tuning may cause instability.
- PID controller is not suitable for all applications.

2.3.2 LQR control

LQR is a control technique which involves the formulation of an optimal control problem on a semi-infinite time interval (Bullo and Lewis, 2004). The system assumes a linear control system illustrated by:

$$\dot{x} = Ax + Bu \tag{2.2}$$

where x is the steady-state mean-square weighted state variable and u is the steady-state mean-square weighted actuator signal. The cost function is:

$$J_{1qr} = \lim_{t \to \infty} E\left(x(t)^T Q x(t) + u(t)^T R u(t)\right) \tag{2.3}$$

where Q and R are positive semi-definite weight matrices. The goal is to calculate feedback gain K such that

$$u = -Kx \tag{2.4}$$

which mnimises the cost function and stabilises the system.

The advantages of LQR are:

- the optimal controller automatically ensures a stable closed-loop system.
- It is fairly simple to implement multiple output system.
- It is robust to a certain degree.

- Tuning procedure is rather simple

The disadvantages are:

- Requires full knowledge of the state to implement the control law (Bullo and Lewis, 2004).
- Control law designed based on linear system may not be as reliable when implemented for nonlinear system.

2.3.3 FLC

First published in (Zadeh, 1965), fuzzy logic controllers are robust systems which allows for handling imprecision and nonlinearity in complex control situations. The setup of such a controller is shown in Figure 2.5.

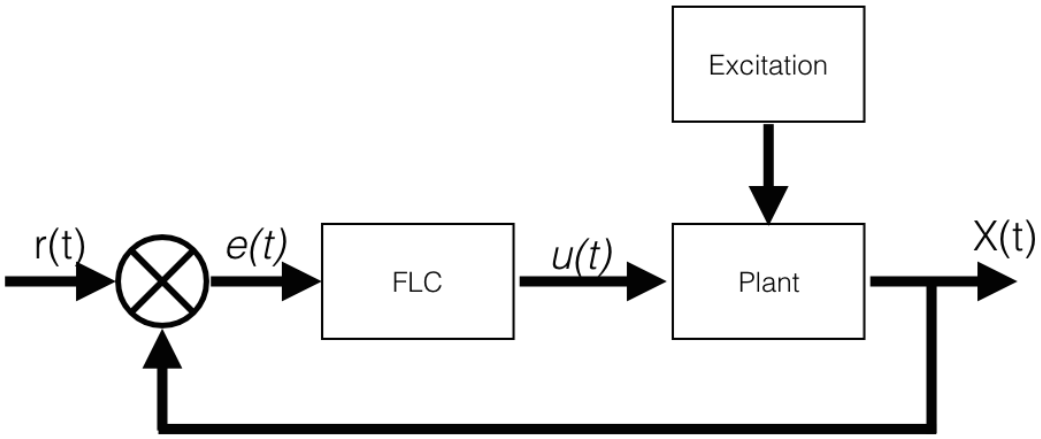

FIGURE 2.5: Schematic of the fuzzy logic controller

In the diagram above $r(t)$ is the reference input, $e(t)$ the error, $u(t)$ the control output and $X(t)$ is the response of the structure. As shown in Figure 2.6 the fuzzy logic controller consists of 4 main components defined as follow

1. Fuzzification - The process by which the measured inputs in the control process is converted into fuzzy membership functions using fuzzy reasoning mechanism.
2. Fuzzy Rules - These are control rules based on expert knowledge of the system to achieve the desired control.
3. Inference Mechanism - Based on the fuzzy rules and for a given fuzzy input the output of the fuzzy logic controller is decided.
4. Defuzzification - The process by which the decided output of the fuzzy logic controller is converted into the required crisp control value.

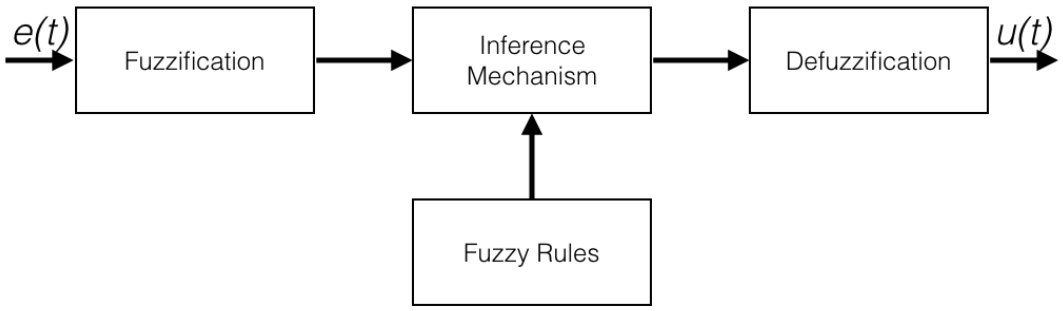

FIGURE 2.6: Components of fuzzy logic controller

The advantages of FLC are:

- Simple and robust.
- Uses human inference and as such allows the implementation of "rule of thumb" experience, intuition and heuristics (Kickert and Mamdani, 1978).
- A mathematical model of the process is not required.
- Able to simply handle nonlinear control.

However, the disadvantage is:

- Because there are no mathematical model of the controller, analysis of the controller's performance becomes challenging.

2.4 Dynamic Response of tall structures Under Moving Loads

As mentioned in Chapter 1, the primary objective of this research is to investigate the effectiveness of the Coriolis effect induced by longitudinal motion through a tall flexible structures. Tall flexible structures generally have an infinite number of degrees of freedom, however they could be simply modelled as vertical cantilever beams with the base fixed in the ground (Ali and Moon, 2007). The dynamic response due to the moving load could be investigated using the beam structure as the primary structure. There are many works presented on the analysis of dynamic response of structures under the influence of moving mass. Works like (Frỳba, 1972; Oguamanam, Hansen, and Heppler, 1998; Olsson, 1991) found approximate analytical solutions to the problem by considering the moving load as a moving force. However in these, the inertial mass and/or the Coriolis and centripetal effect from the interaction of the mass and the beam are neglected. Since the Coriolis component is vital to this research an analytical approach as previously mentioned would not be suitable. Further works have shown a more complete analysis

by considering the moving load as a moving mass and shows the importance in particular for large masses, high velocities and substantial deflection (Cifuentes, 1989; Akin and Mofid, 1989; Michaltsos, Sophianopoulos, and Kounadis, 1996).

The numerical approach of Finite Element Method (FEM) has garnered much attention due to its flexibility and ease by which the mass effects may be taken into account. In (Wu and Lin, 2000; Ye and Chen, 2009), the authors investigated the dynamic response using moving finite element method. The aforementioned investigations, however, focus on the effect of the moving load on an initially stationary structure. Additionally, the mass traverses once, usually with constant velocity, over the structure. To the best of the author's knowledge few investigations have gone into using the effects of an accelerated moving mass to attenuate the vibration of tall flexible structure by means of cyclic motion.

2.5 Coriolis Effect

Gaspard-Gustave Coriolis was a 19th century French mathematician whose most notable work came in the field of mechanics and engineering mathematics. In his most notable work (Coriolis, 1835) he investigated the rotation of a waterwheel where he showed that a particle in a rotating frame of reference experiences an extra force now called the Coriolis acceleration. Basically when there is a mass located in a rotating system, if that mass is located at some distance away from the pivot of rotation the mass will experience a force called the centrifugal force. However, Coriolis found that if that mass has motion relative to the rotating system then it appears to be affected by some additional force which we now call the Coriolis force.

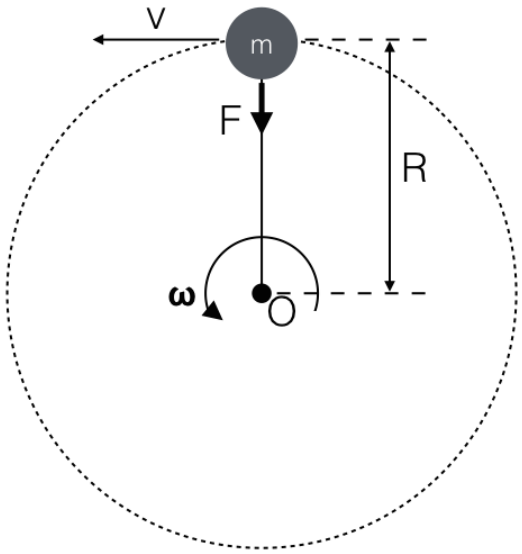

FIGURE 2.7: Forces acting on a stationary mass in a rotating system

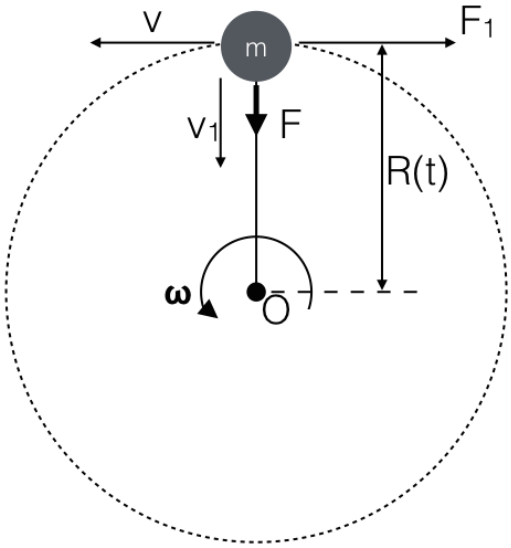

FIGURE 2.8: Forces acting on a translating mass in a rotating system

This is shown in Figures 2.7 and 2.8 where we see a stationary mass m in a rotating system with angular velocity ω and at some distance R from the pivot of rotation O will experience some force (centripetal) F where in this case F is

$$F = m \cdot \omega \times \omega \times R \tag{2.5}$$

Should m no longer be stationary but starts to have some motion relative to the rotation of the system v_1, then the mass will experience an additional (Coriolis) force F_1 where in this case F_1 is

$$F_1 = 2m \cdot \omega \times v_1 \tag{2.6}$$

2.6 Ship Stabilising Systems

Since the 17th century researchers have been investigating roll-damping devices. In 1861, William Froude studied the effect of a water-filled tank on the roll motion of a ship which led to the proposal of anti-roll tank systems. Since then researchers have proposed and implemented several devices and system to reduce the roll response of vessels. This section presents common approaches to date to reduce roll response and highlights the advantages and disadvantages of such systems. As mentioned in Section 2.1, these can be divided into two categories: internal and external system.

2.6.1 Internal Systems

Internal stabilisation systems are usually weight-based systems and work on the principle of generating moments to counteract the undesired (roll)

motion by carefully manipulating weight within the vessel. Common approaches are anti-roll tanks and gyroscopic stabilisers.

Anti-roll Tanks

The most common type of anti-roll tank in use is the U-tube tank which consists of two reservoirs connected by a water duct. Anti-roll tanks reduce the roll response of ships by means of motion of fluid within the tank which has the same period of the ship motion but a quarter of period behind the rolling motion, as a result the fluid motion produces a counteractive moment (Perez, 2010). These systems can either be passive or active through valves and pumps. The principal advantages of this system are there are no hydrodynamic drag effect and they are effective at zero forward speed (Townsend, Murphy, and Shenoi, 2007). However the disadvantages are they occupy large spaces and produce weight issues, as well as stability issues due to sloshing (Perez, 2010; Townsend, Murphy, and Shenoi, 2007).

Gyroscopic Stabilisers

Gyroscopic stabilisers consist of a large rotating flywheel which generates moments by means of its inertial property to eliminate rolling of the vessel. This method is used to a lesser extent in comparison to other methods. The principal advantages of this system type are like anti-roll tanks they provide no hydrodynamic drag effect and operate at zero forward speed (Townsend, Murphy, and Shenoi, 2007). However the drawbacks are they increase the weight of the vessels, produce large stress on the hull and has limited stabilisation capability (Perez, 2010).

2.6.2 External Systems

External stabilisation systems generally work on the principle of hydrodynamic interactions to generate forces and moments outside the hull of the ship to reduce the undesired ship roll motion (Townsend, Murphy, and Shenoi, 2007). Common approaches are bilge keels, fins and rudder control.

Bilge Keels

Bile keels are simply just long narrow ridges mounted to the bilge which generate drag forces that act perpendicular to them to counteract ship roll motion. These devices are passive in nature. The principal advantages are they can still have some effect at low speeds (generally in the range of 10-20% roll reduction) (Sellars and Martin, 1992), they are lightweight and provide no space occupancy (Townsend, Murphy, and Shenoi, 2007). However, they create hydrodynamic drag, are exposed to elements in the water so vulnerable to damage, not appropriate for all ships and have dependence on forward speed, hence ineffective at zero forward speed (Perez, 2010).

Fin Stabilisers

Fin stabilisers consist of a pair of hydrofoils mounted on the side of the ship's hull which can be either passive or actively controlled, to generate hydrodynamic lift to counteract the ship's roll response. The principal operational advantages are they have high performance roll reduction and easy control system design. However the drawbacks are they create hydrodynamic drag and are ineffective at low and zero forward speeds. Additionally, for effective performance they require control system with sensors and powerful hydraulic actuators (Perez, 2010). They are also exposed to elements in the water, including other vessels passing by so vulnerable to damage, creates the possibility of underwater noise pollution which can affect sonar systems and in severe conditions may cause dynamic stall (Perez, 2010).

Rudder Control

The ship's rudder can be used to mitigate roll motions by creating short rudder impulses (Söder et al., 2013). This is an active control technique and is usually a feature of autopilot. The advantages of this type of system are they have medium-high performance, they do not occupy large spaces, require no physical modifications to vessels and can be combined with other stabilisers to increase performance. However, they are ineffective at low and zero forward speeds, create hydrodynamic drag and for high performance requires sophisticated control systems as well as rudder machinery upgrade (Perez, 2010).

2.7 The Proposed Research

As mentioned in Section 2.5, a mass with motion relative to a rotary system experiences the so called Coriolis effect. This could provide an alternative approach to vibration control in particular for cases where lateral space is insufficient for effective counteractive motion. For example tall flexible structures, when these structures vibrate they undergo a certain amount of rotational motion and any motion in the longitudinal direction will induce Coriolis effect which may be used to attenuate these structures. This was investigated in (Matsuhisa et al., 1995; Viet, Anh, and Matsuhisa, 2011) for pendulum systems. They investigated a system where a mass moves in the radius direction to prevent the swing of gondola. This concept is similar to a child's up-down motion to pump a swing (Tea and Falk, 1968; Curry, 1976). In this case the child alternates the up-down motion to amplify the swing and maximisation of this depends on the timing of the motion (Piccoli and Kulkarni, 2005). In (Viet, 2015) the author studied this concept used to control the sway of a crane.

In principle this could be applied to tall flexible structures and by extension to rolling structures. In terms of structural control, as mentioned earlier these structures are being built taller, thinner, lighter and more flexible and conventional systems make use of the lateral space. However, as these

structures become taller and thinner, conventional systems may not have adequate space for effective motion. Longitudinal motion provides an alternative approach. In terms of roll-stabilising systems, this approach also offers an alternative to the conventional systems currently in place which could address some of the challenges these systems currently face.

The system proposed for roll stabilising system is an active control system where water flows in the radial direction through some channel of the ship to generate restoring forces to mitigate ship's roll response. Since the vessel will be in water, sea openings can be placed on areas immersed in water (for example the base of the hull) which will allow water to be pumped into the stabilising system. The advantages of such type system are no complicated control is necessary as the water is simply pumped in one direction with a constant velocity, requires no external fixture so should create no hydrodynamic drag effect, operates at zero forward speed, provides no weight issues, no stability issues as the water flow will always generate positive stabilising effect and has no dependency on any external parameters other than the volume and velocity of water-flow, and the angular motion of the vessel.

Chapter 3

Methodology

3.1 Overview

The research problem is that long period tall, slender and flexible structures, and rolling structures are susceptible to unwanted vibrations, and in some cases do not have sufficient space in the lateral direction for conventional mass dampers to be effective. Following this, the present study investigates the attenuation of the dynamic response of tall flexible structures and rolling structures through the use of coupled longitudinal or radial motion inducing Coriolis Effect. The primary focus of the study is on tall building structures and ship rolling motion. In these, three types of damping mechanism were investigated. The first damping mechanism involves the use of a moving mass through a tall slender structure, the second damping mechanism involves the use of fluid-flow through the structure just to study the effect and then was later proposed as a mechanism for reducing the rolling of ship. The third damping mechanism involves the use of a mutli-degree-of-freedom mass damper to attenuate a super tall building structure (over 300m). The use of both the inertial effect of a conventional mass damper and the coupled effect of the so-called Coriolis damper can allow effective control of the dynamic response of the building. Additionally, the Coriolis damper is coupled with the conventional mass damper to allow for a greater degree of angular motion than that would be allowed by the vibration of the building structure alone. Therefore enhancing the Coriolis effect and consequently increasing the damping effect of the system. A proposal for the control of the hybrid mechanism is given using the theory of Fuzzy Logic.

The primary purpose of the study is to investigate the effect of response reduction and propose ways to improve effectiveness.

This chapter will highlight the steps and procedures undertaken throughout the process of the research. Overview of the reserach questions or hypthesis and their rrationales will be given. Details about the research design, research methods and their appropriateness will be illustrated. Mentioning of limitations and assumptions will be put forward.

3.2 Research Questions or Hypothesis and their Rationales

3.2.1 Research Questions and Hypothesis

When an object or structure experiences some degree of angular or rotational motion, any coupled motion in the longitudinal or radial direction will induce Coriolis Effect which affects the motion of the primary structure and or vice versa. Careful maneouvring of the longitudinal/radial motion can be used to effectively reduce the response of the primary structure. The questions here are what is the effect of reduction and how can it be improved?

3.2.2 Rationale

As mentioned earlier, tall slender flexible structures are susceptible to long period vibrations. The direction of evolution of tall structures is towards lightness and are often featured with increased flexibility and a lack of sufficient inherent damping making them even more vulnerable (Kareem, Kijewski, and Tamura, 1991; Ali and Moon, 2007). This presents a challenge for conventional mass dampers that usually utilise lateral motion for effect. As the height to width ratio increases, the effect of conventional measures decreases. Therefore it is important to find effective measures to reduce their response.

Similarly, rolling structures in low damping conditions face these challenges. For a more specific case, ships are vulnerable to roll motion which is the major contributor to capsizing. This roll motion can be induced in both rough and calm sea conditions. As a result great emphasis is placed on finding measures to reduce roll motion.

3.3 Research Design

This research is a quantitative study of the effect of reduction through several case studies, analytical and numerical approaches which include Finite Element Method, Runge-Kutta Method and Newmark Method.

3.3.1 Moving Mass Through Tall Structure

Overview

For this investigation, the damping effect of a moving mass through a tall building structure subjected to a large displacement and allowed free response was investigated. In order to illustrate the application of the concept in a realistic scenario, a benchmark model was used based on the Shinjuku Mitsui Building and the happenings of the March 11, 2011 earthquake in East Japan.

In this study, Finite Element Method (FEM) was employed to model, analyse and investigate the damping effect of a moving mass through a tall building structure. A common practice for tall building structures is to simply model them as a vertical cantilever beam with their base fixed in the ground with the top allowed to freely vibrate (Ali and Moon, 2007). As such, in this investigation the building structure was modelled as an Euler-Bernoulli beam structure. The moving mass was modelled using the Moving Finite Element Method (MFEM) which easily takes into account the inertial, centrifugal and Coriolis effect of the coupled effect of the moving mass and the tall structure. For the purpose of the study the numerical analysis was carried out using the program MATLAB.

The dynamic response of the primary structure was obtained using the Newmark's time stepping method. As this investigation was only a preliminary into developing a strategy for active control of structural vibrations using longitudinal motion of a moving load, the focus was on the damping effect and not on implementation parameters. The equations of dynamic equilibrium was solved at each nodal point of the primary structure for the selected time steps. For the case of the investigation, the point of interest was at the top of the structure. Following this the dynamic response at the top of the primary structure was analysed and compared to that of the response at similar position for the case of the undamped primary structure to clearly demonstrate the damping effect due to the moving mass.

In order to investigate the effect of damping of the proposed concept certain parameters of the moving mass system was varied to determine their correlation with damping effect. These were the mass of the damper and the stroke length/velocity of the moving mass.

Using energy considerations analytical results of the equations of motion were found and verified with the numerical results.

Benchmark Problem

On March 11, 2011 Japan experienced one of its most devastating earthquake in recent history famously called the Great East Japan Earthquake. In the aftermath of this earthquake tall buildings in Tokyo were still oscillating even thirty minutes after. One such building was the Shinjuku Mitsui Building which according to reports had a deflection at the top just over two meters. Taking from this case, the Shinjuku Mitsui Building was used as the benchmark model for this investigation.

The Shinjuku Mitsui Building has a height of 225m with a natural vibration period of 5.6 seconds in the longitudinal direction and 5.9 seconds in the transverse direction (Hori, Kurino, and Kurokawa, 2016). The effective weight of the Shinjuku Mitsui building is approximately 2.77×10^8N (Hori, Kurino, and Kurokawa, 2016).

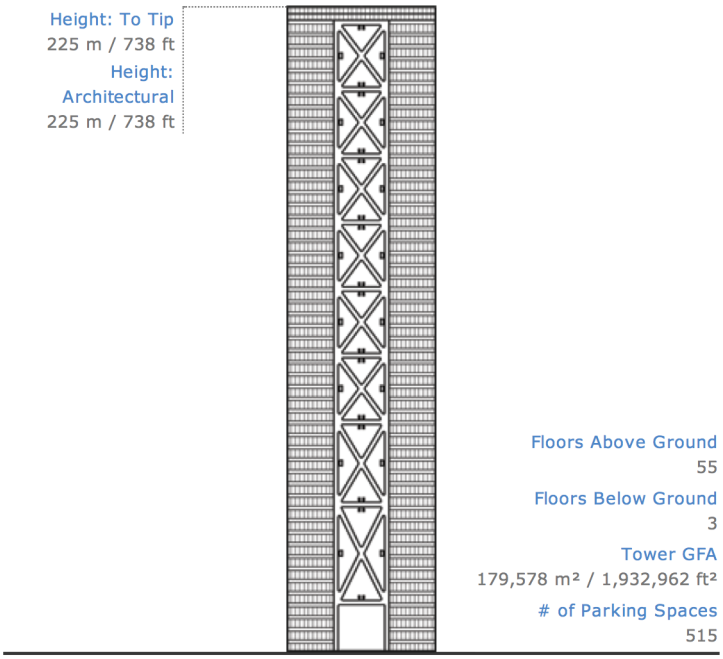

FIGURE 3.1: Schematic of the Shinjuku Mitsui Building (Council on Tall Buildings and Urban Habitat)

3.3.2 Radial Water-flow Through Rolling Ship

Overview

In this investigation, the roll response of a ship subjected to radial water-flow was investigated. The ship was analysed under two conditions. These are free roll decay, where the ship is given an initial displacement and allowed free response, and excited roll, where the ship is subjected to excitations of harmonic beam waves. The free roll decay investigation was used to determine the effect of damping of the radial water-flow on the ship while the excited roll investigation was used to determine the effect of roll response reduction of the radial water-flow on the ship. To illustrate the application of the concept in this investigation, a benchmark Ro-Ro vessel was chosen. Stability of Ro-Ro ships has been extensively researched over the years as they are prone to unstable conditions (Surendran et al., 2005).

For this study, Lagrangian Mechanics was employed to model, analyse and investigate the effect on roll response of the ship by the radial water-flow. The parametric roll of the ship was modelled as a single degree of freedom (SDOF) model while the water-flow was modelled with another degree of freedom (translation). Together, the roll of ship and radial water-flow formed a damped system with two-degrees-of-freedom (angular displacement of ship and translation of water). In order to qualitatively investigate

the rolling response of the ship with the radial water-flow, numerical simulations with the coupled motions of rolling of the ship and the radial water-flow were carried out and compared to analytical results. In this investigation the coupled motions are treated as a nonlinear dynamical system, however the analytical results are linearly approximated.

The dynamic response of the ship was obtained using the 4th Order Runge-Kutta single step method. The numerical results were compared to the linear approximated analytical results for the case of free roll decay and the linear approximated steady state results for the case of excited roll.

In order to investigate the effect of roll response of the system certain parameters of the water-flow system were varied to determine their correlation to roll response. These were the volume and velocity of water-flow.

Benchmark Problem

As mentioned earlier, the test ship used in this investigation was a Ro-Ro vessel. There have been several accidents involving Ro-Ro ships. Even as recent as on April 16, 2014 when the MV Sewol capsized off the coast of South Korea while carrying 476 people resulting in the deaths of 304 people. The parameters used in this investigation were taken from (Surendran et al., 2005) and is shown in Table 3.1.

TABLE 3.1: Parameters of a Ro-Ro Ship (Surendran et al., 2005)

Parameter	Symbol	Value
Length overall	L_{OA}	192.60 m
Length between perpendiculars	L_{BP}	177.60 m
Beam	B	28.00 m
Depth	D	18.00 m
Draught	T	7.50 m
Displacement	Δ	22012 t
Transverse meta-centric height	GM	2.66 m
Vertical centre of gravity	KG	13.98 m
Vertical centre of buoyancy	KB	4.40 m
Block coefficient	C_b	0.60

3.3.3 Multi-degree-of-freedom Enhanced Coriolis Effect Damper

Overview

In this investigation, the previous moving mass system through a tall building structure was modified in order to enhance its effect. The newly modified system consisted of a moving mass located at the top of the primary structure. This mass damper is coupled with a fixture which is allowed angular motion, as such the angular motion is driven by the translational mass at the top. Fitted to the angular fixture is a moving mass which is allowed translational motion along the fixture. This newly proposed system was analysed

under two conditions. These were free response, where the primary structure was initially displaced and allowed to freely oscillate, and seismic response, where the system was excited by recordings of the past Loma Prieta earthquake on October 17, 1989.

The free response investigation was done to determine the effect of damping of the modified system and to see to what extent were there improvements. The seismic response was used to determine the robustness and effectiveness of the modified system in the events of actual earthquake conditions to reduce the response of the primary structure. Additionally, control law based on the concept of Fuzzy Logic Theory was proposed for the modified system to effectively reduce the response of the primary structure. For the purpose of this investigation, a benchmark model was used based on a super tall structure investigated in (Yang et al., 2004).

For this study, Lagrangian Mechanics was employed to model, analyse and investigate the effect on the dynamic response of the primary structure. The building structure was simply modelled as a two degree of freedom model with translational motions in the horizontal direction. The mass damper at the top is modelled as a SDOF oscillator also with translational motion in the horizontal direction opposing that of the primary structure. The mass damper fitted to the oscillating fixture was modelled as a two-degree-of-freedom (2DOF) system which includes the translation along the fixture and the angular motion due to being fitted to the angular fixture. Together, the complete system had five degrees of freedom (translations of the primary structure, translation of the mass damper at the top, angular motion of the mass fitted to the fixture and translation of the mass along the fixture).

The dynamic response of the structure was obtained using the Runge-Kutta single step method.

Benchmark Problem

Yang et. al (Yang et al., 2004) investigated a super tall building which is also used as the benchmark model for the case of this investigation. The building considered has a height of 306 metres and has a height to width ratio of 7:3 therefore making it very vulnerable to excitation. The total mass of the building is 153,000 tons and has a first natural frequency of 1 rad/s.

Seismic Response

On October 17, 1989 the San Francisco and Moneterey Bay regions experienced a severe earthquake. This earthquake was used as the benchmark seismic model in this investigation. For this study we will refer to this earthquake as the Loma Prieta Earthquake. The data for this can be found in MATLAB which contains 200 Hz data of the Loma Prieta earthquake in the Santa Cruz Mountains courtesy of Joel Yellin at the Charles F. Richter Seismological Laboratory, University of California, Santa Cruz. The time histories for this earthquake are shown in Figures 3.4 and 3.5.

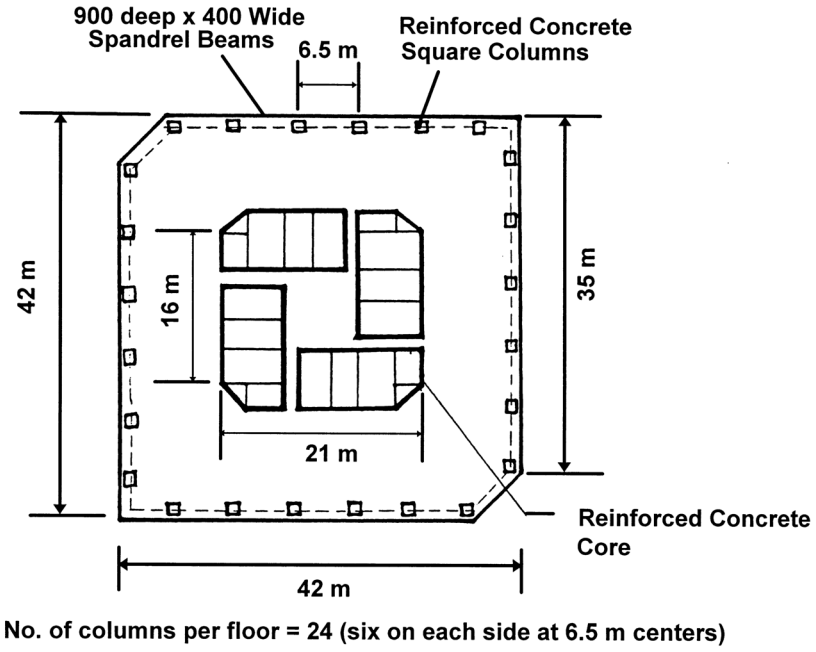

FIGURE 3.2: Plan view of the benchmark building (Yang et al., 2004)

3.3.4 Meaning of the method

Case studies from real and existing scenarios are used as benchmarks to test the robustness of the proposed work and its ability in a more realistic case as a preliminary study.

3.4 Procedure and Analysis

In order to quantitatively investigate this research certain steps and procedures were taken. This section highlights these.

3.4.1 Moving Mass Through Tall Structure

An overview of the procedures taken throughout this investigation is illustrated in Figure 3.6 . First, a simplified physical model of the building structure was created from which analytical equations of motions were derived using the Extended Hamilton's Principle. A finite element model is formulated from the physical model and analysed. The numerical analysis was carried out using Newmark's Method as such:

1. The model was discretised into a number of identical beam elements and nodes.

2. The mass and stiffness matrices of each of these beam elements were determined.

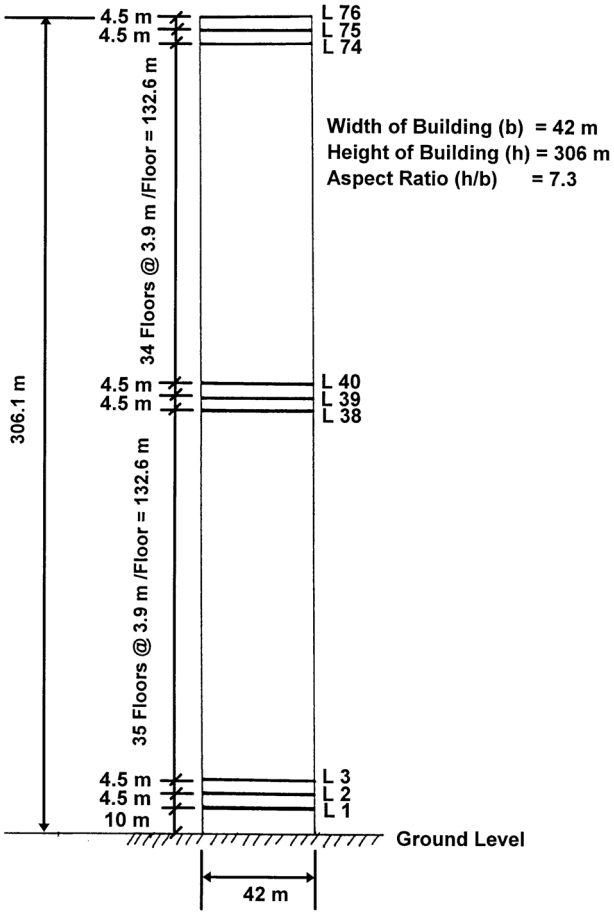

Figure 2. Elevation View of the Building.

FIGURE 3.3: Elevation view of the benchmark building (Yang et al., 2004)

3. The damping matrices of each beam element was determined using Rayleigh damping theory.

4. A fixed stepping time was selected.

5. Motion for the moving mass was proposed based on analysis of the analytical equations of motion.

6. For each time step, the element on which the moving mass is located and the local position of the moving mass on that element was determined.

7. The time dependent shape functions of the beam element were calculated.

8. From this, the mass, stiffness and damping matrices of the moving finite element were determined.

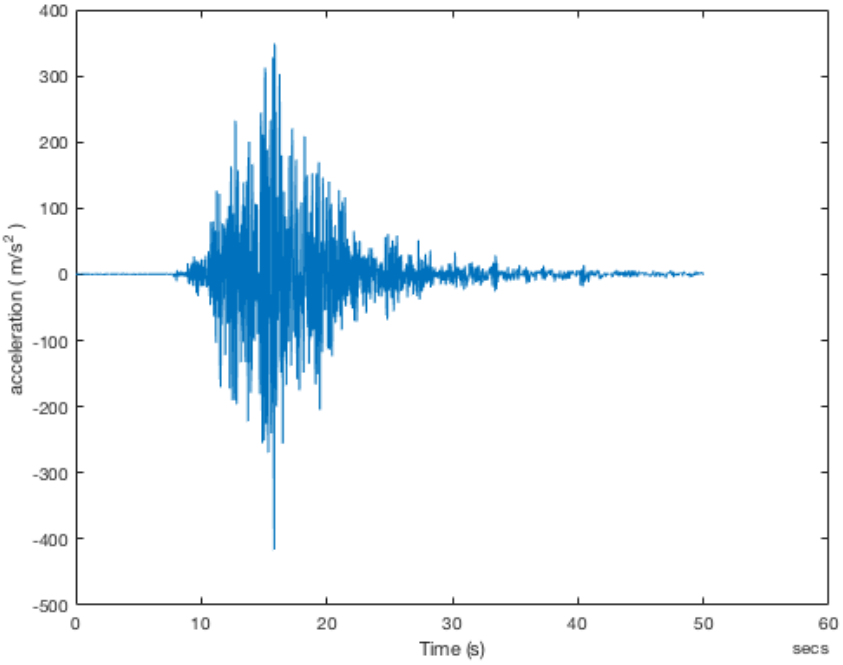

FIGURE 3.4: East-west ground acceleration of the 1989 Loma Prieta earthquake

9. The mass, stiffness and damping matrices of the element on which the moving mass is located were calculated by assembling the matrices of the moving finite element.

10. The instantaneous overall mass, stiffness and damping matrices of the entire system were calculated by assembling all the matrices calculated above.

11. The instantaneous overall force vector was calculated

12. boundary conditions were imposed.

13. The equation of motion was solved using Newmark integration method giving the dynamic responses of the primary structure. The procedures for Newmark method is given in Appendix A.

14. Repeat steps 6 - 13 for all the time steps.

Using energy considerations an analytical expression of the equivalent damping of the system was found.

From analysis of the results, recommendations were made for future investigations which led to the following two investigations.

3.4.2 Radial Water-flow Through Rolling Ship

An overview of the steps taken in analysing the effect of water-flow through a rolling ship is shown in Figure 3.7. Inspired by the results of the previous

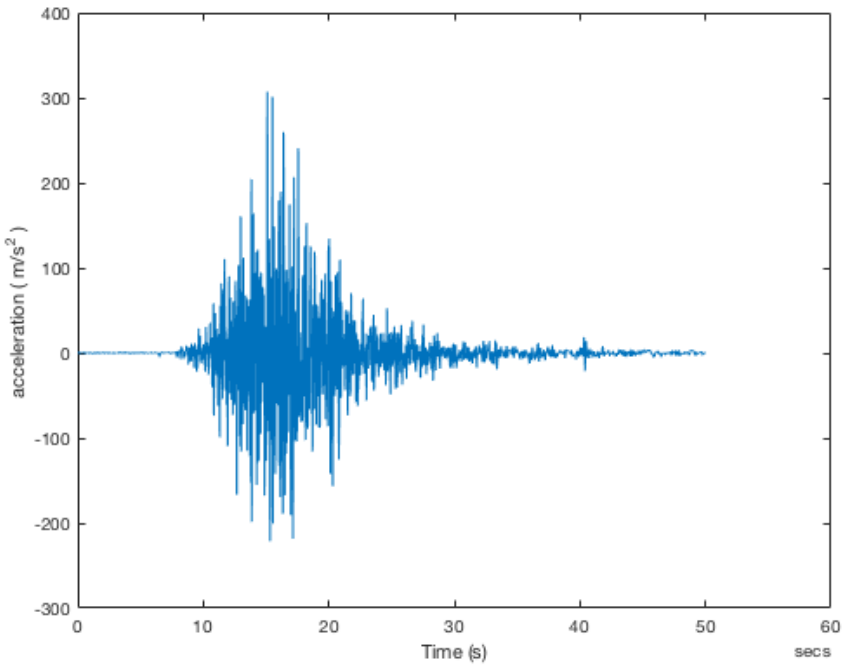

FIGURE 3.5: North-south ground acceleration of the 1989 Loma Prieta earthquake

investigation, the idea of using a constant unidirectional water-flow away from the pivot of the rolling structure to reduce the roll response of ships was proposed. A simplified model of the system was first created from which the equations of motion were derived using Lagragian Mechanics. In order to express the results in a general form, general non-dimensional forms of the equations were found. Numerical analysis of the equations of motion were carried out using the 4th Order Runge-Kutta method. The system was analysed under free roll decay and excited roll. For comparison and validation, the nonlinear system was linearised and approximated to give analytical results. The results were then compared and recommendations for improvement of the system were made.

3.4.3 Multi-degree-of-freedom Enhanced Coriolis Effect Damper

Figure 3.8 highlights the procedures taken throughout this investigation. Inspired by the results of the investigations of the moving mass through the beam structure, a newly modified damper system was proposed to enhance its effect. A physical model of the system was first created from which equations of motion were derived using Lagrangian Mechanics. Numerical analysis of the equations of motion were carried out using Runge-Kutta method. The dynamic response of the primary structure was first analysed to identify the characteristics of the structure. After which, optimal tuned mass damper was proposed using Hartog's method (Den Hartog, 1985). Fuzzy logic control was proposed for the tuned mass damper. The system was then fitted

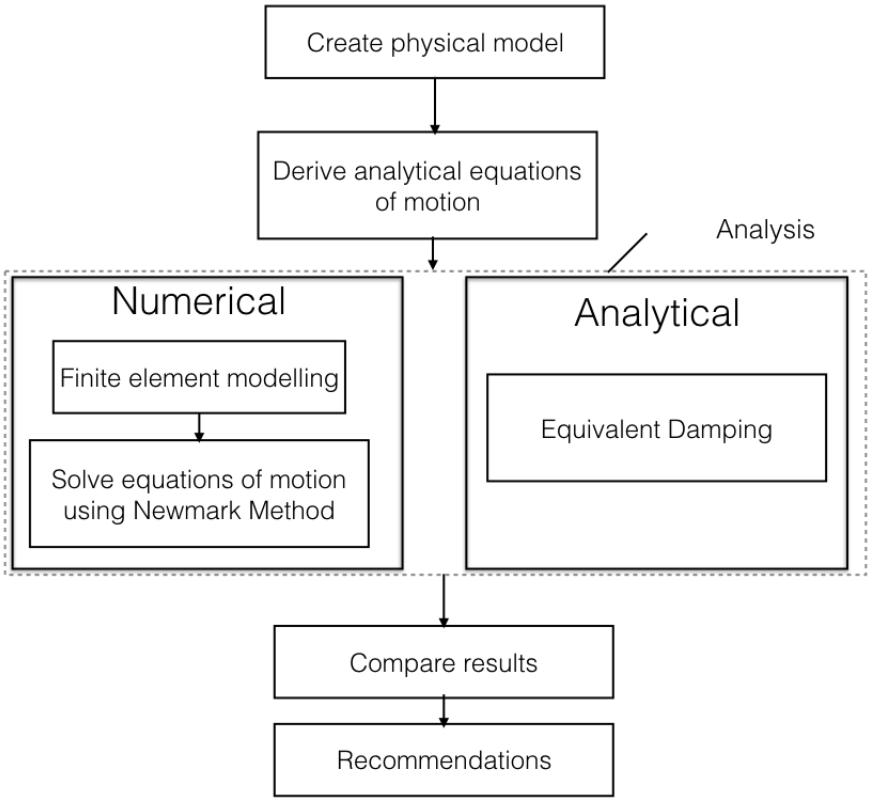

FIGURE 3.6: Steps taken in the analysis of a moving mass through tall building structure.

with the proposed Coriolis damper and also controlled using Fuzzy Logic. The results were then compared. The results are then analysed and recommendations for future research were made.

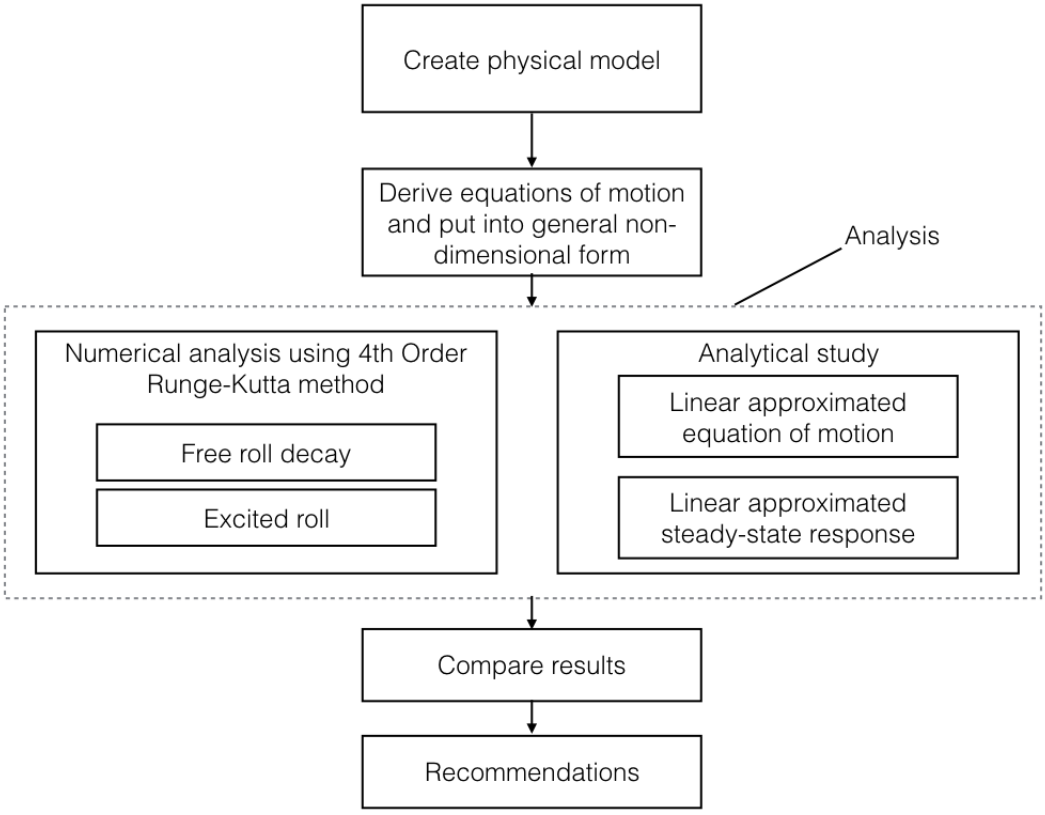

FIGURE 3.7: Steps taken in the analysis of radial water-flow through a rolling ship

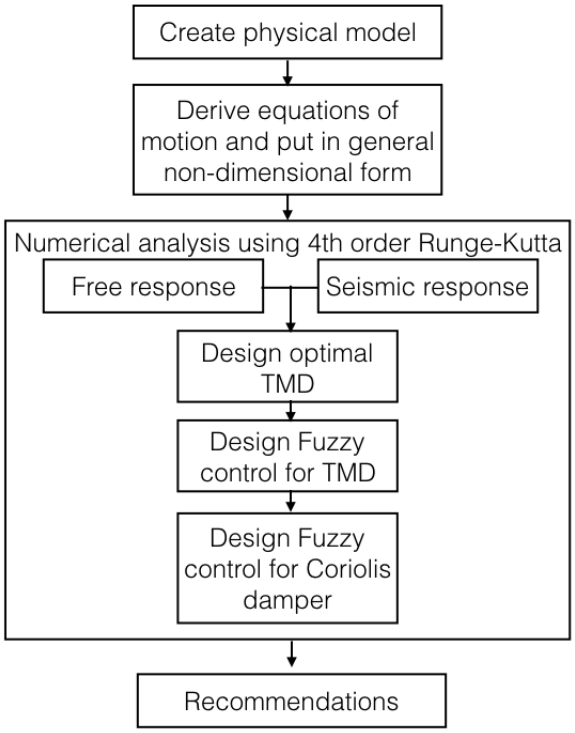

FIGURE 3.8: Steps taken in the analysis of the multi-degrees-of-freedom damped system

Chapter 4

Attenuation of Tall Flexible Structures using Longitudinal Moving Mass: Moving Finite Element Method

4.1 Introduction

In this chapter, a finite element model is formulated to investigate the damping effect of a moving mass on a long-period vibrating vertical cantilever beam. The dynamic response is investigated by modelling the mass as a moving finite element to easily take into account the inertial, centrifugal and Coriolis effect of the moving mass on the structure. The concept of enhancing the effect is also briefly discussed using a multiple-degree-of-freedom damper and a constant positive velocity water-flow damping system as examples.

4.2 Formulation of The Problem

4.2.1 Equations of Motion Through Hamilton's Principle

The equations of motion of the system can be analytically derived using the Extended Hamilton's Principle. The model of the concept is shown in Fig. 4.1. The vibrating primary structure is modelled as an Euler-Bernoulli beam with its bottom end fixed in the ground. The moving mass m moves over the structure and is able to move up and down. The horizontal deflection of the beam is given as $u(y,t)$ and the position of the mass at any time t is the curvilinear coordinate $s(t)$ defined along the height of the beam.

The energy of the system presented is due to (1) the beam and (2) the moving mass.

The kinetic energy of the beam (T_B)

$$T_B = \frac{A\rho}{2}\int_0^H \dot{u}^2 dy \tag{4.1}$$

where A is the cross-section of the beam, ρ is the material density and $u(y,t)$ is the horizontal deflection of the beam. For the beam rotary inertia is ignored.

The kinetic energy of the mass (T_m)

$$T_m = \frac{1}{2}m[\dot{s}^2 + \dot{u}^2 + 2\dot{u}\dot{s}u']_{y=s} \tag{4.2}$$

where m is of the moving mass, $s(t)$ is the position of the mass. In this paper, prime, $()'$, and dot, $(\dot{})$, are the derivatives with respect to y and t respectively. The moving mass is considered to be a particle so the polar moment of inertia is assumed to be zero.

The total kinetic energy of the system

$$T = T_B + T_m \tag{4.3}$$

The potential energy of the system (V) is only due to the strain energy in the beam. Hence

$$V = \frac{EI}{2}\int_0^H u''^2 dy \tag{4.4}$$

where E is the modulus of elasticity and I the moment of inertia.

Now for the Lagrangian Mechanics which states:

$$L = T - V \tag{4.5}$$

Using Hamilton's principle

$$\int_{t_1}^{t_2} \delta L dt = F \tag{4.6}$$

where F is the force applied to the system.

Considering the beam structure and using Equation (4.5) in Equation (4.6) we get

$$\begin{aligned}\int_{t1}^{t_2}\Big[\delta\left(\frac{A\rho}{2}\int_0^H \dot{u}^2 dy + \frac{1}{2}m[\dot{s}^2 + \dot{u}^2 + 2\dot{u}\dot{s}u']_{y=s}\right)\\ -\delta\left(\frac{EI}{2}\int_0^H u''^2 dy\right)\Big]dt = f_B(y,t)\end{aligned} \tag{4.7}$$

where $f_B(y,t)$ is the force per unit length applied to the beam.

Using integration by parts Equation (4.7) becomes

$$\begin{aligned}\int_0^H (A\rho\ddot{u} + EIu'''')dy\\ +m[\ddot{u} + 2\dot{s}\dot{u}' + \ddot{s}u' + \dot{s}^2u'']_{y=s} = f_B(y,t)\end{aligned} \tag{4.8}$$

In the case of free response where the only force applied to the beam would be due to the motion of the moving mass, $f_B(y,t) = 0$. The interaction between the beam and the moving mass is given by the second part of

Equation (4.8).

To find the equation of motion of the moving mass we consider the s coordinate and use Langrange Principle

$$\frac{d}{dt}\left(\frac{\partial L}{\partial \dot{s}}\right) - \frac{\partial L}{\partial s} = f_s(t) \tag{4.9}$$

where $f_s(t)$ is the force applied to the moving mass, we get

$$m[\ddot{s} + \ddot{s}u']_{y=s} = f_s(t) \tag{4.10}$$

4.2.2 Motion of Moving Mass

In Equation (4.8) the $2m\dot{s}\dot{u}'$ term is the Coriolis component of the inertial effects due to the interaction of the moving mass and the vibrating beam. Examination of the Coriolis effect induced in the system shows its correlation of its effectiveness with the motion of the moving mass. It is worth mentioning also that the dissipation of the system depends on the nature of the velocity of the moving mass ($\dot{s}$). When $\dot{s}$ is positive, the system dissipates energy and when $\dot{s}$ is negative the system accumulates energy. The nature of $\dot{s}$ changes in one cycle, therefore there is an alternation of dissipation and accumulation of energy in the system in a cycle. Therefore in order to ensure an overall dissipation as large as possible at the end of a cycle this can only be achieved if the period of dissipation is made as large as possible while the period of accumulation is made as small as possible. From this, we see that for damping effects the moving mass should move up when the angular velocity of the primary structure is close to maximum and down when angular velocity is close to zero. Furthermore, it is known that the primary structure experiences zero and maximum angular velocities twice per cycle. As such, the moving mass should move with twice the frequency of the system. It should be noted that a reverse of this motion will generate an amplification effect.

Further examination of the Coriolis effect also reveals that for maximum effect the velocity of the moving mass should be maximum at the moment the primary structure has maximum angular velocity. From this we prescribe the motion of the moving mass to be

$$s(t) = s_0 - bsin(2\omega_1 t - \psi) \tag{4.11}$$

where s_0 is the height from ground to mid-point between maximum y (s_{max}) and minimum y (s_{min}), ω_1 is the first natural frequency of the structure, ψ is the phase angle at the start of the cycle and

$$b = \frac{1}{2}(s_{max} - s_{min}) \tag{4.12}$$

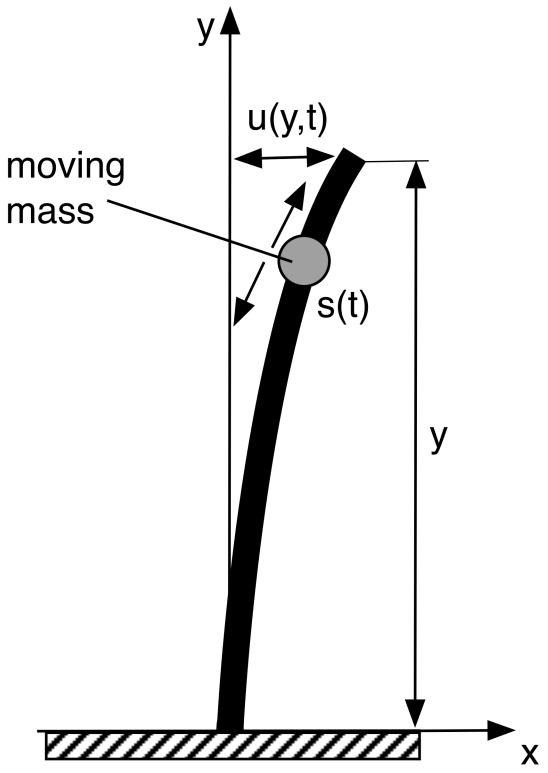

FIGURE 4.1: Vibrating vertical cantilever beam with a moving mass on it.

4.3 Finite Element Method

In this section the finite element approach is illustrated.

Figure 4.2 shows the finite element model of the system. The beam of height H is discretised in n number of elements of height h, and $n+1$ number of nodes. The moving mass m moves up and down over the beam with acceleration and velocity $\ddot{s}$ and $\dot{s}$ respectively. The Figure 4.3 illustrates the nodal forces of the element (s_e^{th} element) on which the mass is located at time t. The position of the moving mass on the s_e^{th} element is given by $y_m(t)$.

4.3.1 The Primary Structure

Using FEM the primary structure is modelled as n number of beam elements as shown in Figure 4.2. The structure has mass, damping and stiffness matrices, $[M]$, $[C]$ and $[K]$ respectively. The mass and stiffness matrices are obtained by assembling all the element matrices. One way to define the damping matrix is to use Rayleigh damping (Craig and Kurdila, 2006)

$$[C] = a_0[M] + a_1[K] \tag{4.13}$$

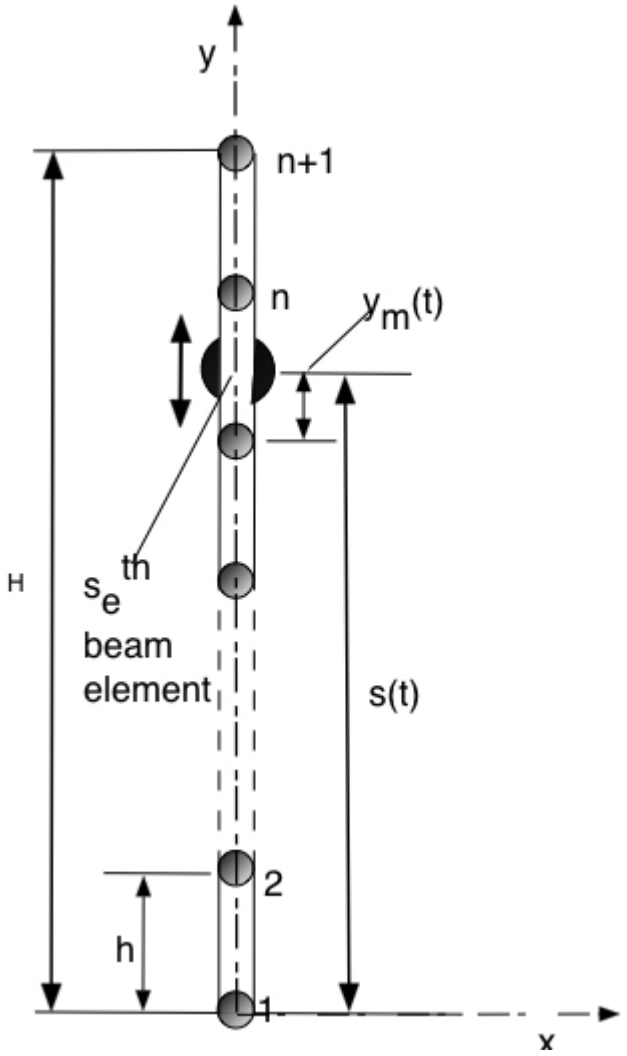

FIGURE 4.2: FEM Model of vertical cantilever beam with moving mass

the damping factors are given by:

$$\zeta_r = \frac{1}{2}\left(\frac{a_0}{\omega_r} + a_1\omega_r\right) \tag{4.14}$$

a_0 and a_1 are found by choosing damping ratios (ζ_r) in two modes with the corresponding natural frequencies (ω_r).

4.3.2 Moving Finite Element

In this study the moving finite element method is employed in order to easily take into consideration all the internal forces acting on the system due to the interaction of the vibrating beam and the moving mass. These include the inertial forces, centripetal forces and most important the Coriolis effect. These forces are described below.

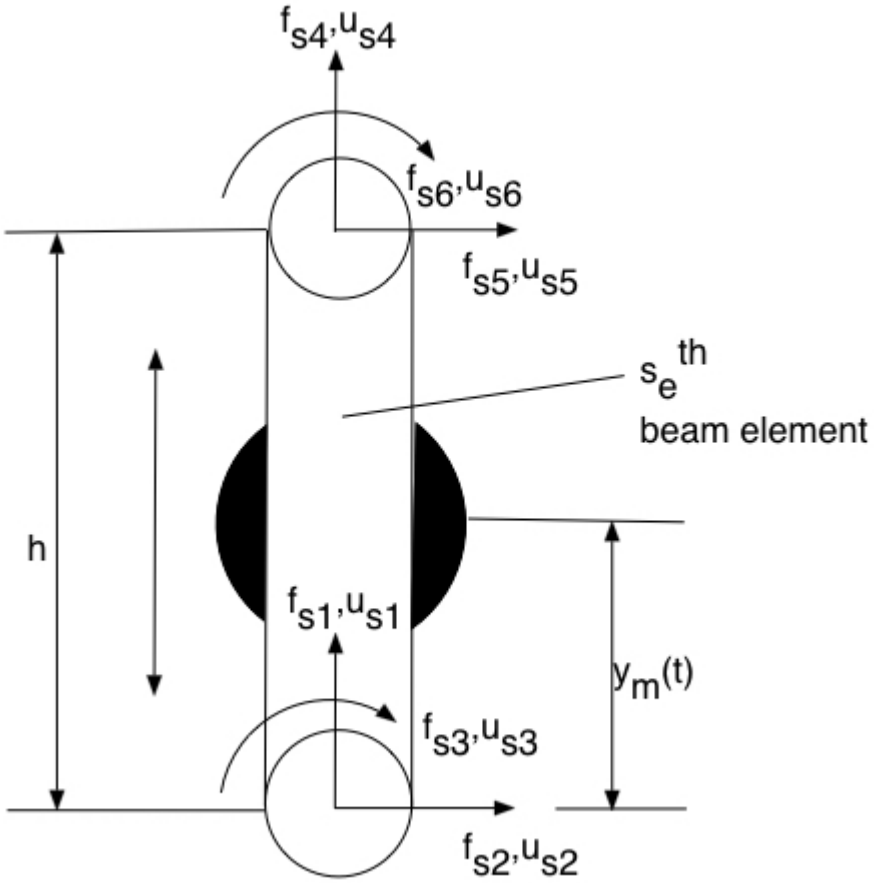

FIGURE 4.3: beam element on which moving mass is located

Nodal Forces of Moving Finite Element

The vibration and curvature of the beam induce forces due to the interaction between the beam and the moving mass. From this point the parameters of $f(y,t)$, $u(y,t)$ and $s(t)$ are simply represented as f, u and s respectively. Taking into account the transverse (x) and longitudinal (y) direction we get:

Transverse (x) force component f_x:

$$f_x = m\frac{d^2u_x}{dt^2}\delta(y-s) \tag{4.15}$$

Longitudinal (y) force component f_y:

$$f_y = m\frac{d^2u_y}{dt^2}\delta(y-s) \tag{4.16}$$

where u_y and u_x respectively represent the longitudinal (y) displacement and transverse (x) deflection of the beam at position y and time t. $\delta(y-s)$ represents the Dirac-delta function.

For transverse direction

$$\frac{du_x}{dt} = \frac{\partial u_x}{\partial y}\frac{\partial y}{\partial t} + \frac{\partial u_x}{\partial t}\frac{\partial t}{\partial t} \tag{4.17}$$

which gives

$$\frac{du_x}{dt} = u'_x\dot{y} + \dot{u}_x \tag{4.18}$$

And

$$\begin{aligned}\frac{d^2u_x}{dt^2} = &\frac{\partial u'_x}{\partial y}\frac{\partial y}{\partial t}\dot{y} + \frac{\partial u'_x}{\partial t}\frac{\partial t}{\partial t}\dot{y} \\ &+u'_x\frac{d\dot{y}}{dt} + \frac{\partial \dot{u}_x}{\partial y}\frac{\partial y}{\partial t} \\ &+\frac{\partial \dot{u}_x(y,t)}{\partial t}\frac{\partial t}{\partial t}\end{aligned} \tag{4.19}$$

which gives

$$\begin{aligned}\frac{d^2u_x}{dt^2} = &\ddot{u}_x + 2\dot{u}'_x\dot{y} \\ &+u'_x\ddot{y} + u''_x\dot{y}^2\end{aligned} \tag{4.20}$$

For longitudinal direction

$$\frac{du_y}{dt} = \frac{\partial u_y}{\partial y}\frac{\partial y}{\partial t} + \frac{\partial u_y}{\partial t}\frac{\partial t}{\partial t} \tag{4.21}$$

which gives

$$\frac{du_y}{dt} = u'_y\dot{y} + \dot{u}_y \tag{4.22}$$

Assuming the beam is inextensible, the first term can be ignored and Equation (4.22) can be approximated as

$$\frac{du_y}{dt} \approx \dot{u}_y \tag{4.23}$$

And

$$\frac{d^2u_y}{dt^2} = \frac{\partial \dot{u}_y}{\partial y}\frac{\partial y}{\partial t} + \frac{\partial \dot{u}_y}{\partial t} \tag{4.24}$$

which gives

$$\frac{d^2u_y}{dt^2} = \dot{u}'_y\dot{y} + \ddot{u}_y \tag{4.25}$$

again using the assumptions above we can approximate Equation (4.25) as

$$\frac{d^2u_y}{dt^2} \approx \ddot{u}_y \tag{4.26}$$

Substituting Equation (4.20) into Equation (4.15) and Equation (4.26) into Equation (4.16) we get

$$f_x = m[\ddot{u}_x + 2\dot{u}'_x\dot{y} + u'_x\ddot{y} + u''_x\dot{y}^2]\delta(y-s) \tag{4.27}$$

since $\dot{y} = \dot{s}$ and $\ddot{y} = \ddot{s}$, we get

$$f_x = m[\ddot{u}_x + 2\dot{u}'_x\dot{s} + u'_x\ddot{s} + u''_x\dot{s}^2]\delta(y-s) \tag{4.28}$$

$$f_y = m\ddot{u}_y\delta(y-s) \tag{4.29}$$

From this we can get the equivalent nodal forces (f_{si}) of the s_e^{th} element.

$$f_{si} = N_i m\ddot{u}_y \qquad (i = 1, 4) \tag{4.30}$$

$$f_{si} = N_i m[\ddot{u}_x + 2\dot{u}'_x\dot{s} + u'_x\ddot{s} + u''_x\dot{s}^2] \qquad (i = 2, 3, 5, 6) \tag{4.31}$$

where N_i $(i = 1-6)$ are shape functions of the beam element as given in (Clough and Penzien, 2003):

$$\begin{aligned} N_1 &= 1 - \xi \\ N_2 &= 1 - 3\xi^2 + 2\xi^3 \\ N_3 &= [\xi - 2\xi^2 + \xi^3]h \\ N_4 &= \xi \\ N_5 &= 3\xi^2 - 2\xi^3 \\ N_6 &= [-\xi^2 + \xi^3]h \\ &with \\ \xi &= \frac{y_m}{h} \end{aligned} \tag{4.32}$$

where as shown in Fig. 4.3, h is the height of the s_e^{th} beam element and y_m is the distance between the moving mass m and the bottom end of the s_e^{th} beam element at time t.

The longitudinal (y) and transverse (x) displacements can be shown to be

$$\begin{aligned} u_y &= N_1 u_{s1} + N_4 u_{s4} \\ u_x &= N_2 u_{s2} + N_3 u_{s3} + N_5 u_{s5} + N_6 u_{s6} \end{aligned} \tag{4.33}$$

where u_{si} $(i = 1-6)$ are displacements of the nodes of the beam element on which the moving mass m, locates.

Substituting Equation (4.33) into Equation (4.30) and Equation (4.31) and writing in matrix form yields equation

$$\{f\} = [m]\{\ddot{u}\} + [c]\{\dot{u}\} + [k]\{u\} \tag{4.34}$$

where

$$\begin{aligned} \{f\} &= [f_{s1} \quad f_{s2} \quad f_{s3} \quad f_{s4} \quad f_{s5} \quad f_{s6}]^T \\ \{\ddot{u}\} &= [\ddot{u}_{s1} \quad \ddot{u}_{s2} \quad \ddot{u}_{s3} \quad \ddot{u}_{s4} \quad \ddot{u}_{s4} \quad \ddot{u}_{s5} \quad \ddot{u}_{s6}]^T \\ \{\dot{u}\} &= [\dot{u}_{s1} \quad \dot{u}_{s2} \quad \dot{u}_{s3} \quad \dot{u}_{s4} \quad \dot{u}_{s4} \quad \dot{u}_{s5} \quad \dot{u}_{s6}]^T \\ \{u\} &= [u_{s1} \quad u_{s2} \quad u_{s3} \quad u_{s4} \quad u_{s4} \quad u_{s5} \quad u_{s6}]^T \end{aligned} \tag{4.35}$$

$$[m] = m \begin{bmatrix} N_1^2 & 0 & 0 & N_1N_4 & 0 & 0 \\ 0 & N_2^2 & N_2N_3 & 0 & N_2N_5 & N_2N_6 \\ 0 & N_3N_2 & N_3^2 & 0 & N_3N_5 & N_3N_6 \\ N_4N_1 & 0 & 0 & N_4^2 & 0 & 0 \\ 0 & N_5N_2 & N_5N_3 & 0 & N_5^2 & N_5N_6 \\ 0 & N_6N_2 & N_6N_3 & 0 & N_6N_5 & N_6^2 \end{bmatrix} \tag{4.36}$$

$$[c] = 2m\dot{s} \begin{bmatrix} 0 & 0 & 0 & 0 & 0 & 0 \\ 0 & N_2N_2' & N_2N_3' & 0 & N_2N_5' & N_2N_6' \\ 0 & N_3N_2' & N_3N_3' & 0 & N_3N_5' & N_3N_6' \\ 0 & 0 & 0 & 0 & 0 & 0 \\ 0 & N_5N_2' & N_5N_3' & 0 & N_5N_5' & N_5N_6' \\ 0 & N_6N_2' & N_6N_3' & 0 & N_6N_5' & N_6N_6' \end{bmatrix} \tag{4.37}$$

$$[k] = m \begin{bmatrix} 0 & 0 & 0 & 0 & 0 & 0 \\ 0 & k_{22} & k_{23} & 0 & k_{25} & k_{26} \\ 0 & k_{32} & k_{33} & 0 & k_{35} & k_{36} \\ 0 & 0 & 0 & 0 & 0 & 0 \\ 0 & k_{52} & k_{53} & 0 & k_{55} & k_{56} \\ 0 & k_{62} & k_{63} & 0 & k_{65} & k_{66} \end{bmatrix} \tag{4.38}$$

where $k_{ij} = \ddot{s}N_iN_j' + \dot{s}^2N_iN_j''$

[m], [c], [k] are respectively the mass, damping and stiffness matrices of the moving finite element. It is evident from Equation (4.32) that these matrices are time-dependent.

4.3.3 Entire Structural System

Equation of Motion

The equation of motion of the entire structural system is governed by

$$[\hat{M}]\{\ddot{u}\} + [\hat{C}]\{\dot{u}\} + [\hat{K}]\{u\} = [\hat{F}] \tag{4.39}$$

where $[\hat{M}]$, $[\hat{C}]$ and $[\hat{K}]$ are the overall mass, damping and stiffness matrices respectively. $\{\ddot{u}\}$, $\{\dot{u}\}$, and $\{u\}$ are the acceleration, velocity and displacement vectors respectively. While $[\hat{F}]$ is the overall external force vector at any time t.

Mass, Stiffness and Damping Matrices

The mass, stiffness and damping matrices are obtained by assembling the element matrices and imposing boundary conditions. For this the element matrices of the moving finite element are taken into consideration. As such

$$\hat{K}_{ij} = K_{ij} \qquad (i, j = 1 - n) \tag{4.40}$$

$$\hat{M}_{ij} = M_{ij} \qquad (i, j = 1 - n) \tag{4.41}$$

$$\hat{C}_{ij} = C_{ij} \qquad (i, j = 1 - n) \tag{4.42}$$

except for the s_e^{th} element where

$$\hat{K}_{sisj} = K_{sisj} + k_{ij} \qquad (i,j = 1-6) \tag{4.43}$$

$$\hat{M}_{sisj} = M_{sisj} + m_{ij} \qquad (i,j = 1-6) \tag{4.44}$$

$$\hat{C}_{sisj} = C_{sisj} + c_{ij} \qquad (i,j = 1-6) \tag{4.45}$$

Overall Force Vector

The overall force is due only to the forces in the s_e^{th} beam element on which the moving mass locates. As such the overall force vector takes the form

$$[\hat{F}] = [0 \quad ... \quad f_{s1} \quad f_{s2} \quad f_{s3} \quad f_{s4} \quad f_{s5} \quad f_{s6} \quad ...]^T \tag{4.46}$$

where the nodal forces are found using Equation (4.30) and Equation (4.31).

Solution of Equation of Motion

The solution to the equation of motion can be obtained by numerical integration. There are several methods that exist, but for the purpose of this paper we use Newmark's method as illustrated in (Rajasekaran, 2009).

4.4 Quantitative Equivalent Damping Ratio

An analytical approach for finding an explicit expression of the equivalent damping ratio ζ_{eqv} in terms of the parameters of the system is given using the approximation (Liang et al., 2011):

$$\zeta_{eqv} = \frac{1}{4\pi}\frac{E_d}{E_0} \tag{4.47}$$

where E_d represents the energy dissipation capacity of the system and E_0 represents the maximum potential energy of the system.

4.4.1 Equations of Motion: Fourier Method

Let us consider the case for free vibration. Then Equation (4.8) can be written as

$$\int_0^H \left(A\rho \frac{\partial^2 u(y,t)}{\partial t^2} + EI \frac{\partial^4 u(y,t)}{\partial t^4} \right) dy$$
$$+m \left[\frac{\partial^2 u(y,t)}{\partial t^2} + 2\frac{\partial s(t)}{\partial t}\frac{\partial u(y,t)}{\partial y \partial t} + \frac{\partial^2 s(t)}{\partial t^2}\frac{\partial u(y,t)}{\partial y} + \frac{\partial s(t)}{\partial t}^2 \frac{\partial^2 u(y,t)}{\partial y^2} \right]_{y=s} = 0 \tag{4.48}$$

Equation (4.48) can be conveniently written by means of separation of variables, assuming:

$$u(y,t) = U(y)W(t) \tag{4.49}$$

where $U(y)$ is the known shape function of the beam and $W(t)$ defines the amplitude of vibration with time t.

Therefore, putting Equation (4.49) into Equation (4.48), and rearranging we get:

$$\begin{aligned}\left[\int_0^H A\rho U(y)dy + mU(s)\right]\frac{\mathrm{d}^2W(t)}{\mathrm{d}t^2} + 2m\frac{\mathrm{d}s(t)}{\mathrm{d}t}\frac{\mathrm{d}U(s)}{\mathrm{d}s}\frac{\mathrm{d}W(t)}{\mathrm{d}t} \\ + \left[m\left(\frac{\mathrm{d}^2s(t)}{\mathrm{d}t^2}\frac{\mathrm{d}U(s)}{\mathrm{d}s} + \frac{\mathrm{d}s(t)}{\mathrm{d}t}^2\frac{\mathrm{d}^2U(s)}{\mathrm{d}s^2}\right) + \int_0^H EI\frac{\mathrm{d}^4U(y)}{\mathrm{d}y^4}dy\right]W(t) = 0\end{aligned} \tag{4.50}$$

Using boundary conditions for uniform cantilever beam, we get the general form of the solutions for $U(y)$ and $W(t)$ as

$$F(t) = A_n sin\bar{\omega}t + B_n cos\bar{\omega}t \tag{4.51}$$

$$U(y) = C_1 sin\beta y + C_2 cos\beta y + C_3 sinh\beta y + C_4 cosh\beta y \tag{4.52}$$

Now it can be seen that Equation (4.50) is in the form

$$\bar{M}\ddot{W}(t) + \bar{C}\dot{W}(t) + \bar{K}W(t) = 0 \tag{4.53}$$

or

$$\ddot{W}(t) + 2\zeta_{eqv}\bar{\omega}\dot{W}(t) + \bar{\omega}^2W(t) = 0 \tag{4.54}$$

where

$$\begin{aligned}\bar{\omega}^2 = \frac{1}{\int_0^H A\rho U(y)dy + mU(s)}\left[m\left(\frac{\mathrm{d}^2s(t)}{\mathrm{d}t^2}\frac{\mathrm{d}U(s)}{\mathrm{d}s} + \frac{\mathrm{d}s(t)}{\mathrm{d}t}^2\frac{\mathrm{d}^2U(s)}{\mathrm{d}s^2}\right)\right. \\ \left. + \int_0^H EI\frac{\mathrm{d}^4U(y)}{\mathrm{d}y^4}dy\right]\end{aligned} \tag{4.55}$$

4.4.2 Energy Consideration

The normalised energy of the system is

$$\bar{E}(t) = \frac{1}{2}\dot{W}(t)^2 + \frac{1}{2}\bar{\omega}^2W(t)^2 \tag{4.56}$$

Now the derivative with respect to time of the normalised energy gives us the dissipation energy of the system. That is

$$\frac{\mathrm{d}\bar{E}(t)}{\mathrm{d}t} = -\bar{D}(t) \tag{4.57}$$

where $\bar{D}$ is the dissipation energy. Therefore

$$\bar{D}(t) = \frac{2m}{\int_0^H A\rho U(y)dy + mU(s)}\left[\frac{\mathrm{d}s(t)}{\mathrm{d}t}\frac{\mathrm{d}U(s)}{\mathrm{d}s}\frac{\mathrm{d}W(t)}{\mathrm{d}t}^2 - \frac{\Omega W(t)^2}{4\left(\int_0^H A\rho U(y)dy + mU(s)\right)}\right] \tag{4.58}$$

where

$$\Omega = \left[\left(\frac{\mathrm{d}^3 s(t)}{\mathrm{d}t^3}\frac{\mathrm{d}U(s)}{\mathrm{d}s} + \frac{\mathrm{d}^2 s(t)}{\mathrm{d}t^2}\frac{d}{dt}\left(\frac{\mathrm{d}U(s)}{\mathrm{d}s}\right)\right.\right.$$
$$\left.\left. +2\frac{\mathrm{d}s(t)}{\mathrm{d}t}\frac{\mathrm{d}^2 s(t)}{\mathrm{d}t^2} + \frac{d}{dt}\left(\frac{\mathrm{d}^2 U(s)}{\mathrm{d}s^2}\right)\right)\left(\int_0^H A\rho U(y)dy + mU(s)\right)\right.$$
$$\left. -m\frac{\mathrm{d}U(s)}{\mathrm{d}t}\left(m\left(\frac{\mathrm{d}^2 s(t)}{\mathrm{d}t^2}\frac{\mathrm{d}U(s)}{\mathrm{d}s} + \frac{\mathrm{d}s(t)}{\mathrm{d}t}^2\frac{\mathrm{d}^2 U(s)}{\mathrm{d}s^2}\right)\right) + \int_0^H EI\frac{\mathrm{d}^4 U(y)}{\mathrm{d}y^4}dy\right] \tag{4.59}$$

Using the equivalent damping ratio for a viscous damper (Equation(4.47)) we get

$$\zeta_{eqv} = \frac{1}{4\pi\bar{E}_0}\int_0^t \bar{D}(t)dt \tag{4.60}$$

where t is some arbitrary time frame over which the integration takes place. Equation (4.60) therefore relates the equivalent damping ratio in terms of the parameters of the system and as such the equivalent damping can be found over the time period of the system ($t = \tau$) given the parameters of the system.

4.4.3 Fundamental Frequency with moving mass: Dunkerley's Equation

The Dunkerley's equation can be used to give the approximate value of the fundamental frequency of a composite system which considering only the first natural frequency can be written as (Rao, 2011):

$$\frac{1}{\omega_1^2} = \frac{1}{\omega_{11}^2} + \frac{1}{\omega_{22}^2} = \frac{1}{\omega_{11}^2} + a_{ij}m \tag{4.61}$$

where ω_1, ω_{11} and ω_{22} are the first natural frequency of the system with the moving mass, the first natural frequency of the beam and the first natural frequency of the moving mass attached to the beam respectively. Now a_{22} is the flexibility influence coefficient which is the deflection at point i due to a

load at point j. Here a_{ij} is defined as:

$$a_{ij} = s(t)^3 \frac{1}{3EI} \tag{4.62}$$

4.5 Results and Discussion

4.5.1 Numerical Example

In the 2011 Great East Japan Earthquake tall buildings in Tokyo were oscillating even thirty minutes after. One such building was the Shinjuku Mitsui Building which according to reports, had deflection at the top of almost two meters.

As an example consider the Shinjuku Mitsui Building modelled as a vertical cantilever beam fixed at the base. The properties of the beam are listed in Table 4.1. The beam had a natural vibration period of 6 seconds. Most mass damper system in structures are designed to be within a mass ratio (μ) range of $1 - 10\%$, so this will be used as the benchmark.

TABLE 4.1: Analysis parameters

Parameter	Symbol	Value
Height of beam	H	225 m
Material density of beam	ρ	7860 kg/m^3
Area	A	15.83 m^2
Mass of beam	M	2.8×10^8 kg
Elasticity of beam	E	1.47×10^{12} N/m^2
Moment of inertia of beam	I	19.95 m^4

The dimensionless stroke length (β) of the moving mass is given as

$$\beta = \frac{b}{H} \tag{4.63}$$

The parameters for the proposed damping system are chosen as $\mu = 0.01 - 0.1$ and $\beta = 1/10 - 1/2$. For all these cases $s_0 = 168.75$ m.

4.5.2 Case 1: Prescribed Motion of Moving Mass

The motion of the mass is prescribed as such given in Equation (4.11). For this ω_1 is first calculated for each case of μ for which the author lets $\omega_1 = \omega_1(s_0)$. This is shown in Table 4.2

For all the cases the primary structure is given an initial displacement $u_0 = 2$ m.

Numerical analysis is carried out using FEM where the beam was discretised into two hundred and twenty five identical elements. The inherent damping of the primary structure was chosen to be zero to clearly illustrate

TABLE 4.2: First natural frequency of system model

μ	Period τ (s)	$\omega_1(s_0)$ (rad/s)
0.01	5.944	1.057
0.03	6.047	1.039
0.05	6.148	1.022
0.08	6.289	0.999
0.10	6.385	0.984

the damping effect due the the damping system. Equation (4.39) is numerically integrated using Newmark Method. The dynamic responses at the top of the structure subjected to a moving mass are shown in Figures 4.4 - 4.8.

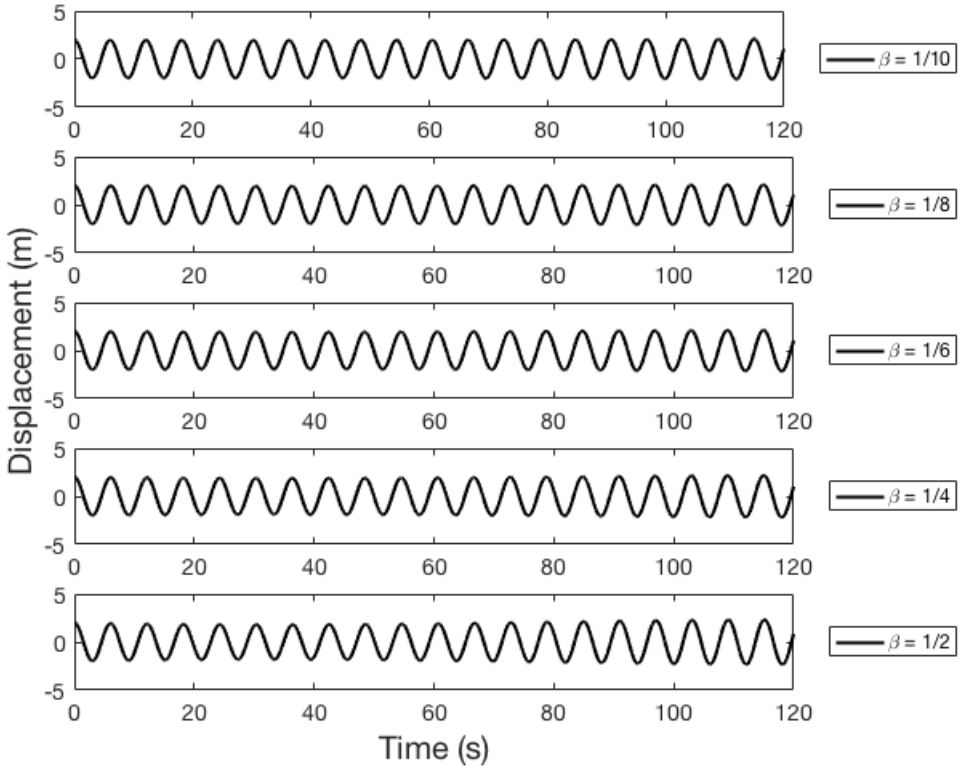

FIGURE 4.4: Dynamic response at the top for $\mu = 0.01$ for (a) $\beta = 1/10$ (b) $\beta = 1/8$ (c) $\beta = 1/6$ (d) $\beta = 1/4$ and (e) $\beta = 1/2$

From these we see there was no visible damping effect for the case of the small mass ($\mu = 0.01$) for short stroke lengths, but as the stroke length increases we notice more visible damping effect. This is also true for an increase in mass ratio as there were visible damping effects for the other cases of mass ratio.

Additionally, for the cases of the larger mass ratios and longer stroke lengths, the results show that at some point the system experiences no damping effect and instead began amplifying the primary structure. This is as a

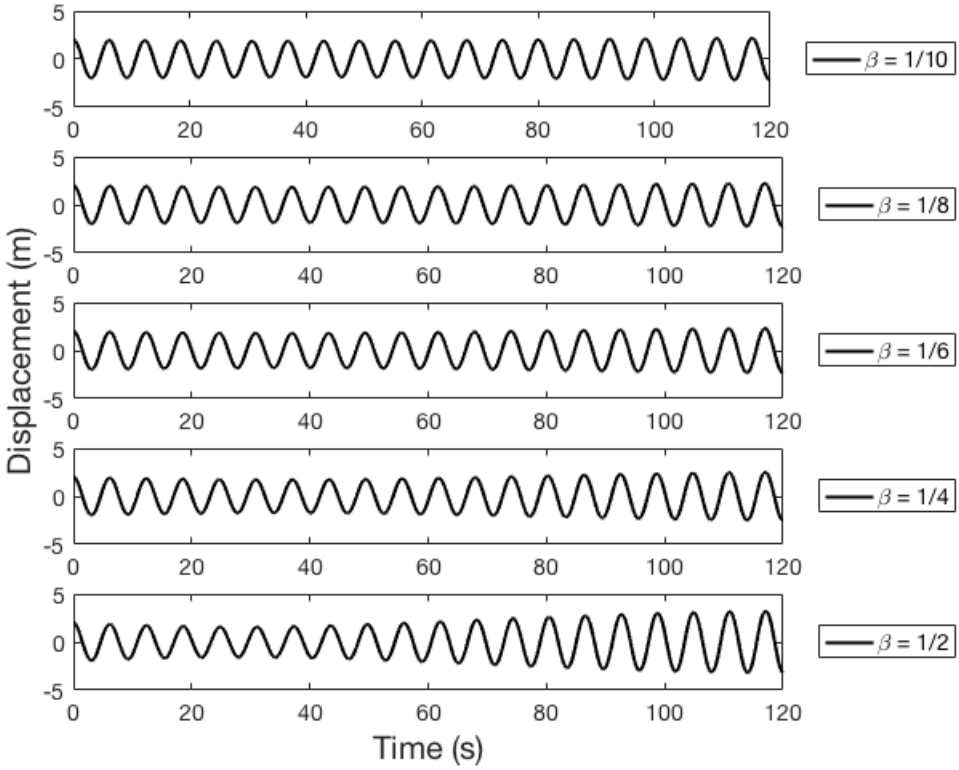

FIGURE 4.5: Dynamic response at the top for $\mu = 0.03$ for (a) $\beta = 1/10$ (b) $\beta = 1/8$ (c) $\beta = 1/6$ (d) $\beta = 1/4$ and (e) $\beta = 1/2$

result of the fixed motion of the moving mass along the structure causing a phase shift in each cycle. For example, the dynamic response of the system for one cycle and the motion of the damping system is shown in Figure 4.9 , for the case of $\mu = 0.1$ and $\beta = 1/2$. From this we see position of the moving mass is slightly below that of the starting position at time $t = 0$. Which means the moving mass is slightly ahead of the primary structure and this is as a result of an increase in the time period of the structure. This means that the system is now experiencing phase shift and this phase shift, while it may be insignificant in one cycle, if the moving mass continue with fixed motion the phase shift will continue to change until the system no longer experiences damping effect. At that point the phase shift $\psi = \pi/2$ and from this point forward the system will experience amplification effect.

4.5.3 Case 2: Synchronised Mass Motion

As mentioned above, a continuous fixed motion of the moving mass will lead to a phase shift in the system which then makes the damping system no longer effective after some point. As such it is vital for the moving mass to be monitored and constantly adjusted so as to ensure continuous damping of the structure. In order for this to happen, the phase shift between the

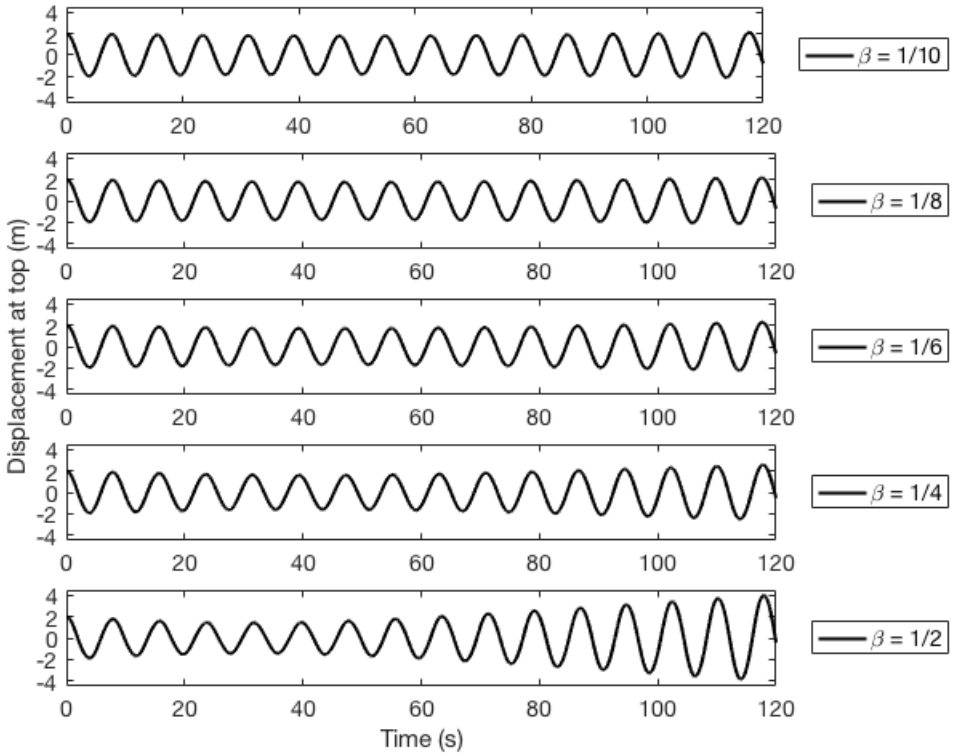

FIGURE 4.6: Dynamic response at the top for $\mu = 0.05$ for (a) $\beta = 1/10$ (b) $\beta = 1/8$ (c) $\beta = 1/6$ (d) $\beta = 1/4$ and (e) $\beta = 1/2$

moving mass and the response of the primary structure will need to be as close as possible to zero and should never exceed $\pi/2$.

A simple preliminary feedback control system is presented below. Since the phase shift at the end of one cycle is not so significant, to save on monitoring and readjusting time the feedback system can monitor the position of the moving mass and readjust at the end of each cycle (such as for this case presented we readjust when displacement of primary structure is positive and velocity is zero). If at the end of the cycle depending on whether the motion of moving mass is ahead or behind the motion of the primary structure, the velocity of the moving mass is then adjusted in order to minimise the phase shift. The results for all the cases of μ and for longest stroke length of $\beta = 1/2$ are shown in Figures 4.10 - 4.14.

This feedback and readjustment method is quite effective and produced consistent damping effect throughout the extended time period. The damping ratio (ζ) is calculated using the logarithmic decrement

$$\zeta = \frac{1}{2\pi} \ln \frac{u_0}{u_1} \tag{4.64}$$

where u_1 is the amplitude at the top at time period τ. The results for these are shown in Figure 4.15.

From the results we see the concept is capable of producing substantial

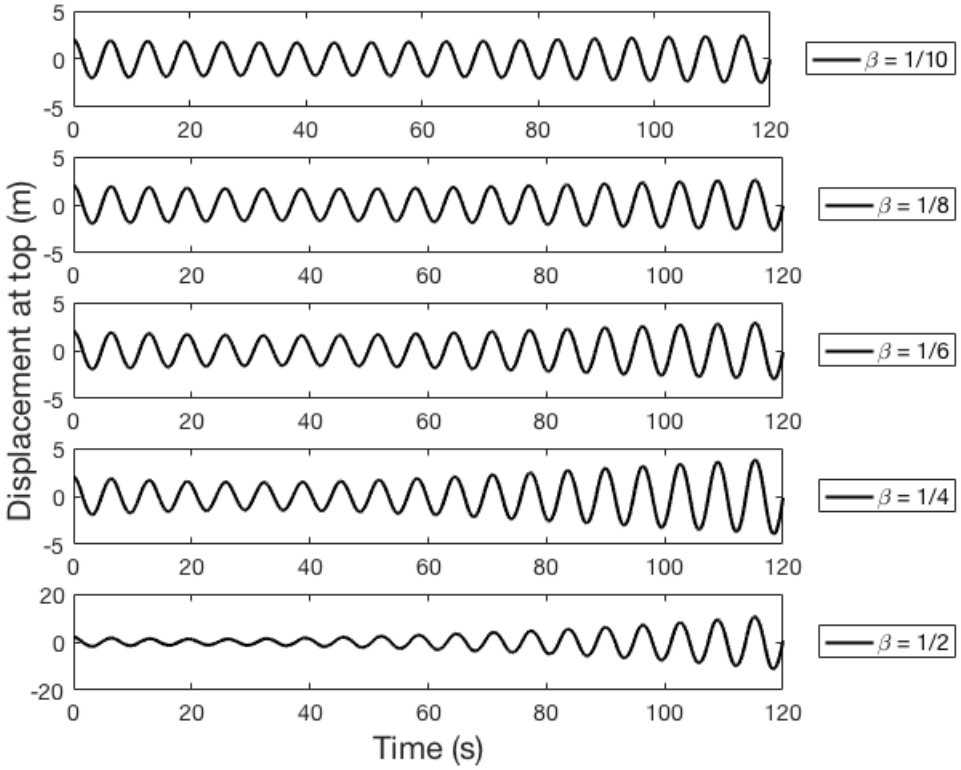

FIGURE 4.7: Dynamic response at the top for $\mu = 0.08$ for (a) $\beta = 1/10$ (b) $\beta = 1/8$ (c) $\beta = 1/6$ (d) $\beta = 1/4$ and (e) $\beta = 1/2$

damping effect, however it is also seen that this method becomes less effective as the mass ratio increases. This highlights the importance of the need for continuous feedback and adjustment of the moving mass, in particular for the cases of larger mass ratios and longer stroke lengths.

4.5.4 Verification with Equivalent Damping

The equivalent damping can be found using Equation (4.47) given we know certain parameters of the system. Consider a moving mass moving with motion given by Equation (4.11). The beam motion is such as given by Equation (4.49). In order to arrive at an analytical solution certain assumptions have to be made. The author assumes the natural frequency of the system is fixed and is equal to the natural frequency of the system at time $t = 0$ ($\omega_1 = \bar{\omega} = \omega(s_0)$). This can be found using Equation (4.61). It should be noted that this value is always smaller than the actual value (Rao, 2011). Furthermore the author assumes the deflections at the top of the beam are small as such the deflection can be assumed for an initial deflection $u_0 = 2$m as:

$$U(y) = 2\left[1 - cos\left(\frac{\pi y}{2H}\right)\right] \tag{4.65}$$

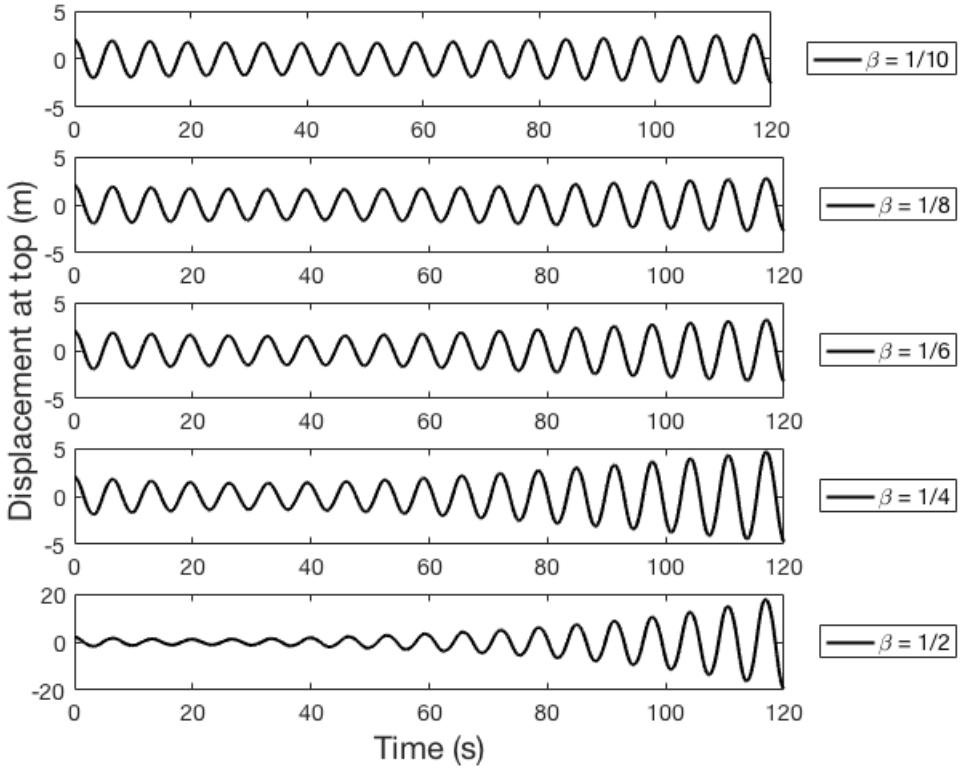

FIGURE 4.8: Dynamic response at the top for $\mu = 0.10$ for (a) $\beta = 1/10$ (b) $\beta = 1/8$ (c) $\beta = 1/6$ (d) $\beta = 1/4$ and (e) $\beta = 1/2$

Using the above assumptions and the parameters from Section 4.5.2 the equivalent damping ratio was found integrating over the time period of the system ($t = \tau = \frac{2\pi}{\omega(s_0)}$). The results for the different stroke lengths and mass ratios are shown in Figure 4.16 - 4.20.

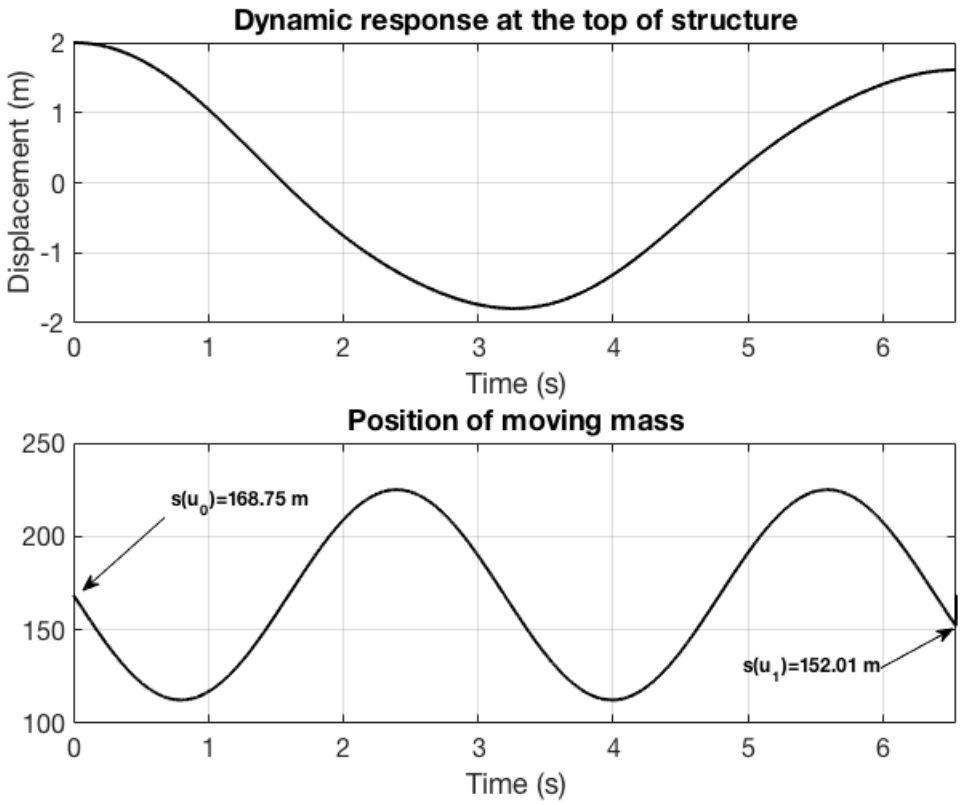

FIGURE 4.9: Dynamic response of structure and motion of mass for $\mu = 0.1$ and $\beta = 1/2$ for one cycle

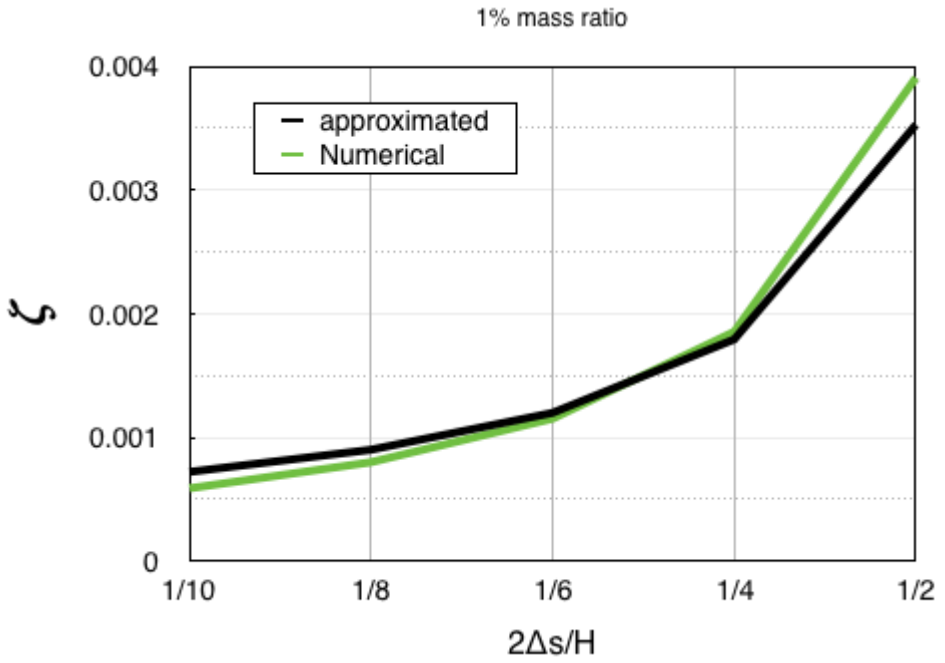

FIGURE 4.16: Comparison of the approximated equivalent damping ratio and the numerical damping ratio for $\mu = 1\%$

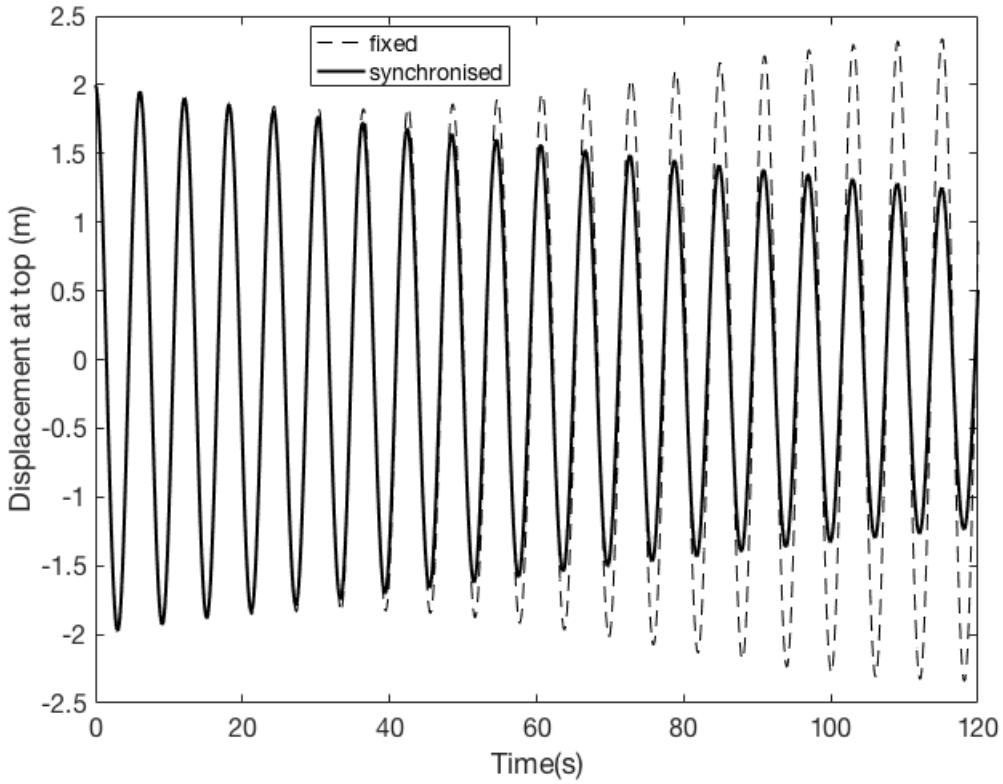

FIGURE 4.10: Dynamic response of structure with synchronised motion of damping system for $\mu = 0.01$ and $\beta = 0.5$

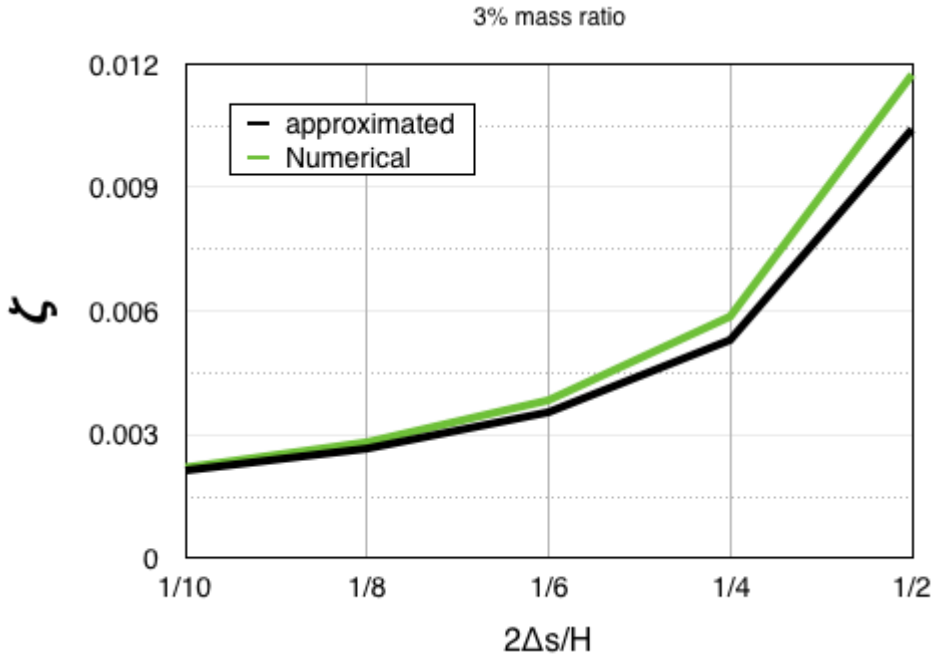

FIGURE 4.17: Comparison of the approximated equivalent damping ratio and the numerical damping ratio for $\mu = 3\%$

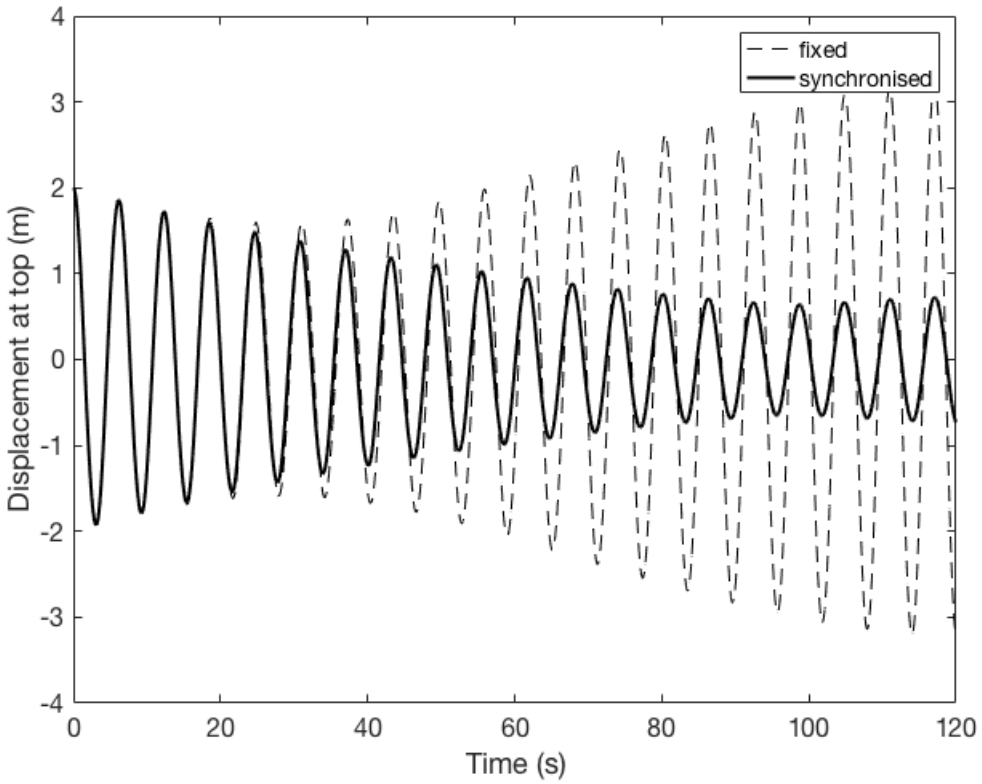

FIGURE 4.11: Dynamic response of structure with synchronised motion of damping system for $\mu = 0.03$ and $\beta = 0.5$

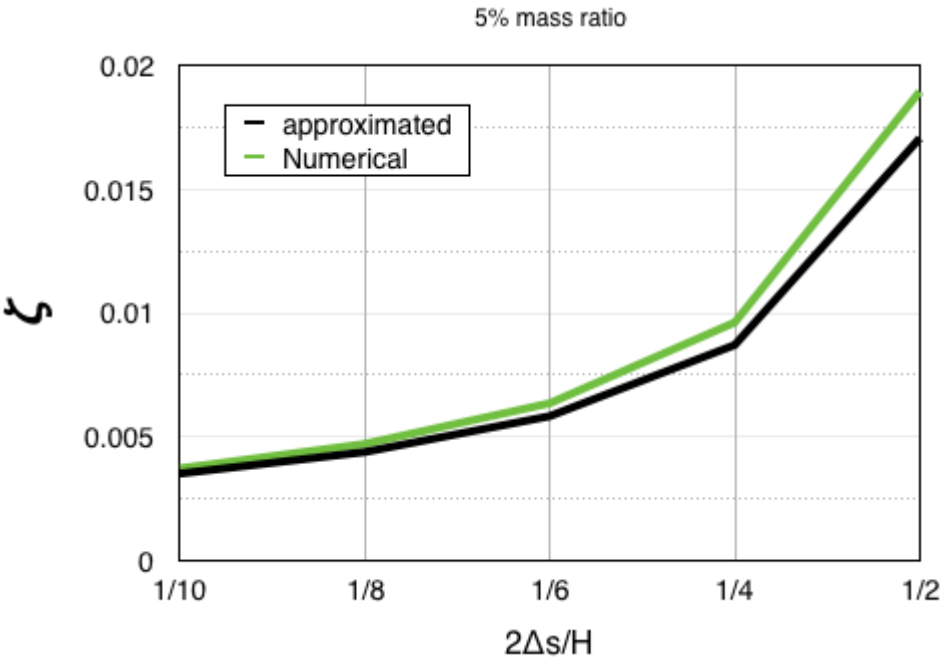

FIGURE 4.18: Comparison of the approximated equivalent damping ratio and the numerical damping ratio for $\mu = 5\%$

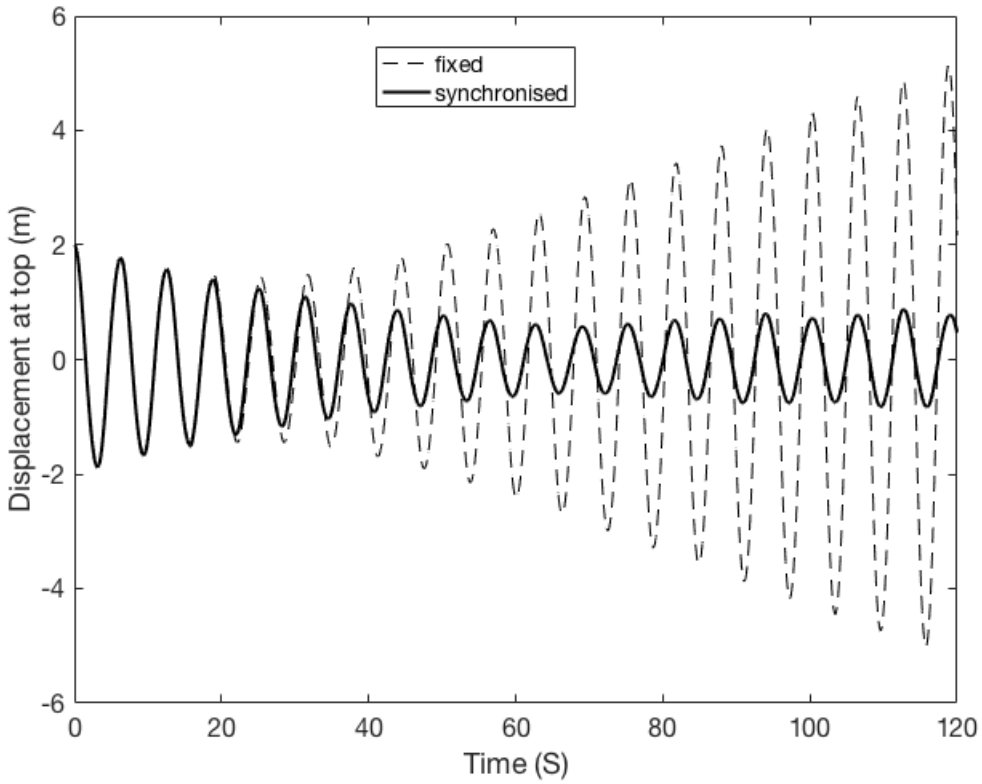

FIGURE 4.12: Dynamic response of structure with synchronised motion of damping system for $\mu = 0.05$ and $\beta = 0.5$

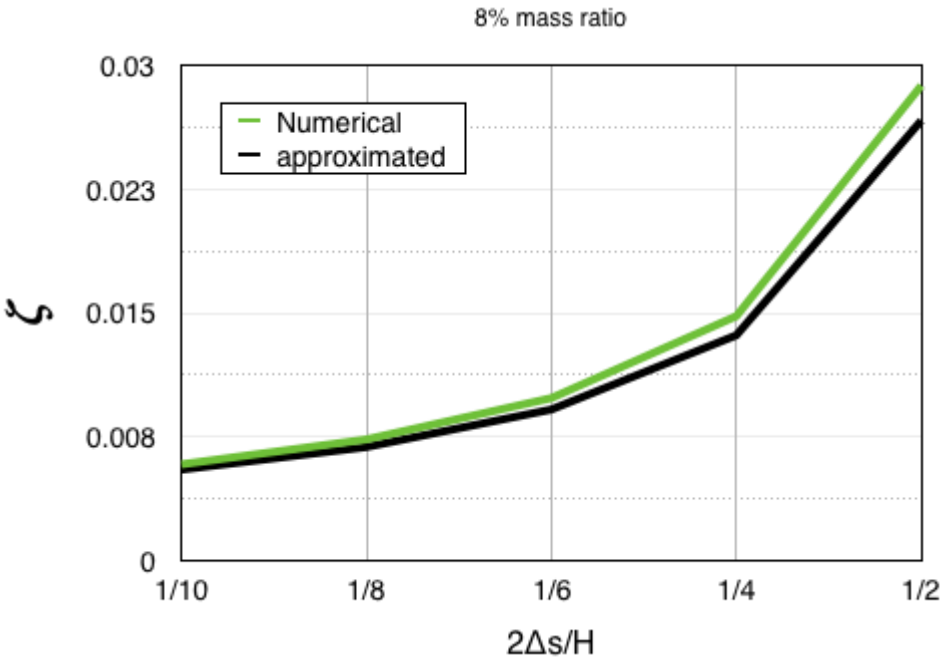

FIGURE 4.19: Comparison of the approximated equivalent damping ratio and the numerical damping ratio for $\mu = 8\%$

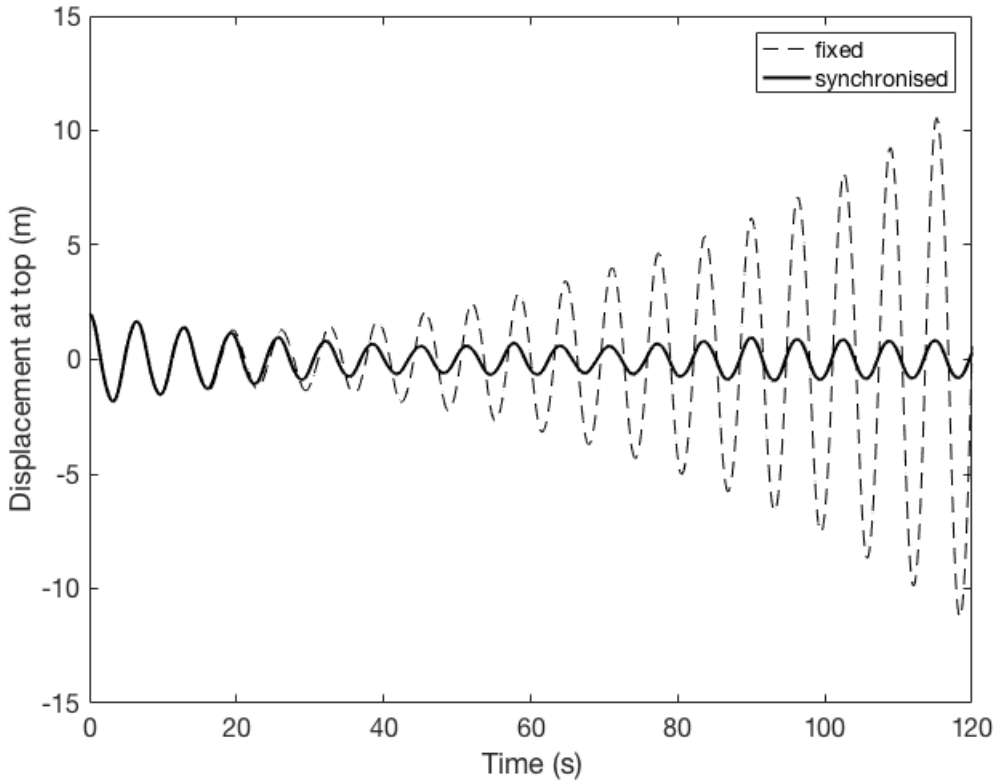

FIGURE 4.13: Dynamic response of structure with synchronised motion of damping system for $\mu = 0.08$ and $\beta = 0.5$

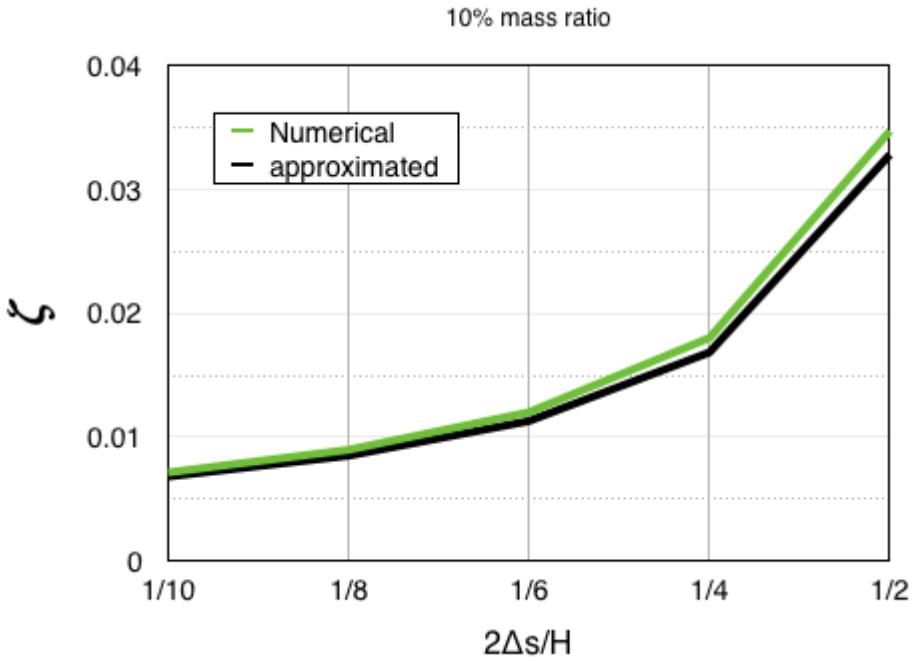

FIGURE 4.20: Comparison of the approximated equivalent damping ratio and the numerical damping ratio for $\mu = 10\%$

From the results the approximated equivalent damping ratio seems to

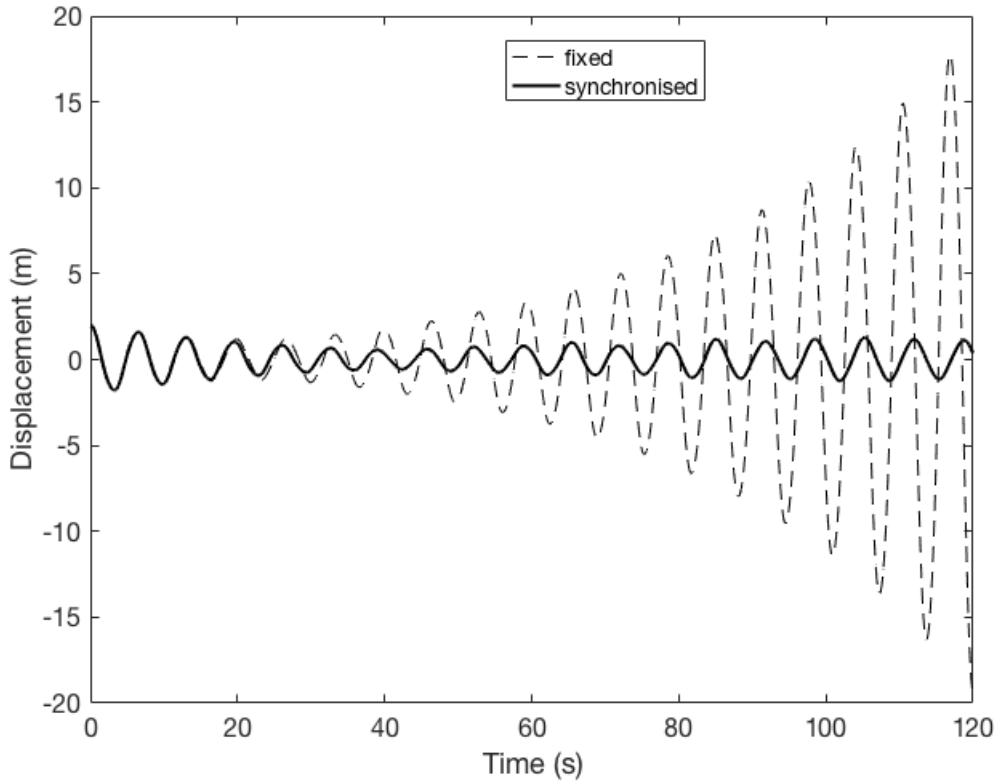

FIGURE 4.14: Dynamic response of structure with synchronised motion of damping system for $\mu = 0.1$ and $\beta = 0.5$

agree well with the numerical damping ratio for the specified mass ratios and stroke lengths.

4.5.5 Practical Implications

The concept presented in this chapter is an idea to attenuate long period oscillation of building structures, in particular in the event of large excitation, to reduce the response to an acceptable degree. This theory of damping measure is quite attractive, however at present technical limitations prevent this measure from being a practical concept for damping tall building structures. In particular the speed required of the moving mass is of concern. The peak speed of the moving mass as it relates to the dimensionless stroke length (β) is shown in Figure 4.21.

However, the concept as is, is quite feasible for long, thin and flexible structural systems such as beams, frames, etc. Especially if the motion of the structure is dominated by the lowest mode of vibration.

It is worth mentioning that the Coriolis effect generated by the moving mass can be enhanced. As mentioned in 'Motion of Moving Mass' section there are several parameters that influence the Coriolis effect, one of which is the degree of angular motion. As such we can enhance the effect as illustrated in Figure 4.22 . The damping system has multiple degrees of freedom with

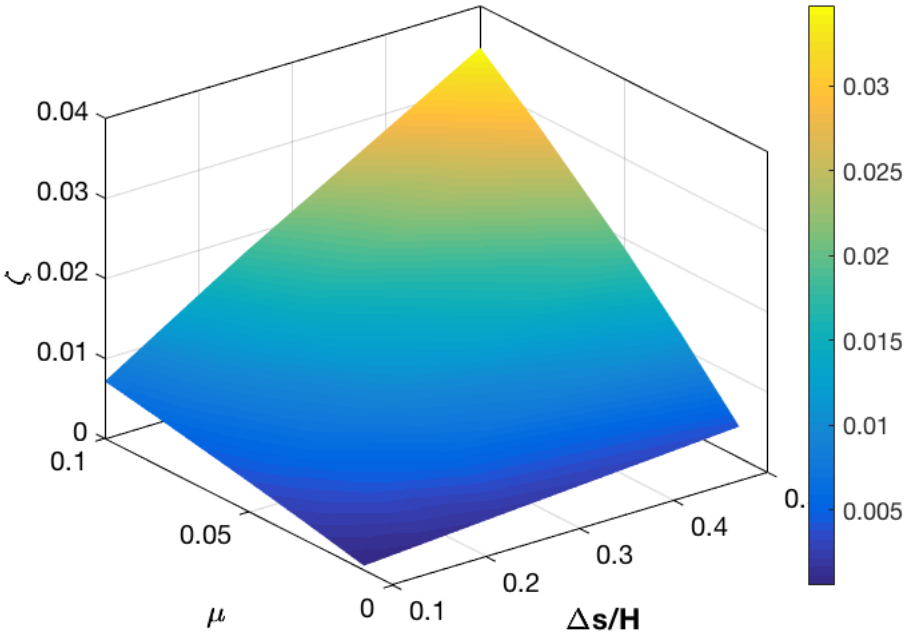

FIGURE 4.15: Effects of dimensionless stroke length (β) and mass ratio (μ) on the damping ratio (ζ) of the system for synchronised motion.

a moving mass translating along an axis with angular motion. The angular motion of the pendulum and the up-down motion of the mass is carefully synchronised with the motion of the primary structure to maximise damping effect.

One way to realise this is to have a driver located at the top of the structure moving laterally facilitating angular motion of the oscillating fixture about its pivot, while the moving mass translates along it (See Figure 4.23). It should be noted that this driver can be actively or passively driven. Additionally, the inertial properties of the driving mechanism and the oscillating fixture can add to the attenuating effect of the moving mass, much like a Tuned Mass Damper (TMD).

Another parameter that influences the Coriolis effect is the velocity of moving mass. Careful examination of the Coriolis component of Equation (4.8) reveals a positive velocity yields positive damping effect and a negative velocity yields negative damping effect. Since the motion of the moving mass is cyclic, this means in one cycle the system goes through alternating phase of damping and attenuation but with careful manoeuvring the period of damping is greater at the end of the cycle. However, if the velocity were to remain positive throughout the whole cycle, this would increase the overall damping effect. This is shown by having the primary structure having a pipe through it which allows the flow of fluid. For this case water-flow is used (See Figure 4.24). The basic idea is to attenuate the long period vibration of the primary structure using high speed water flow in the positive (up) direction.

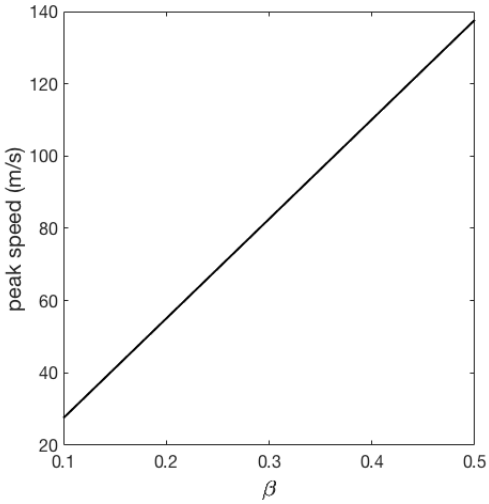

FIGURE 4.21: The peak speed of moving mass for each dimensionless stroke length β

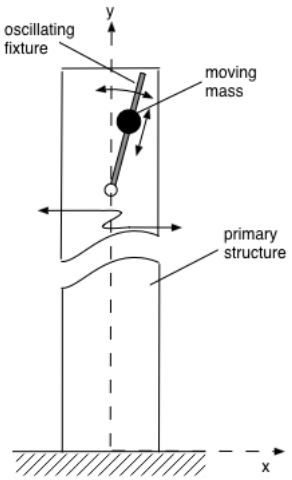

FIGURE 4.22: Illustration of the concept of a multiple-degree-of-freedom enhanced Coriolis effect damper

The previous moving finite element model is slightly altered to take into consideration the waterflow effect. The water is pumped upwards with a constant velocity. As such Equation (4.8) becomes:

$$\begin{aligned} &\int_0^H (A\rho\ddot{u} + EIu'''')dy \\ +\rho_f A_f &\int_0^H (\ddot{u} + 2\dot{s}\dot{u}' + \dot{s}^2 u'') = f_B(y,t) \end{aligned} \tag{4.66}$$

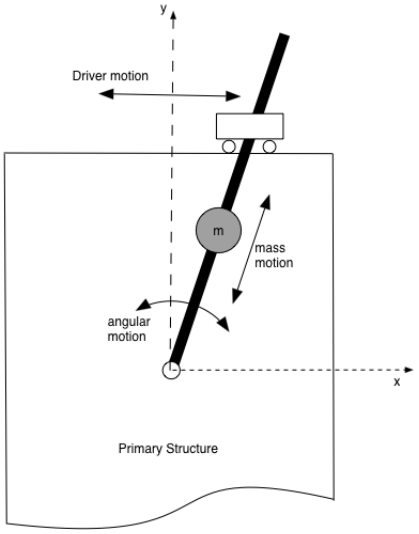

FIGURE 4.23: Example mechanism of a multiple-degree-of-freedom enhanced Coriolis effect damper

and Equations (4.36 - 4.38) becomes:

$$[m] = \rho_f A_f \int_0^H \begin{bmatrix} N_1^2 & 0 & 0 & N_1N_4 & 0 & 0 \\ 0 & N_2^2 & N_2N_3 & 0 & N_2N_5 & N_2N_6 \\ 0 & N_3N_2 & N_3^2 & 0 & N_3N_5 & N_3N_6 \\ N_4N_1 & 0 & 0 & N_4^2 & 0 & 0 \\ 0 & N_5N_2 & N_5N_3 & 0 & N_5^2 & N_5N_6 \\ 0 & N_6N_2 & N_6N_3 & 0 & N_6N_5 & N_6^2 \end{bmatrix} \tag{4.67}$$

$$[c] = 2\rho_f A_f \dot{s} \int_0^H \begin{bmatrix} 0 & 0 & 0 & 0 & 0 & 0 \\ 0 & N_2N_2' & N_2N_3' & 0 & N_2N_5' & N_2N_6' \\ 0 & N_3N_2' & N_3N_3' & 0 & N_3N_5' & N_3N_6' \\ 0 & 0 & 0 & 0 & 0 & 0 \\ 0 & N_5N_2' & N_5N_3' & 0 & N_5N_5' & N_5N_6' \\ 0 & N_6N_2' & N_6N_3' & 0 & N_6N_5' & N_6N_6' \end{bmatrix} \tag{4.68}$$

$$[k] = \rho_f A_f \dot{s}^2 \int_0^H \begin{bmatrix} 0 & 0 & 0 & 0 & 0 & 0 \\ 0 & N_2N_2'' & N_2N_3'' & 0 & N_2N_5'' & N_2N_6'' \\ 0 & N_3N_2'' & N_3N_3'' & 0 & N_3N_5'' & N_3N_6'' \\ 0 & 0 & 0 & 0 & 0 & 0 \\ 0 & N_5N_2'' & N_5N_3'' & 0 & N_5N_5'' & N_5N_6'' \\ 0 & N_6N_2'' & N_6N_3'' & 0 & N_6N_5'' & N_6N_6'' \end{bmatrix} \tag{4.69}$$

For this case ρ_f, A_f and $\dot{s}$ are the density of the fluid, area of cross-section of the pipe and velocity of fluid flow respectively.

We integrate these over the height of the primary structure to get for each element

$$[m] = \frac{\rho_f A_f h}{420} \begin{bmatrix} 140 & 0 & 0 & 70 & 0 & 0 \\ 0 & 156 & 22h & 0 & 54 & -13h \\ 0 & 22h & 4h^2 & 0 & 13h & -3h^2 \\ 70 & 0 & 0 & 140 & 0 & 0 \\ 0 & 54 & 13h & 0 & 156 & -22h \\ 0 & -13h & -3h^2 & 0 & -22h & 4h^2 \end{bmatrix} \tag{4.70}$$

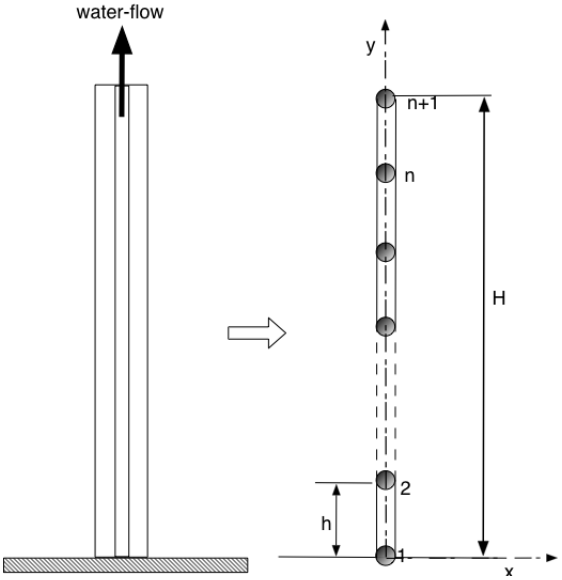

FIGURE 4.24: Simplified model of structure with water-flow through it and the finite element modelling

$$[c] = \frac{2\rho_f A_f \dot{s}}{60} \begin{bmatrix} 0 & 0 & 0 & 0 & 0 & 0 \\ 0 & -30 & 6h & 0 & 30 & -6h \\ 0 & -6h & 0 & 0 & 6h & -h^2 \\ 0 & 0 & 0 & 0 & 0 & 0 \\ 0 & -30 & -6h & 0 & 30 & 6h \\ 0 & 6h & h^2 & 0 & -6h & 0 \end{bmatrix} \tag{4.71}$$

$$[k] = \frac{\rho_f A_f \dot{s}^2}{30h} \begin{bmatrix} 0 & 0 & 0 & 0 & 0 & 0 \\ 0 & -25 & -\frac{300h}{11} & 0 & 25 & -300h \\ 0 & -300h & -225h^2 & 0 & 300h & h^2 \\ 0 & 0 & 0 & 0 & 0 & 0 \\ 0 & 25 & 300h & 0 & -25 & \frac{300h}{11} \\ 0 & -300h & h^2 & 0 & 300h & -225h^2 \end{bmatrix} \tag{4.72}$$

The result for water-flow with mass ratio 1% of the primary structure pumped at velocity 50 ms^{-1} is shown in Figure 4.25. The result shows a similar performance to that of moving mass with $\mu = 1/100$ and $\beta = 1/2$, having damping $\zeta = 0.016$, but with far less than half the maximum speed required to produce this effect. It is clear from the result the method of using high speed water-flow is more effective than sinusoidal motion of a solid mass driven at twice the frequency of the primary structure's oscillation. The extent of which will depend on the pumping capabilities i.e. the volume of water and velocity at which it is pumped.

4.6 Summary

In this study a new concept to control low frequency vibration in tall and thin structures using mass motion in the longitudinal direction was proposed. Unlike conventional concepts, the motion of the mass induces Coriolis force

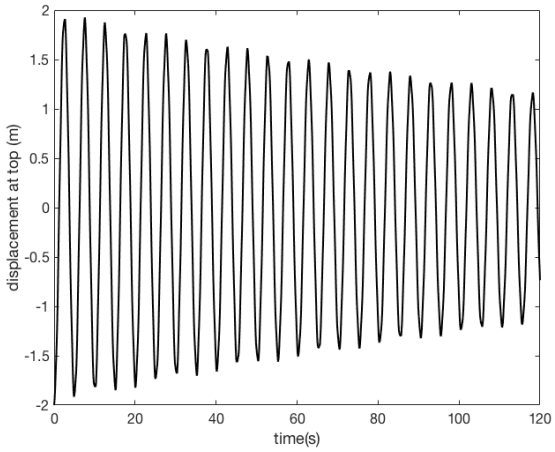

FIGURE 4.25: Dynamic response using water-flow ($\mu = 1/100$ and $\dot{s} = 50\ \mathrm{ms}^{-1}$).

and with the appropriate motion reduces the vibration of the primary structure. The system was modelled using finite element method (FEM) and the dynamic response of the system was analysed. The analysis shows the concept produces substantial damping effect and this effect increases with increases in the mass and degree of motion of the moving mass. Furthermore, in order to effectively attenuate the structure for an extended period of time, the motion of the moving mass needs to be constantly monitored and adjusted so as to keep the phase shift in the system to a minimum. The Coriolis effect can also be enhanced by increasing the degree of angular motion of the moving mass or by it having always-positive velocity. This idea of enhancing the damping effect was introduced and briefly discussed using multiple-degree-of-freedom Coriolis damper (angular motion and translation of moving mass) and also using a constant positive velocity fluid-flow as examples.

This concept of using Coriolis effect to attenuate structures can be applied to any long-period structure that has rotational component where Coriolis effect can be induced. The proposed concept as presented should be considered as a first step to develop an alternative method for control of vibration in flexible structures in the event of large excitations. This concept is particularly attractive for structures with low inherent damping and limited lateral space, and can be applied to a wide variety of structures which includes flexible-type, pendulum-type and rolling-type structures.

Future works will in detail look into enhancing damping effect and will investigate the consideration of other modes of vibration.

Chapter 5

Ship Roll Reduction Using Water-flow Induced Coriolis Effect

5.1 Introduction

In the previous chapter (Chapter 4), it mentioned about the alternation of the Coriolis effect of a cyclic motion of a moving mass through a beam structure and how constant motion away from the pivot would produce a much better overall effect in a cycle. It also explored the concept of using a constant positive flow through the structure. In this chapter, the author builds on the idea and apply it to rolling structures, more specifically ships, where the access to water makes the concept very viable and practical. As such, this chapter proposes and investigates the method of reducing roll response of a ship by inducing Coriolis effect using water-flow in the radial direction of the vessel. The correlations between the velocity and volume of water-flow and the reduction of roll response is quantitatively studied.

5.2 Problem formulation

In this section the equations of the coupled motions of rolling of a ship and fluid flow through the proposed stabilising system are illustrated.

5.2.1 Parametric Roll of Ship

The parametric roll of a ship can be modelled as a single-degree-of-freedom (SDOF) system as given by the popular equations:

Free Roll:

$$(I_{44} + A_{44})\,\ddot{\phi} + B_{44}\dot{\phi} + C_{44}\sin\phi = 0 \tag{5.1}$$

Excited Roll:

$$(I_{44} + A_{44})\,\ddot{\phi} + B_{44}\dot{\phi} + C_{44}\sin\phi = M_w \tag{5.2}$$

where I_{44} is ship inertia, A_{44} is added mass, B_{44} is the damping in the rolling direction, C_{44} is the restoring moment. For simplicity it is very common to assume these parameters to be constant (Himeno, 1981). M_w is the external excitation by the waves. Also $\dot{()}$ represents a derivative with respect to time.

For the case of this study a Ro-Ro ship is considered to show the application of the proposed concept as these vessels are quite prone to capsizing. The parameters for this is given in Chapter 3 in Table 3.1.

In this paper the ship will be excited by regular beam waves modelled as harmonic excitation. Also the nonlinearity in the restoring moment and the damping are neglected.

5.2.2 Coupled Effect of Fluid Flow

The coupled effect due to water-flow induced Coriolis effect is introduced.

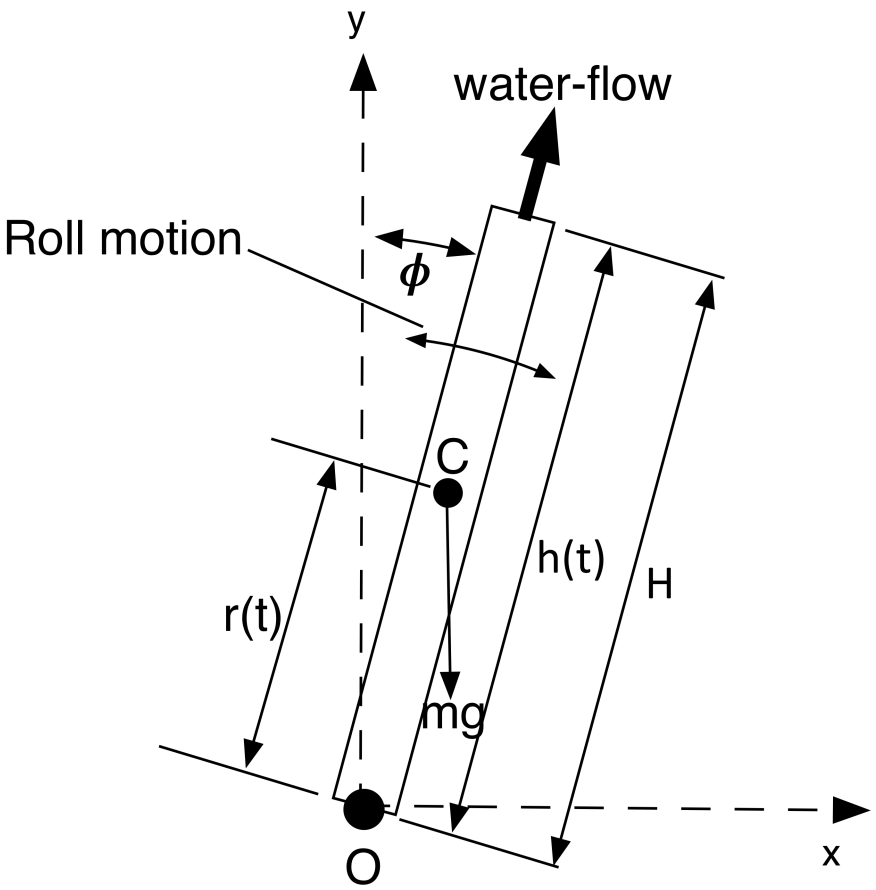

FIGURE 5.1: Illustration of the water-flow coupled effect

Figure 5.1 shows the water flowing through the channels while the ship experiences roll motion. The equations of motion for the effects of the water-flow were derived using Lagrangian mechanics.

Consider the water-flow with a mass m with pivot at O through the channel as shown in Figure 5.1. The centre of mass C is located at a distance $r(t)$ from the pivot, where $r(t)$ is half the height of the water-flow $h(t)$. The set

of generalised coordinates are the angular displacement ϕ of $\bar{OC}$ from the y-axis, and the radial height of the centre of mass C of the fluid from the pivot O.

The kinetic energy (T)

$$T = \frac{1}{2}m\dot{r}^2 + \frac{1}{2}mr^2\dot{\phi}^2 \tag{5.3}$$

The potential energy (V)

$$V = mgr\cos\phi \tag{5.4}$$

Using Lagrangian and the Euler-Lagrange equation and considering only the ϕ coordinate since we are only concerned with the roll motion,

$$L = T - V \tag{5.5}$$

$$\frac{d}{dt}\left(\frac{\partial L}{\partial \dot{\phi}}\right) - \frac{\partial L}{\partial \phi} = 0 \tag{5.6}$$

This gives

$$mr^2\ddot{\phi} + 2mr\dot{r}\dot{\phi} - mgr\sin\phi = 0 \tag{5.7}$$

Therefore Equation 5.1 for free roll becomes

$$\left(I_{44} + A_{44} + J\right)\ddot{\phi} + \left(B_{44} + 2mr\dot{r}\right)\dot{\phi} + \left(C_{44} - mgr\right)\sin\phi = 0 \tag{5.8}$$

and Equation 5.2 for excited roll becomes

$$\left(I_{44} + A_{44} + J\right)\ddot{\phi} + \left(B_{44} + 2mr\dot{r}\right)\dot{\phi} + \left(C_{44} - mgr\right)\sin\phi = M_w \tag{5.9}$$

where $J = mr^2$ is the inertia of the water-flow.

5.2.3 Non-dimensionalised Equations of Motion

The equations of motion are now presented in a generalised non-dimensional form. The variables are described as:

$$\tau = t\sqrt{\frac{C_{44}}{I_{44} + A_{44} + J}} \tag{5.10}$$

$$\tau = \sqrt{\frac{C_{44}}{I_{44} + A_{44} + J}} \tag{5.11}$$

$$\bar{r} = \frac{r}{KG} \tag{5.12}$$

Therefore we get

$$\dot{r} = \left(KG\sqrt{\frac{C_{44}}{I_{44} + A_{44} + J}} \right) \frac{\mathrm{d}\bar{r}}{\mathrm{d}\tau} \tag{5.13}$$

$$\dot{\phi} = \left(\sqrt{\frac{C_{44}}{I_{44} + A_{44} + J}} \right) \frac{\mathrm{d}\phi}{\mathrm{d}\tau} \tag{5.14}$$

$$\ddot{\phi} = \left(\sqrt{\frac{C_{44}}{I_{44} + A_{44} + J}} \right) \frac{\mathrm{d}^2\phi}{\mathrm{d}\tau^2} \tag{5.15}$$

Substituting Equations 5.13 - 5.15 into Equations 5.8 and 5.9, rearranging and letting

$$\alpha = \frac{1}{C_{44}} \tag{5.16}$$

we get

Free Roll:

$$\frac{\mathrm{d}^2\phi}{\mathrm{d}\tau^2} + \left(B_{44}\alpha\dot{\tau} + 2m\bar{r}\alpha\dot{\tau}KG^2\frac{\mathrm{d}\bar{r}}{\mathrm{d}\tau} \right) \frac{\mathrm{d}\phi}{\mathrm{d}\tau} + (1 - mg\bar{r}\alpha KG)\sin\phi = 0 \tag{5.17}$$

Excited Roll:

$$\frac{\mathrm{d}^2\phi}{\mathrm{d}\tau^2} + \left(B_{44}\alpha\dot{\tau} + 2m\bar{r}\alpha\dot{\tau}KG^2\frac{\mathrm{d}\bar{r}}{\mathrm{d}\tau} \right) \frac{\mathrm{d}\phi}{\mathrm{d}\tau} + (1 - mg\bar{r}\alpha KG)\sin\phi = M_w\alpha \tag{5.18}$$

Taylan (Taylan, 2000) found the external excitation M_w as

$$M_w = \omega^2\alpha_m \left(I_{44} + A_{44}\right)\cos\left(\omega_e t\right) \tag{5.19}$$

where ω_e is the frequency of encounter and α_m is the maximum wave slope.

To find ship inertia I_{44} use Weiss formula

$$i = \sqrt{\frac{I_{44}}{\Delta}} \approx 0.4B \tag{5.20}$$

Similar to (Surendran et al., 2005) the added mass A_{44} is assumed to be 20% of ship inertia. B_{44} in this case is such that the ship has a typical hydrodynamic roll damping of 10% and $C_{44} = \Delta gGM$. It should be noted that for fluid flow laminar flow was assumed.

5.3 Results and Discussion

In this section the results are presented. For the first assessment the vessel is investigated under free roll decay with and without the proposed stabilising system. The numerical analysis is carried out using the 4th Order Runge-Kutta Method and for comparison the approximated analytical results for the linearised model of the system is also presented. The system is analysed

for the cases of mass ratio (μ) range 0.01, 0.03 and 0.05 where

$$\mu = \frac{m}{\Delta} \tag{5.21}$$

and non-dimensional velocities of water-flow of 3 - 10.

5.3.1 Free Roll Decay

The system is observed under free roll decay with and without the system. The vessel is initially inclined at an angle $\phi_0 = 60^\circ$. For comparison the nonlinear model is linearised and an approximate analytical solution is also presented using equation

$$\phi(\tau) = \phi_0 \exp -\zeta\omega\tau\sqrt{\frac{I_{44} + A_{44} + J}{C_{44}}} \cos\left(\sqrt{1-\zeta^2}\omega\tau\sqrt{\frac{I_{44} + A_{44} + J}{C_{44}}} + \psi\right) \tag{5.22}$$

where ζ and ω are the damping ratio and natural frequency respectively of the system, assuming constant water-flow height ($h(t) = h(max)$) and ψ is the phase angle. Figures 5.2 - 5.10 show these results for the different cases of mass ratio and velocity.

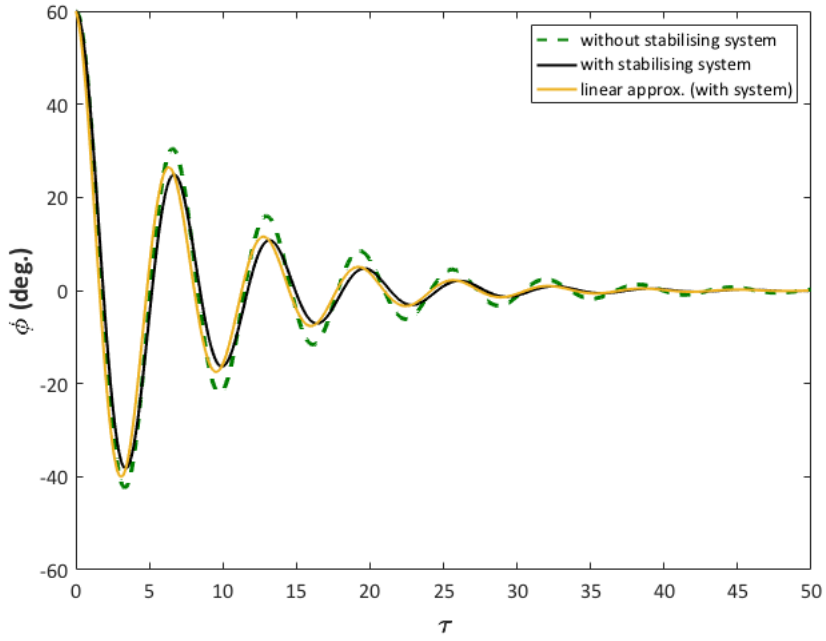

FIGURE 5.2: Free roll decay with and without the stabilising system and comparison with linear approximation of the model with stabilising system on for $\mu = 0.01$ and velocity = $20ms^{-1}$

From the results we see that the proposed stabilising system provides substantial damping effect which increases with the velocity and mass ratio of the water-flow. The system increased the damping ratio in the range of 0.140 - 0.720 for the smallest mass ratio and velocity to the largest mass ratio and

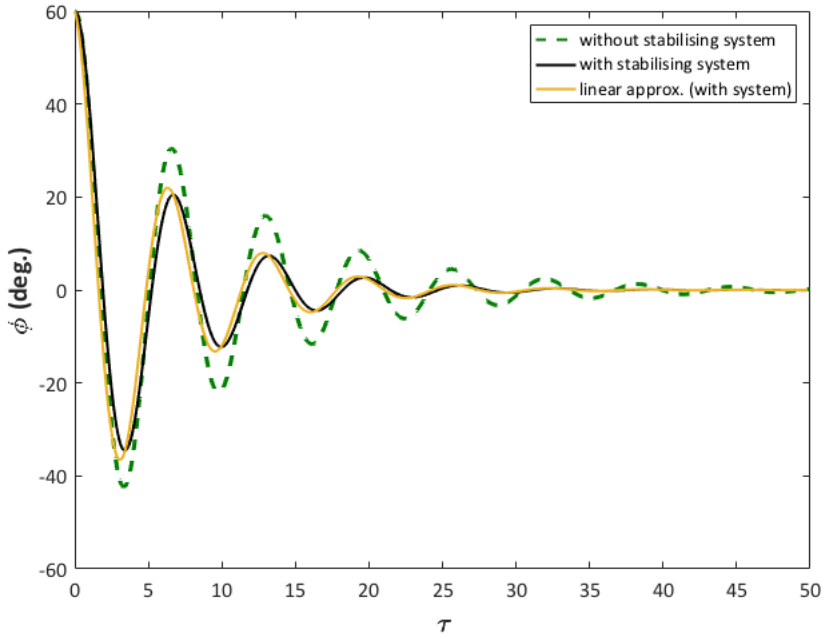

FIGURE 5.3: Free roll decay with and without the stabilising system and comparison with linear approximation of the model with stabilising system on for $\mu = 0.01$ and velocity = $40ms^{-1}$

velocity. Additionally we see that the numerical simulation is in good agreement with the linear analytical solution.

5.3.2 Excited Roll

The system is additionally observed under excited motion from beam waves modelled using Equation (5.19). For the entirety of the analysis a maximum wave slope $\alpha_m = 1/30$ was used and wave encounter frequency (ω_e)

$$\omega_e = \sqrt{\frac{C_{44} - mgr}{I_{44} + A_{44} + J}} \tag{5.23}$$

The parameters of the mass ratio and velocity are similar to those of the free roll decay analysis and for comparison the approximated linear steady-state results are presented using

$$\phi(\tau) = \frac{M_w \alpha}{\mathrm{Y}} \sin\left(\omega_e \tau \sqrt{\frac{I_{44} + A_{44} J}{C_{44}}} - \psi\right) \tag{5.24}$$

$$\mathrm{Y} = \sqrt{\left(1 - mg\bar{r}\alpha KG - \omega_e^2\right)^2 + \left(B_{44}\alpha\dot{\tau} + 2m\bar{r}KG^2\alpha\dot{\tau}^2 \frac{\mathrm{d}\bar{r}}{\mathrm{d}\tau}\right)\omega_e^2} \tag{5.25}$$

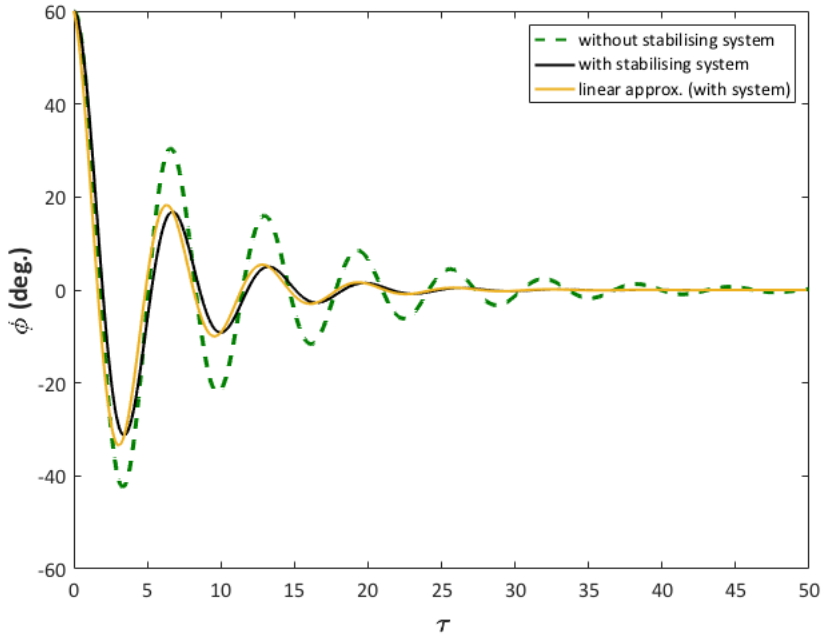

FIGURE 5.4: Free roll decay with and without the stabilising system and comparison with linear approximation of the model with stabilising system on for $\mu = 0.01$ and velocity = $60ms^{-1}$

Figures 5.11 - 5.19 show these results for the different cases of mass ratio and velocity.

5.3.3 Influence of Velocity and Volume of Water-flow: Comment On Limitations

As Coriolis force is dependent on the velocity of flow and the degree of angular motion, the efficiency of roll reduction using the proposed system is expected to increase with the velocity of fluid-flow. Additionally, the effect also increases with increased mass ratios. This is clearly illustrated in Figures 5.20 - 5.22. It shows that the response amplification operator (RAO) is severely reduced as the mass ratio and the velocity ratio is increased. As such the performance of the system is limited by the volume and velocity of fluid-flow which is dependent on the limitations of the pumping system.

Take for example the case of the Ro-Ro vessel presented earlier. For the extreme case of mass ratio 5% and non-dimensional velocity 10.45, using the parameters of the vessel presented in Table 3.1, this corresponds to velocity $\dot{r} = 60$ ms$^-$1 and mass $m = 4402$ t. Now for a channel with a ratio of height to Depth D equal to 1 this results in a required flow rate $Q \approx 3660$ m^{3}s^{-1}. A typical type of pump that would be used for this application would be centrifugal pumps and these are capable of handling flow rates even exceeding 10,000 gpm (Nelik, 1999). They have a general speed operation range of 5 - 200,000 gpm which is equivalent to a maximum approximate flow rate of 13 m^{3}s^{-1}. Which means just considering the flow rate capacity, at the present

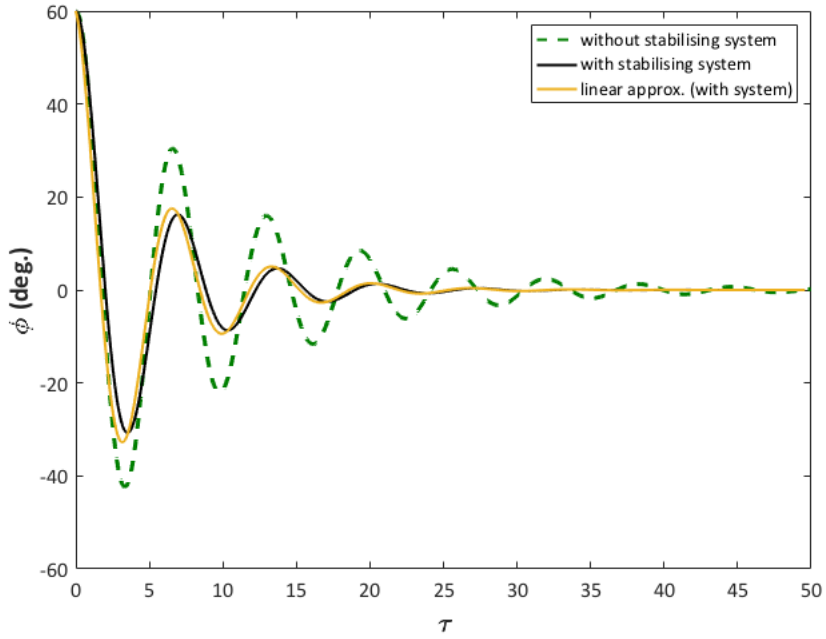

FIGURE 5.5: Free roll decay with and without the stabilising system and comparison with linear approximation of the model with stabilising system on for $\mu = 0.03$ and velocity = $20ms^{-1}$

moment with the available technology, this extreme case of ratios would be impractical for such a large size vessel. Therefore this may pose a problem for larger vessels, however this would be an effective concept for smaller vessels.

5.4 Summary

A new concept for roll reduction of ships has been presented and discussed in this chapter. The system uses water-flow in the radial direction to induce Coriolis effect to create a restoring moment. The system is modelled using two degrees of freedom, one degree for parametric roll of the ship and one degree for the water-flow. A Ro-Ro ship with a typical hydrodynamic roll damping of 10% is used as an example for the purpose of the analysis. The system is analysed under free roll decay and excited roll motion in beam waves for mass ratio 0.01 - 0.05 and velocities 20 ms^{-1} - 60 ms^{-1}. For comparison the approximated linear analytical results are also presented.

The results showed that the stabilising system can substantially increase the damping ratio (damping up to 72%) if the volume and velocity of water-flow are sufficiently large. And the results also showed a substantial reduction of roll angle (more than 71% reduction in roll angle).

The proposed stabilising system provides a fairly simple approach to reducing roll motion and requires no complicated control system, provides no hydrodynamic drag, operates in zero forward speed, no weight issues and

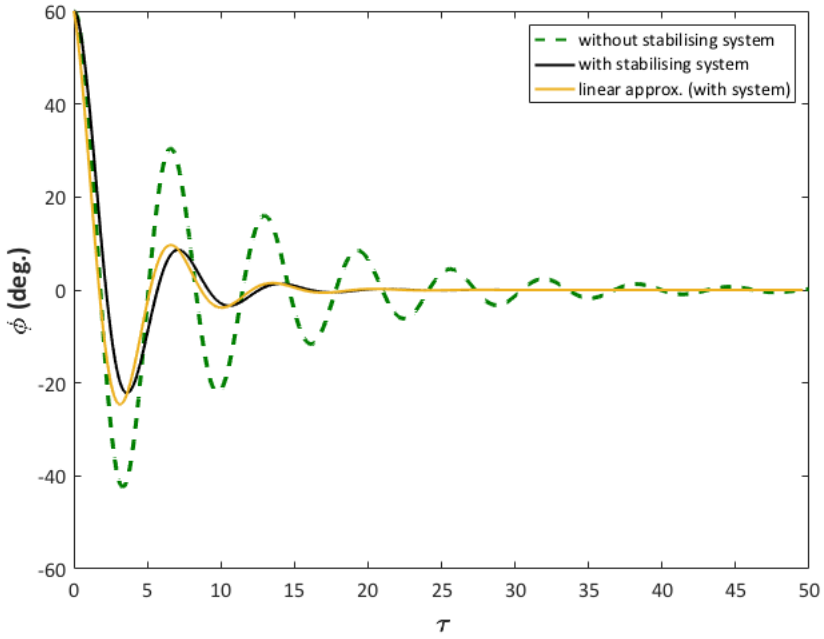

FIGURE 5.6: Free roll decay with and without the stabilising system and comparison with linear approximation of the model with stabilising system on for $\mu = 0.03$ and velocity = $40ms^{-1}$

should have no stability issues as the water flow will always generate positive damping effect and has no dependency on any external parameters other than the volume and velocity of water-flow, and the degree of roll. The system provides substantial roll reduction providing the pump capacity is available for the volume and velocity of water-flow. This is an attractive concept for roll reduction, in particular at present for smaller vessels as they would require smaller pump capacities.

The work presented here should be considered as a preliminary for designing an effective and practical system using fluid-flow to induce Coriolis effect to provide restoring moment.

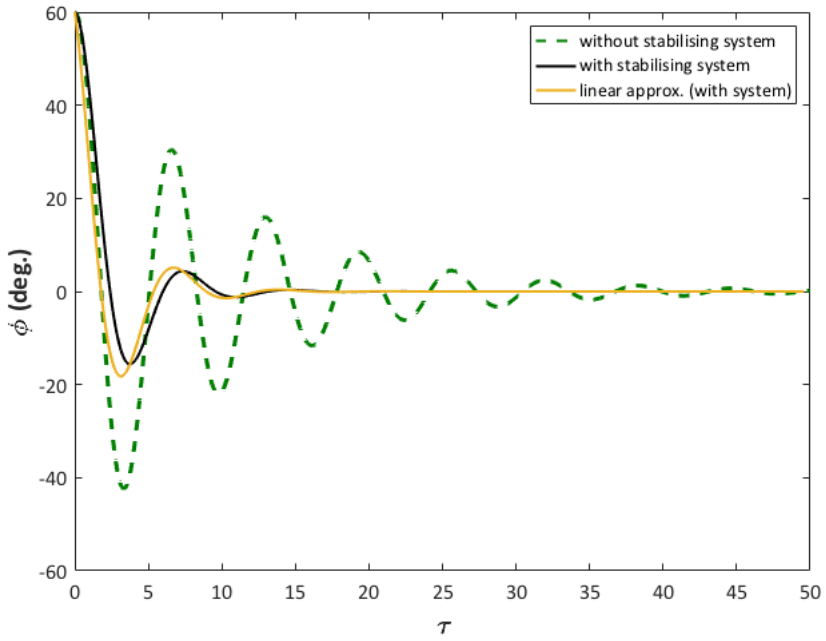

FIGURE 5.7: Free roll decay with and without the stabilising system and comparison with linear approximation of the model with stabilising system on for $\mu = 0.03$ and velocity = $60ms^{-1}$

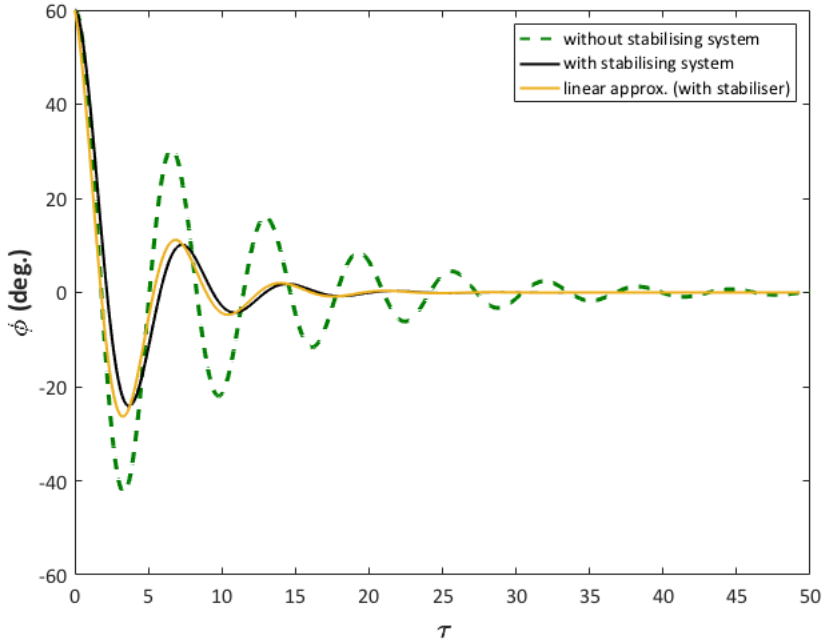

FIGURE 5.8: Free roll decay with and without the stabilising system and comparison with linear approximation of the model with stabilising system on for $\mu = 0.05$ and velocity = $20ms^{-1}$

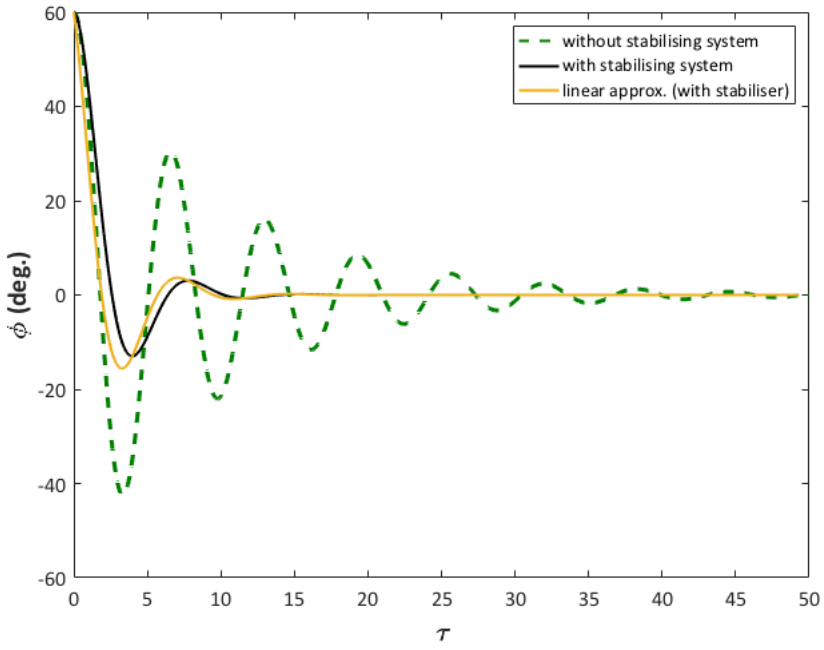

FIGURE 5.9: Free roll decay with and without the stabilising system and comparison with linear approximation of the model with stabilising system on for $\mu = 0.05$ and velocity = $40ms^{-1}$

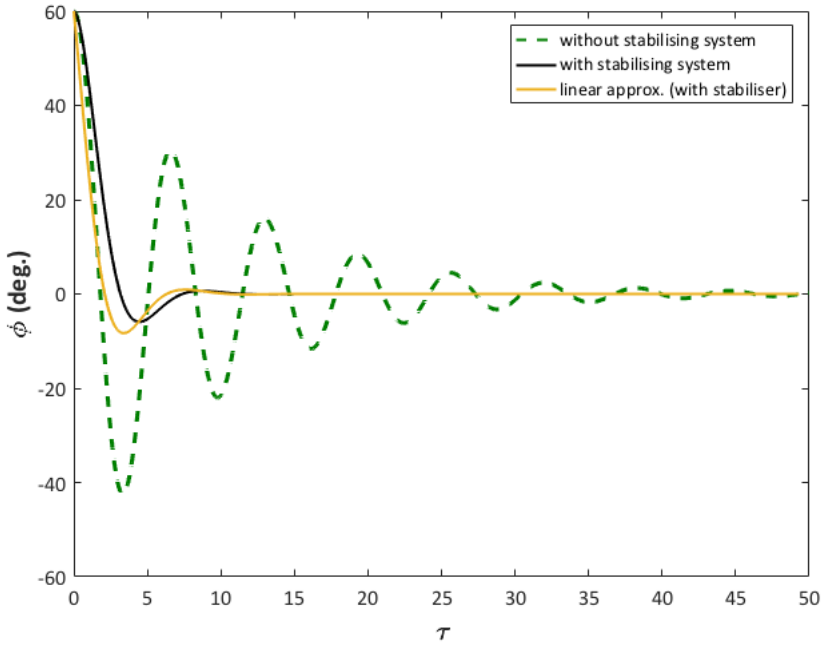

FIGURE 5.10: Free roll decay with and without the stabilising system and comparison with linear approximation of the model with stabilising system on for $\mu = 0.05$ and velocity = $60ms^{-1}$

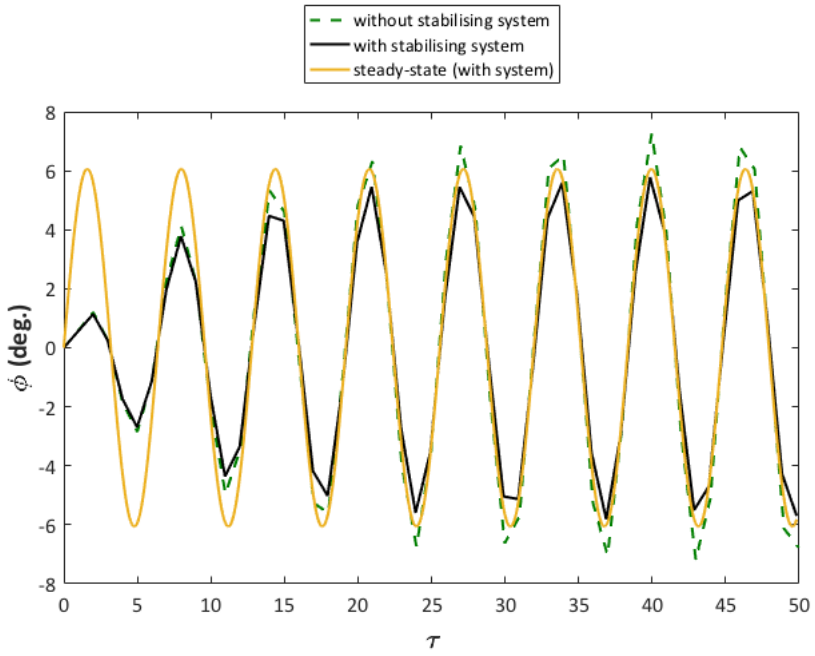

FIGURE 5.11: Excited roll motion with and without the stabilising system and comparison with linear steady-state approximation of the model with stabilising system on for $\mu = 0.01$ and velocity = $20ms^{-1}$

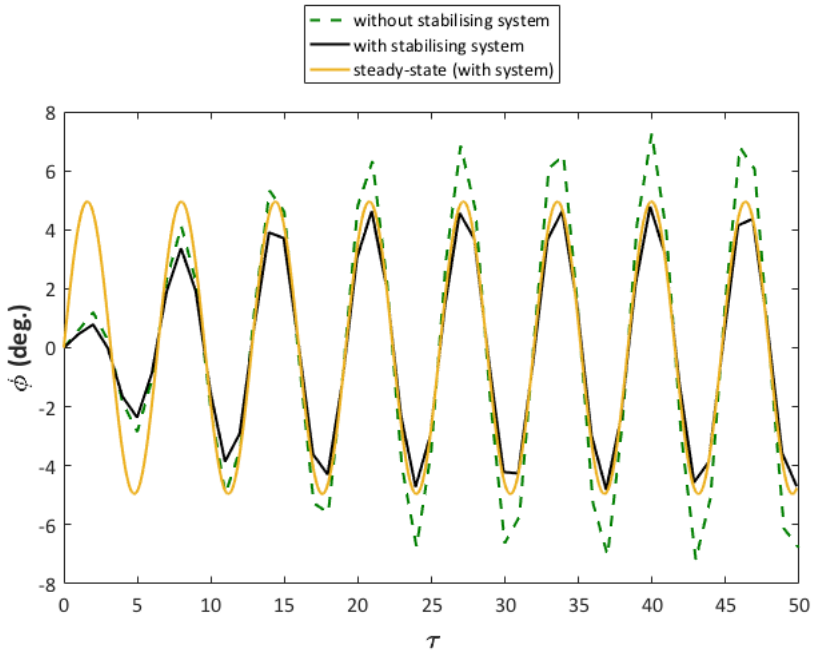

FIGURE 5.12: Excited roll motion with and without the stabilising system and comparison with linear steady-state approximation of the model with stabilising system on for $\mu = 0.01$ and velocity = $40ms^{-1}$

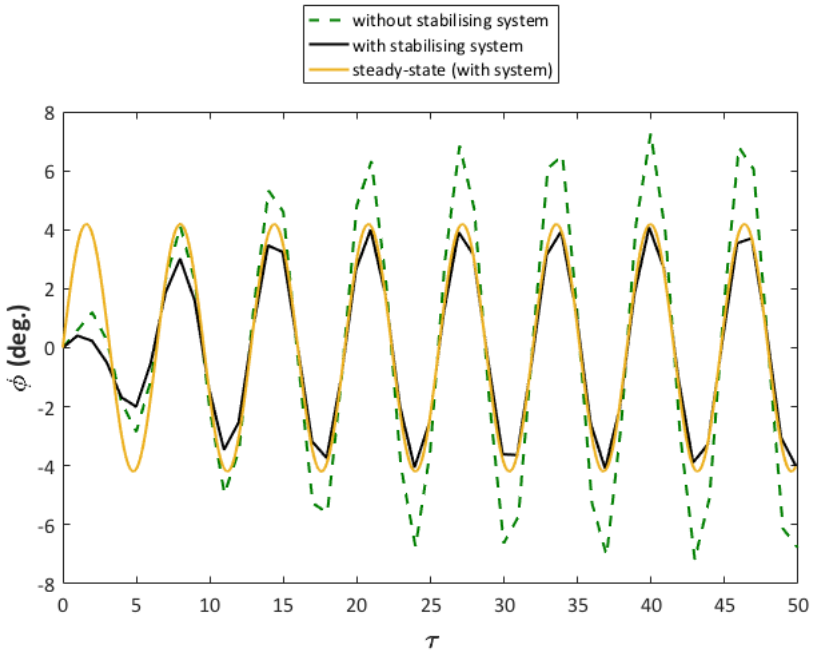

FIGURE 5.13: Excited roll motion with and without the stabilising system and comparison with linear steady-state approximation of the model with stabilising system on for $\mu = 0.01$ and velocity = $60ms^{-1}$

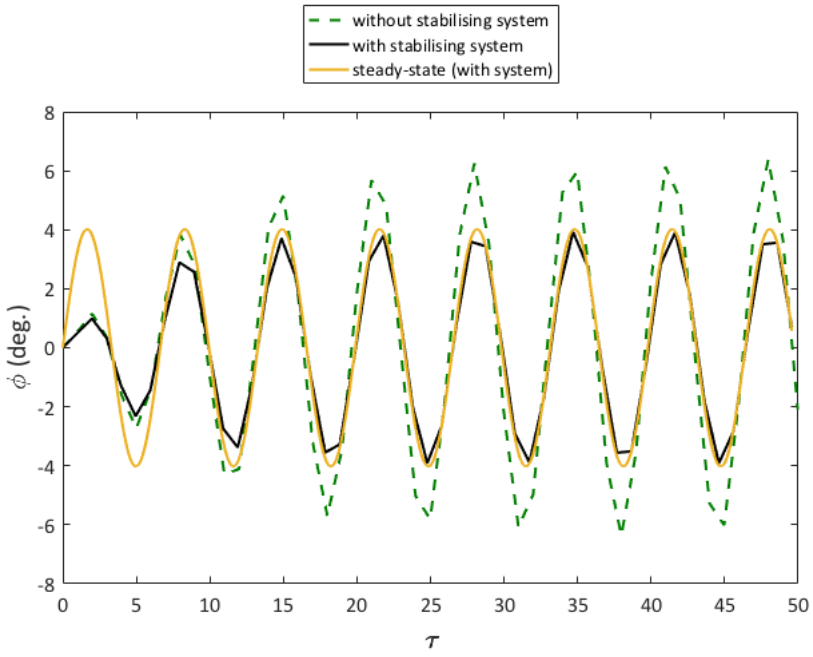

FIGURE 5.14: Excited roll motion with and without the stabilising system and comparison with linear steady-state approximation of the model with stabilising system on for $\mu = 0.03$ and velocity = $20ms^{-1}$

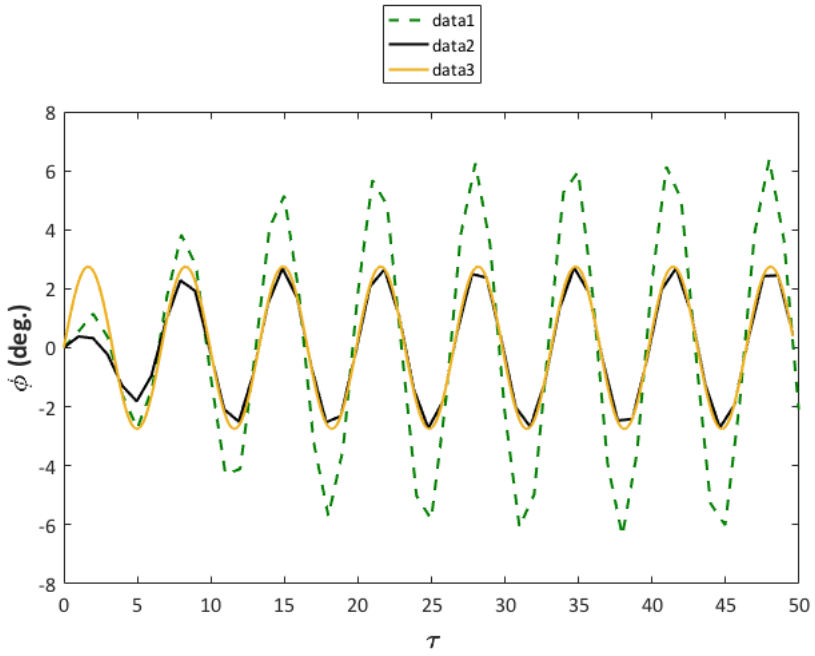

FIGURE 5.15: Excited roll motion with and without the stabilising system and comparison with linear steady-state approximation of the model with stabilising system on for $\mu = 0.03$ and velocity = $40ms^{-1}$

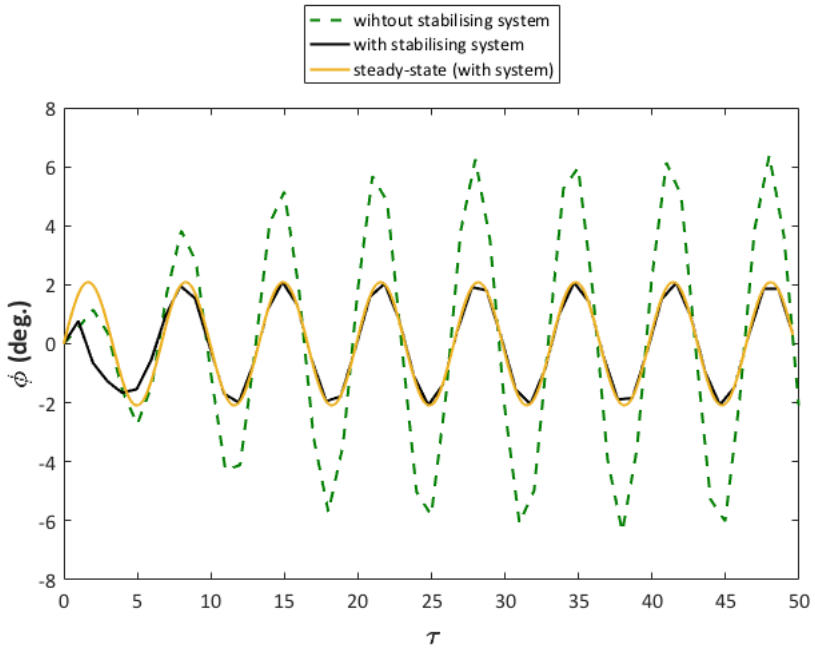

FIGURE 5.16: Excited roll motion with and without the stabilising system and comparison with linear steady-state approximation of the model with stabilising system on for $\mu = 0.03$ and velocity = $60ms^{-1}$

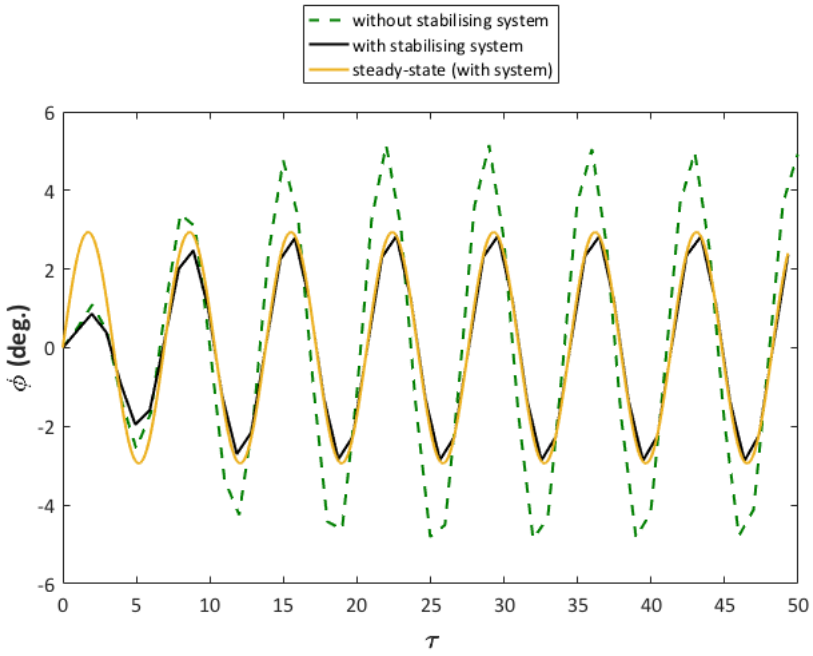

FIGURE 5.17: Excited roll motion with and without the stabilising system and comparison with linear steady-state approximation of the model with stabilising system on for $\mu = 0.05$ and velocity = $20ms^{-1}$

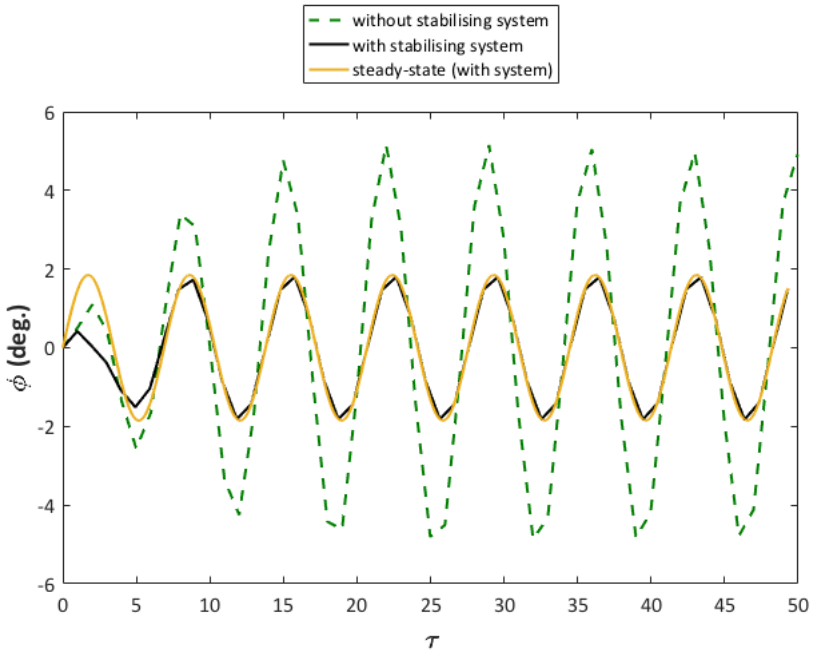

FIGURE 5.18: Excited roll motion with and without the stabilising system and comparison with linear steady-state approximation of the model with stabilising system on for $\mu = 0.05$ and velocity = $40ms^{-1}$

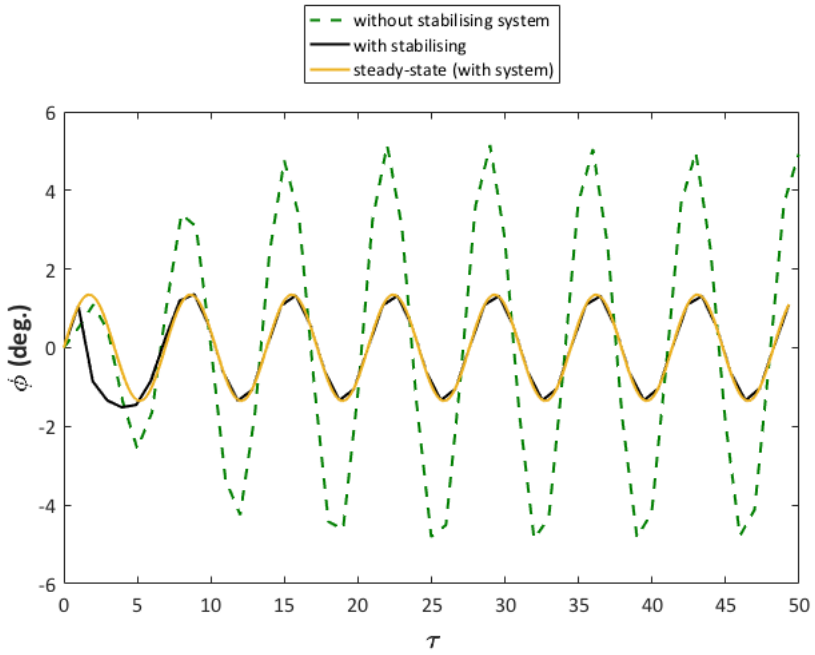

FIGURE 5.19: Excited roll motion with and without the stabilising system and comparison with linear steady-state approximation of the model with stabilising system on for $\mu = 0.05$ and velocity = $60ms^{-1}$

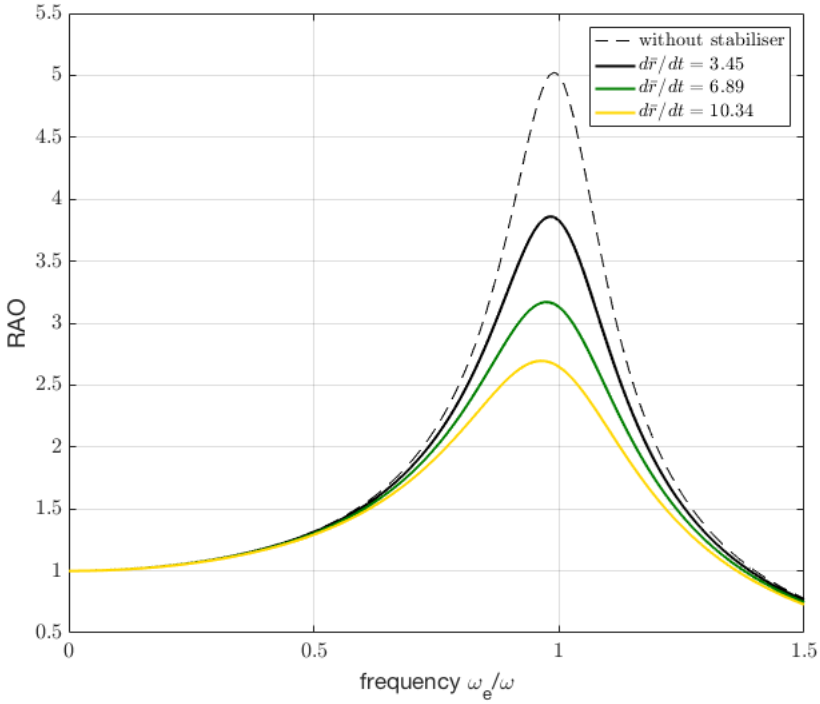

FIGURE 5.20: Response profile of the vessel with 1% mass ratio stabilising system

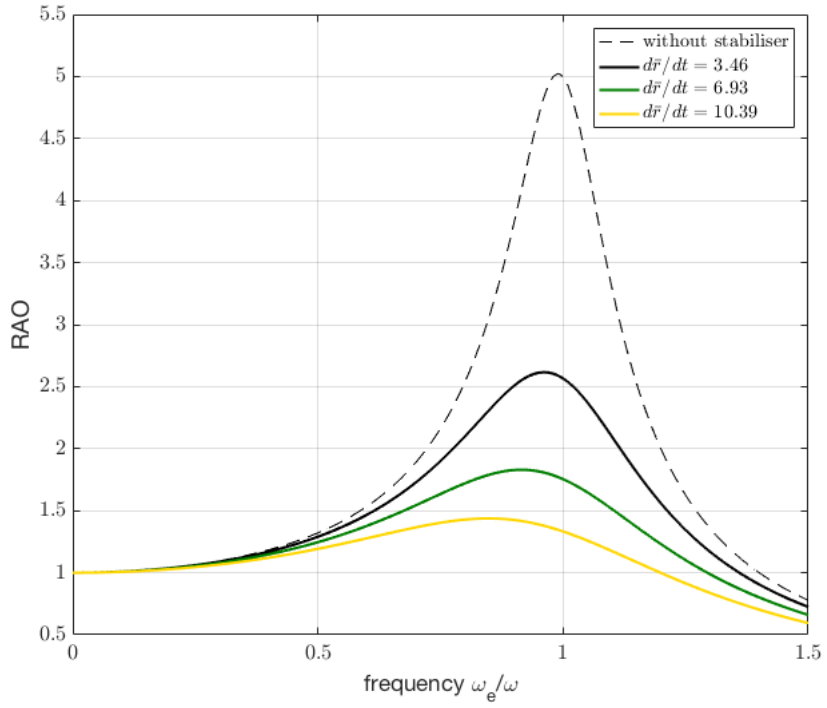

FIGURE 5.21: Response profile of the vessel with 3% mass ratio stabilising system

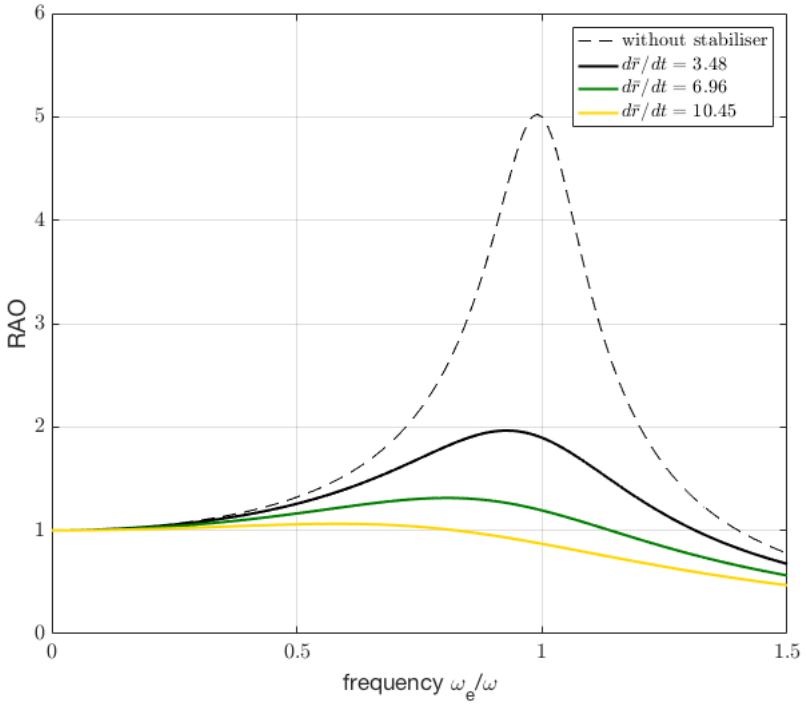

FIGURE 5.22: Response profile of the vessel with 5% mass ratio stabilising system

Chapter 6

Attenuation of Super Tall Structures Using Multi-degree-of-freedom Enhanced Coriolis Effect Damper

6.1 Introduction

In Chapter 4 it is mentioned that the two significant parameters that affect the Coriolis effect are velocity of the translating object (both in magnitude and direction) and the angular displacement of the rotating object. Additionally, in Chapter 5 the concept of enhancing Coriolis effect through the use of constant direction of translational motion away from the pivot of the rotating object was explored and applied to the case of a rolling structure in the form of a ship. Now, this chapter will explore the idea of enhancing the effect by manipulating the angular displacement. For this case the concept is applied to a building structure which would be more practical for this type of structure as it may be less feasible to use a constant direction of translational motion as in the case for a ship.

6.2 Problem Formulation

The system is setup as illustrated in Figure 6.1.

Model

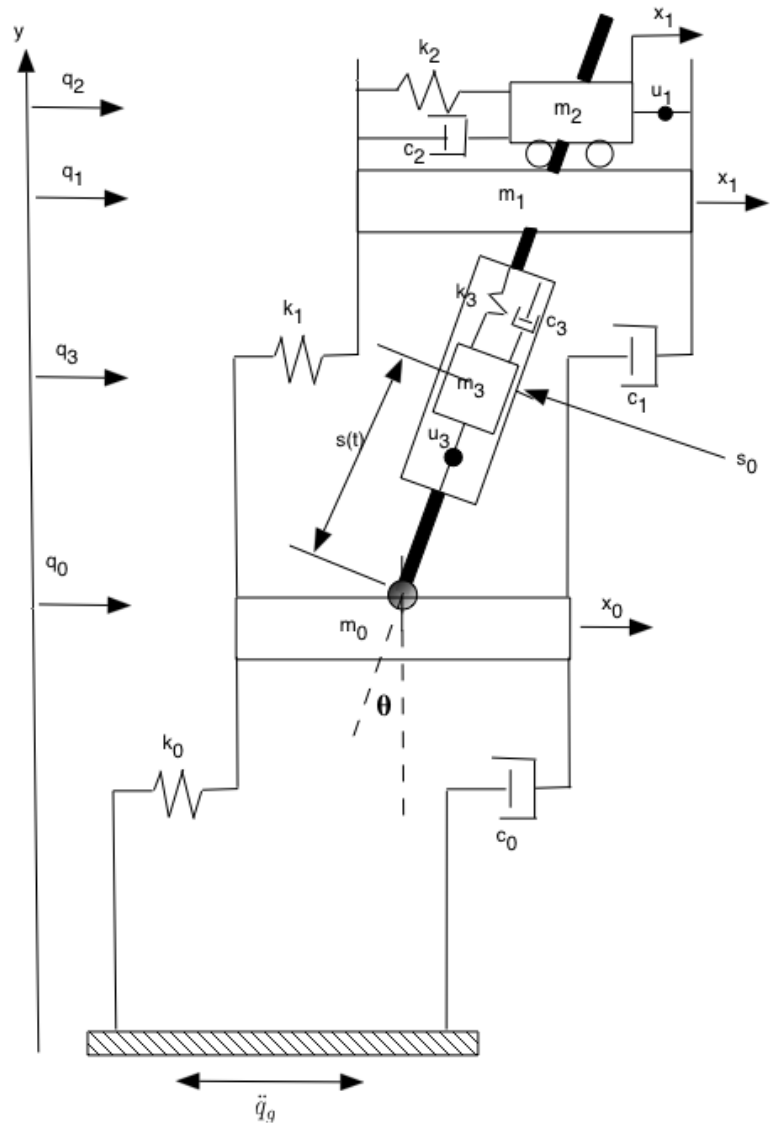

FIGURE 6.1: Model of the enhanced Coriolis damper

Coordinate Parameters

$$q_0 = q_g + x_0 \tag{6.1}$$

$$q_1 = q_0 + x_1 \tag{6.2}$$

$$q_2 = q_1 + x_2 \tag{6.3}$$

$$q_3 = q_g + s\sin\theta \tag{6.4}$$

$$y_3 = y_0 + s\cos\theta \tag{6.5}$$

Where q_0 is the total horizontal displacement of m_0, q_g is the horizontal displacement of ground, x_0 is the relative horizontal displacement of m_0 from the ground, q_1 is the total horizontal displacement of m_1, x_1 is the relative horizontal displacement of m_1 from m_0, q_2 is the total horizontal displacement of

m_2, x_2 is the relative displacement of m_2 from m_1, s is the displacement of m_3 along the angular fixture, s_0 is the height from pivot to neutral point of m_3 along the angular fixture and y_3 is the vertical displacement of m_3.

Using Lagrangian mechanics, the following equations of motions are obtained.

$$\begin{aligned} m_0\ddot{x}_0 + c_0\dot{x}_0 + k_0x_0 - c_1\dot{x}_1 - k_1x_1 \\ +m3\left[\ddot{q}_0 + (2\dot{s}\dot{\theta} + s\ddot{\theta})\cos\theta + (\ddot{s} - s\dot{\theta}^2)\sin\theta\right] = -m_0\ddot{q}_g - u_3\sin\theta \end{aligned} \tag{6.6}$$

$$m_1\ddot{q}_1 + c_1\dot{x}_1 + k_1x_1 - c_2\dot{x}_2 - k_2x_2 = -u_2 \tag{6.7}$$

$$m_2\ddot{q}_2 + c_2\dot{x}_2 + k_2x_2 = u_2 \tag{6.8}$$

$$m_3\left[\ddot{s} + \ddot{q}_0\sin\theta - s\dot{\theta}^2 + g\cos\theta\right] + c_3\dot{s} + k_3(s_0 - s) + = u_3 \tag{6.9}$$

The angular equation of motion can be directly obtained using

$$\theta = \sin^{-1}\left(\frac{2(x_1 + x_2)}{H}\right) \tag{6.10}$$

Therefore

$$\dot{\theta} = \frac{2(\dot{x}_1 + \dot{x}_2)}{H\sqrt{1 - \frac{(x_1+x_2)^2}{H^2}}} \tag{6.11}$$

$$\ddot{\theta} = \frac{8(x_1 + x_2)(\dot{x}_1 + \dot{x}_2)^2}{H^3\left(1 - \frac{(x_1+x_2)^2}{H^2}\right)^{3/2}} + \frac{2(\ddot{x}_1 + \ddot{x}_2)}{H\sqrt{1 - \frac{(x_1+x_2)^2}{H^2}}} \tag{6.12}$$

It should be stated that for this investigation the relative horizontal displacement of the floors and mass dampers from the neutral axis of the primary structure will be given as w_i where $i = 0, 1, 2$ and the numbers correspond to the mass numbers.

6.3 Seismic Excitation

The seismic excitation used throughout the study was taken from the data records of the 1989 Loma Prieta Earthquake. All analyses were conducted using the data as shown in Figure 6.2.

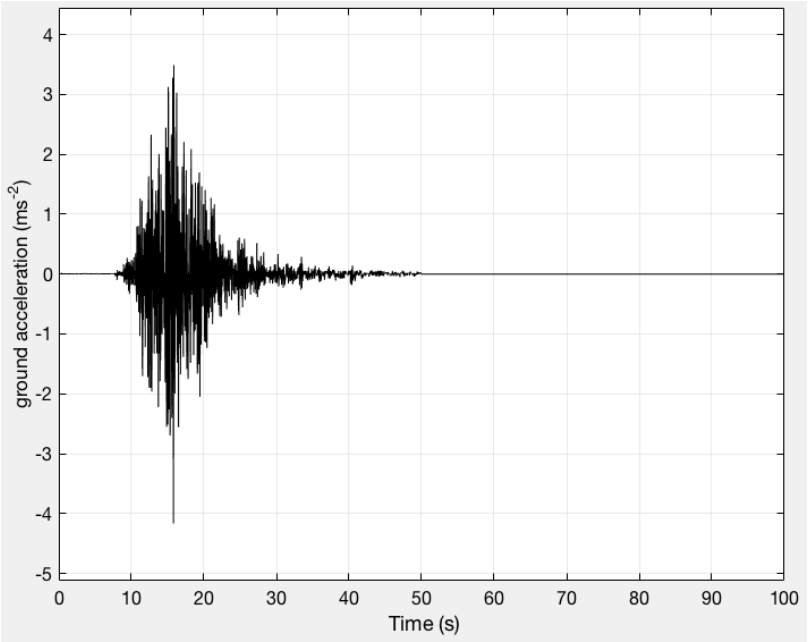

FIGURE 6.2: Ground excitation (Loma Prieta East-West ground acceleration)

6.4 Tuned Mass Damper

6.4.1 Design of TMD

In order to design an effective hybrid enhanced damper the author starts by designing an effective tuned mass damper (TMD) to be later controlled by the chosen control law. In Figure 6.1 m_2 represents this TMD to be actively/semi-actively controlled with stiffness k_2 and damping coefficient c_2. Following the procedures taken in (Connor, 2003) based on the Hartog's principles for optimal parameters (Den Hartog, 1985), the optimal parameters are found for the case of periodic excitation. From this the various H were given as

$$H_5 = \frac{\sqrt{\left[\Omega_2^2 - \rho^2\right]^2 + \left[2\zeta_2\rho\Omega_2\right]^2}}{|D_3|} \tag{6.13}$$

$$H_7 = \frac{\rho}{|D_3|} \tag{6.14}$$

where

$$\begin{aligned} |D_3| = \{ &\left[-\Omega_2^2\rho^2\mu_2 + \left(1-\rho^2\right)\left(\Omega_2^2 - \rho^2\right) - 4\zeta\zeta_2\Omega_2\rho^2\right]^2 \\ &+4\left[\zeta\rho\left(\Omega_2^2 - \rho^2\right) + \zeta_2\Omega_2\rho\left(1-\rho^2\left(1+\mu_2\right)\right)^2\right]\} \end{aligned} \tag{6.15}$$

where ρ is the dimensionless frequency ratio of the forced frequency to the frequency of the primary structure.

There are no analytical solution to find the optimal tuning frequency and optimal damping ratio in terms of the mass ratio due to the dependency of the damping ratio of the primary structure ζ (Connor, 2003). As such the equations can be solved numerically for a range of ρ values, given we know the values for the mass ratio, damping ratio of primary structure and mass damper, and tuning frequency. According to (Connor, 2003),plots of H_5 versus ρ can be generated for various Ω_2 and ζ_2 values and the combination of these values that produces the lowest peak value of H_5 can be taken as the optimal state. The behavioural data for these are plotted below in Figures 6.3 and 6.4 for different values of mass ratios and damping ratio of primary structure.

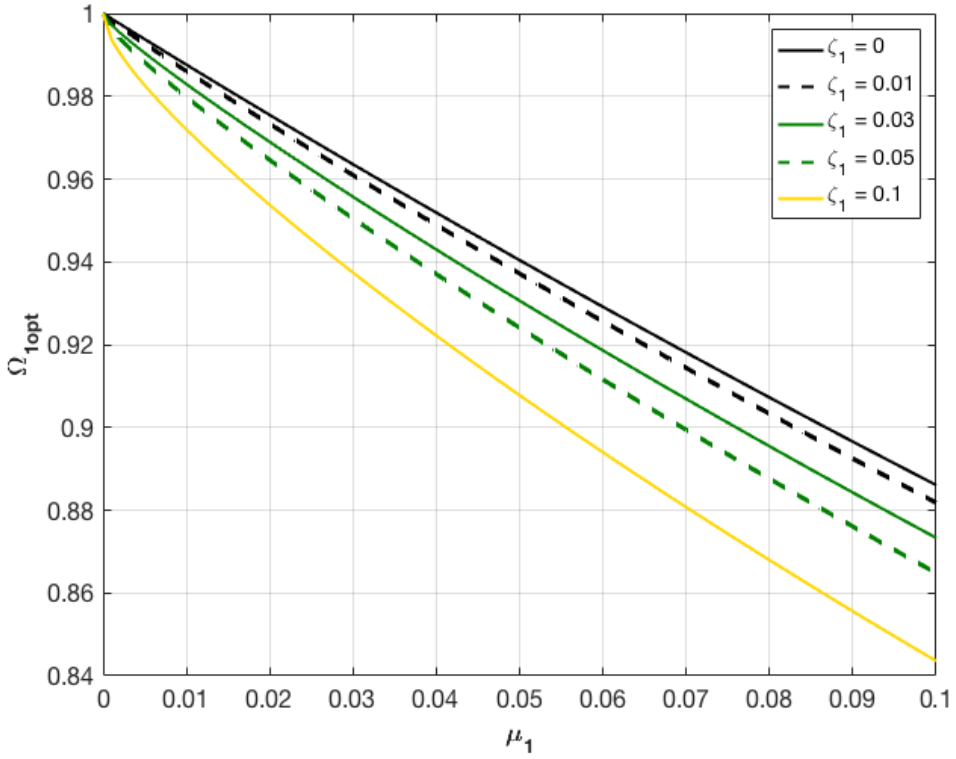

FIGURE 6.3: Optimal tuning frequency Ω_2 for TMD

6.4.2 Performance of TMD

In Chapter 3 it is mentioned about a benchmark model for a super tall building structure used in (Yang et al., 2004) with height 306 m, mass of 153,000 tons and first natural frequency of 1 rad/s. The building is also given a damping ratio of 1%. The performance of the TMD designed above is tested by incorporating it into this model. The TMD used has a mass of 5% of the primary structure and using these parameters optimal parameters for the damping and tuning frequency ratios were determined. The system is excited by the Loma Prieta earthquake mentioned in Chapter 3. The time

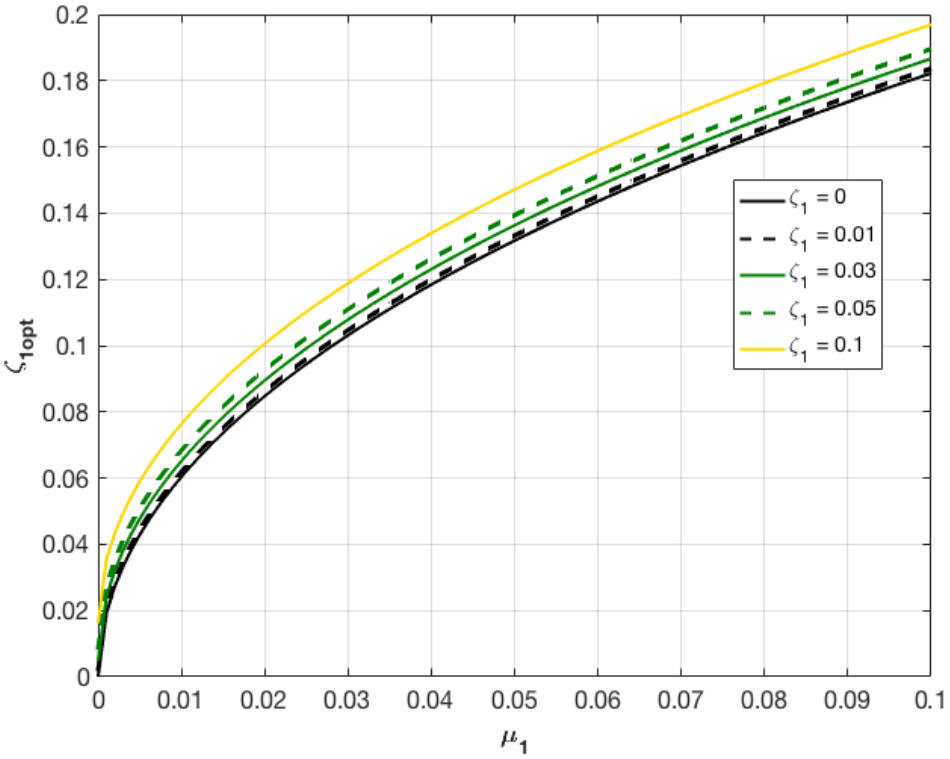

FIGURE 6.4: Optimal damping ratio ζ_2 for TMD

history of the response of the system with and without the TMD, and the response of the TMD are shown in Figures 6.5 - 6.7.

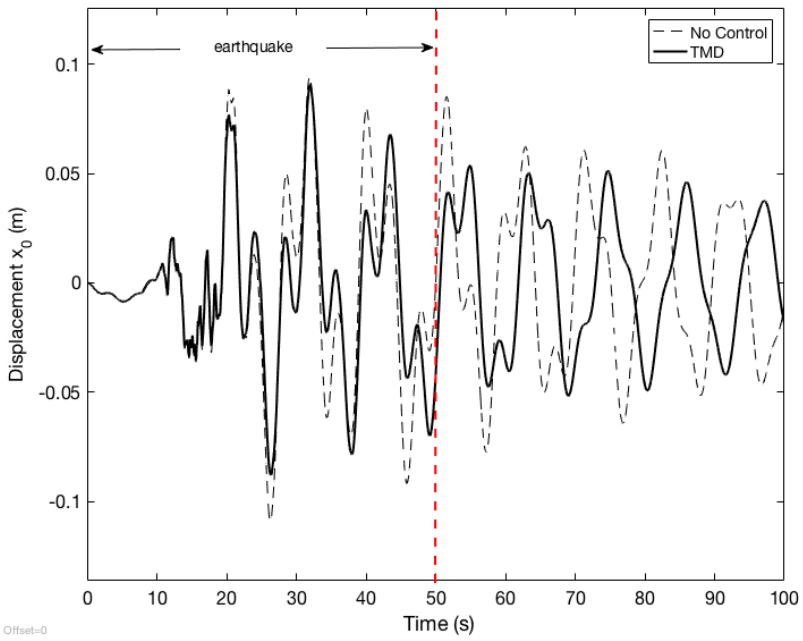

FIGURE 6.5: Dynamic response of the 2nd floor

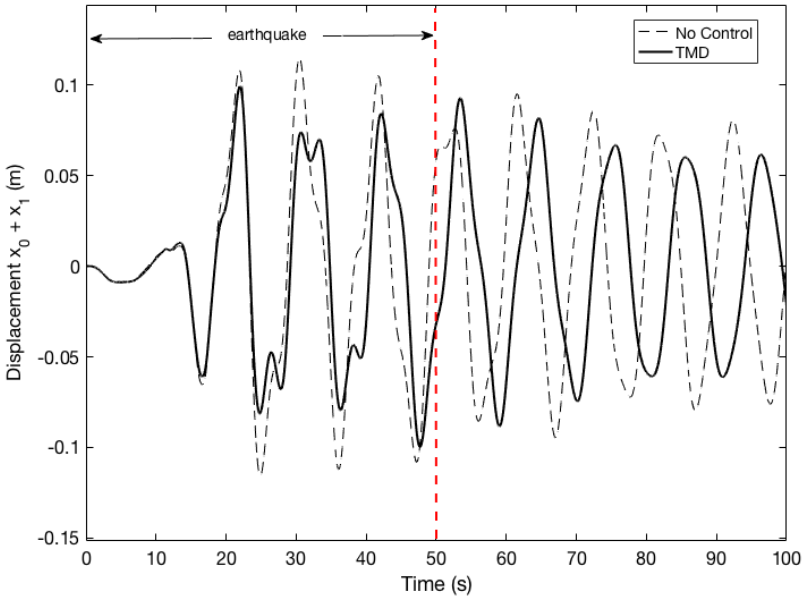

FIGURE 6.6: Dynamic response of the top floor

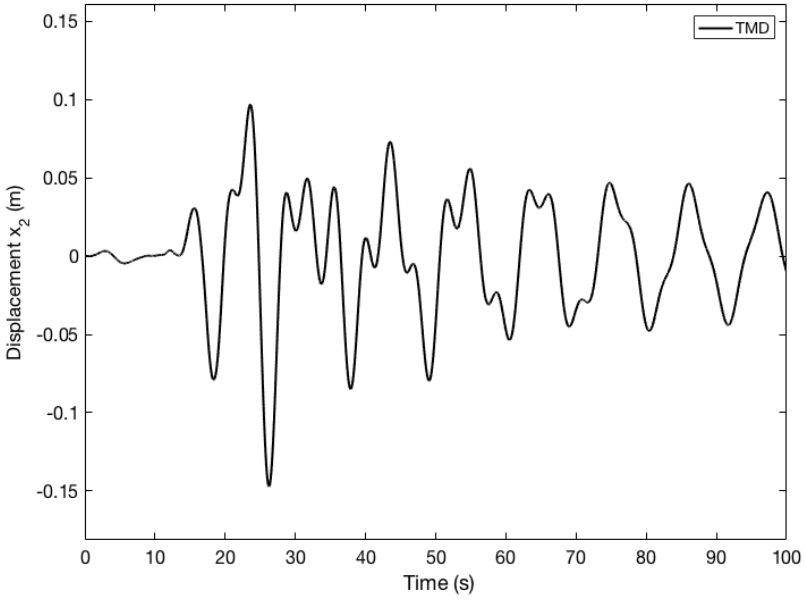

FIGURE 6.7: Response of TMD

From the results we see that the TMD was able to reduce the response of the primary structure due to seismic excitation and was able to attenuate the response after excitation was removed.

6.5 Active Tuned Mass Damper

In the previous section the optimal frequency and damping ratio under periodic excitation for a TMD were found. However, TMDs are not very effective for reducing vibrations when the forced frequency varies from the fundamental frequency of the primary structure. As such, in order to improve the

effectiveness of the TMD, one method is to apply control law. In this section an active tuned mass damper (ATMD) system is designed and application of control law by means of Fuzzy Logic Controller is applied.

6.5.1 Design of Controller

As mentioned in Section 2.3.3, the FLC allows implementing human inference into a control system, it is quite robust and able to simply handle nonlinear control. Giving these, a FLC is implemented for the control of this system. In this investigation, for the fuzzification process, gaussian membership functions are chosen as shown in Figures 6.8 and 6.9. The fuzzy rules are based on an "IF-THEN" system and the linguistic variables are as described in Table 6.1

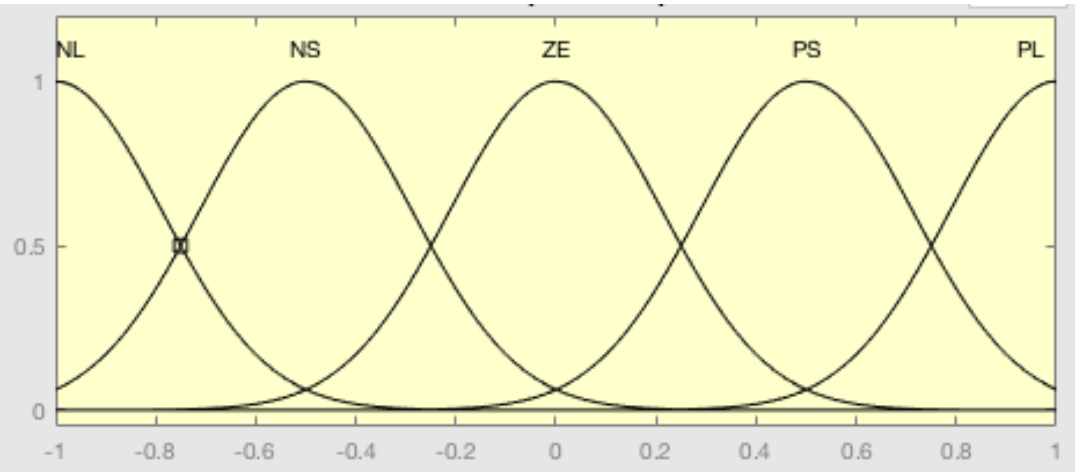

FIGURE 6.8: Fuzzy membership functions for input

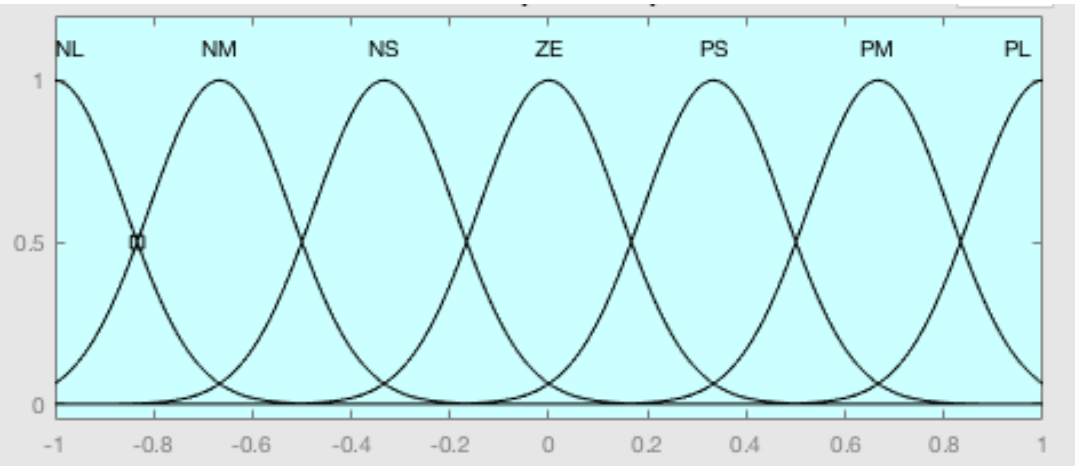

FIGURE 6.9: Fuzzy membership functions for output

The input variables for the fuzzy control are the displacement and velocity of the top floor of the primary structure x_1 and $\dot{x}_1$ respectively. The output is the control force u_2 to the mass damper. The controller is a Mamdani controller and the rule base is shown in Table 6.2. The rule base form is:

TABLE 6.1: Description of fuzzy variables

Variable	Description
NL	Negative Large
NM	Negative Medium
NS	Negative Small
ZE	Zero
PS	Positive Small
PM	Positive Medium
PL	Positive Large

if $\text{Input}_1 = XX$ and $\text{Input}_2 = XX$ then $\text{Output} = XX$

TABLE 6.2: Fuzzy rules

Velocity $\dot{x}_1$	Displacement x_1				
	NL	NS	ZE	PS	PL
NL	PL	PM	PS	PS	ZE
NS	PM	PM	PS	ZE	ZE
ZE	PS	PS	ZE	NS	NS
PS	ZE	ZE	ZE	NM	NM
PL	ZE	NS	NS	NM	NL

6.5.2 Performance of ATMD

The benchmark model analysed in the previous section will now be analysed incorporating the newly designed ATMD. The parameters from before are the same including the excitation parameters. The time history of the response of the system with and without the ATMD as well as comparisons from the previous investigations are shown in Figures 6.10 and 6.11. Additonally the responses of the mass dampers are shown in Figure 6.12.

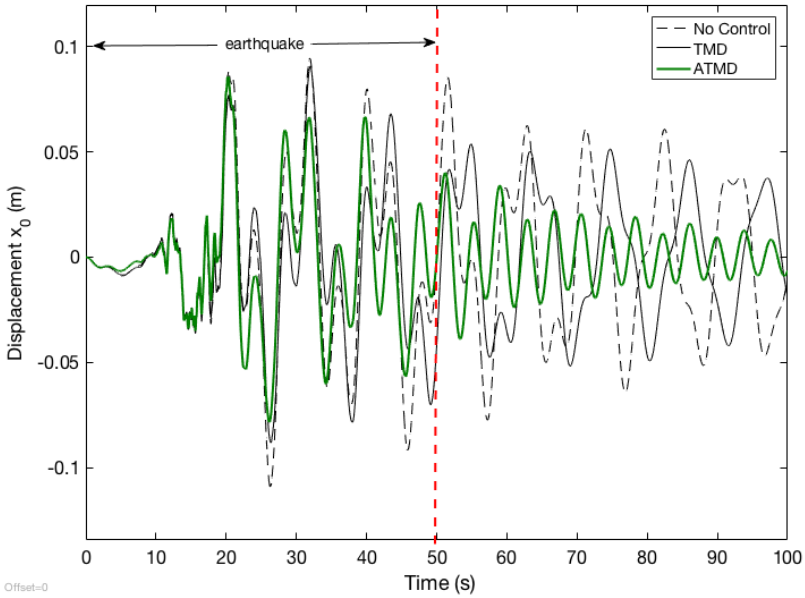

FIGURE 6.10: Dynamic response of the 2nd floor

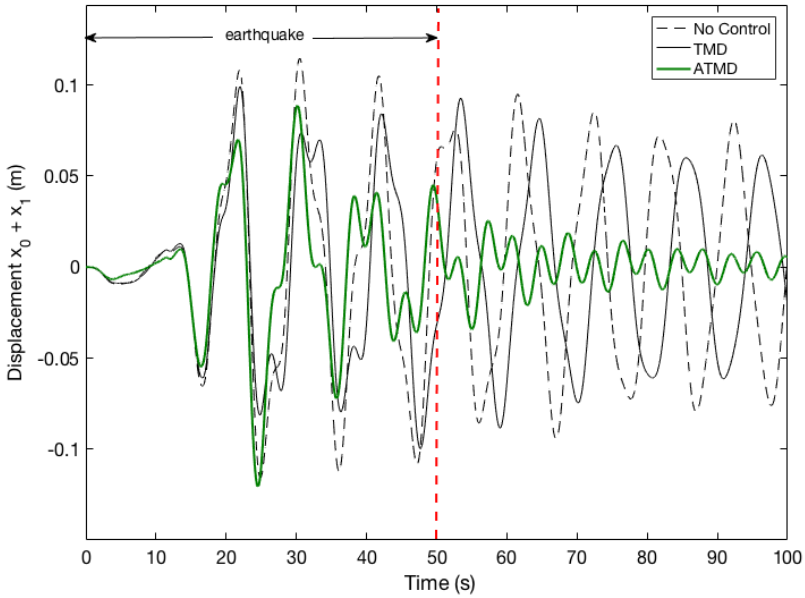

FIGURE 6.11: Dynamic response of the top floor

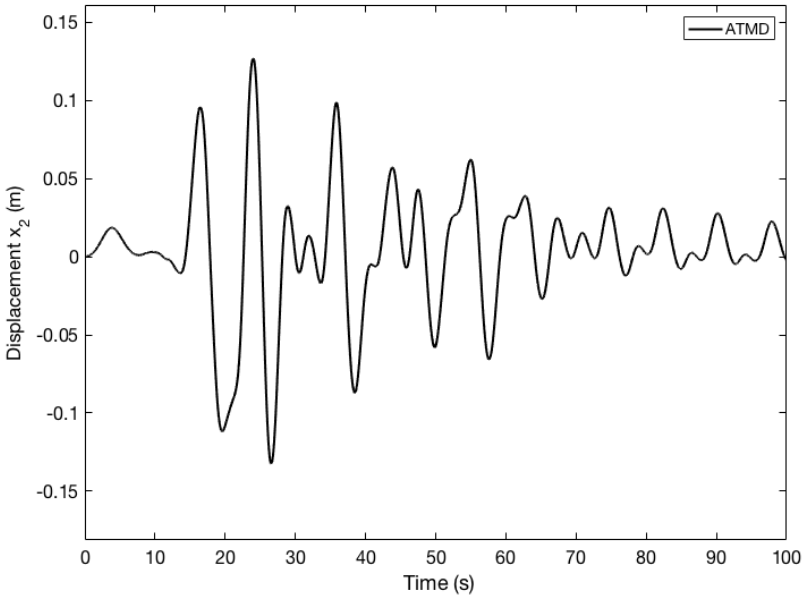

FIGURE 6.12: Response of mass dampers

The results show an improved performance for the ATMD system to reduce the response of excited primary structure

6.5.3 Stability of Fuzzy Logic Controller for ATMD

Stability proof for fuzzy logic controllers have been a concern over the years. Researchers have often criticised the stability of closed-loop fuzzy logic controllers (Feng, 2006), and to this day, no analytical solution exists due to the complex non-linearities of fuzzy logic systems (Lee, 1990; Elkhatib and Soraghan, 2008). However, many approaches to stability issues concerning fuzzy logic controllers have been investigated over the years, and a common approach is through Lyapunov stability theory (Feng, 2006). As such, the stability of the ATMD fuzzy logic system was analysed on the basis of Lyapunov's direct method. For this the Lyapunov theorem for global stability states that given a positive definite function $V(x)$ then if the derivative of this function is (Slotine and Li, 1991):

1. negative definite then the equilibrium at the origin is globally asymptotically stable

Using energy as the Lyapunov function we get

$$V(x,\dot{x}) = \frac{1}{2}M\dot{x}^2 + \frac{1}{2}Kx^2 \tag{6.16}$$

where this is the sum of the kinetic and potential energy of the system.

Taking the general form of the equation as

$$M\ddot{x} + C\dot{x} + Kx = F \tag{6.17}$$

then we get the derivative of the Lyapunov function as

$$\dot{V}(x,\dot{x}) = M\dot{x}\ddot{x} + Kx\dot{x} = M\dot{x}\frac{1}{M}(F - C\dot{x} - Kx) + Kx\dot{x}$$
$$\dot{V}(x,\dot{x}) = F\dot{x} - C\dot{x}^2 \tag{6.18}$$

According to stability theorem in order for the system to be globally asymptotically stable about the equilibrium at the origin then $\dot{V}(x,\dot{x}) < 0$ and since the second term in Equation 6.18 is negative then to ensure that $\dot{V}$ is always negative then the first term should also be negative. Based on this, the first term can only be negative if the force F is always opposing the velocity $\dot{x}$. Using this the rule bases from Table 6.2 are such that the overall force applied to the primary structure is always opposing the velocity. Thus, the system is globally asymptotically stable.

6.6 Hybrid Structural Control Using ATMD with Proposed Coriolis Damper

In this section the motion of the previously designed ATMD is used to enhance the Coriolis effect of the proposed damper. This is done through increasing angular motion as while the primary structure may experience a small horizontal displacement at the top, the proposed damper is connected to the translating mass damper which therefore the angular displacement will be due to a sum of the horizontal displacement of the primary structure and the mass damper. Again the benchmark model from previous sections is used, using the same parameters for the model. This time for the damping system, since it consists of 2 mass dampers the combination of the 2 mass dampers will be 5% of the primary structure. The effect of their ratio will be analysed to highlight the influence of the Coriolis effect from the proposed concept. The proposed concept will also be controlled using fuzzy logic controller which is designed as follow.

6.6.1 Design of Coriolis damper

Like for the ATMD designed in the previous section, an effective TMD parameters are designed. For this an equivalent inverted pendulum system is considered. From this we can see that the frequency of such a system is

$$\omega_\theta = \sqrt{\frac{|1 - \mu_3\alpha_s|}{1 + \mu_3\alpha_s^2}} \tag{6.19}$$

where μ_3 is the ratio of the Coriolis mass m_3 to the mass of the ATMD m_2, and α_s is the ratio of the neutral position of the Coriolis mass s_0 from the pivot to the height of the primary structure H. Again, from analysis of the Coriolis effect we know the frequency of the sliding mass should be at about twice the frequency of the oscillating mass. Therefore the ratio of the frequency can be

expressed as

$$\frac{\omega_3}{\omega_2} \approx 2\omega_\theta = 2\sqrt{\frac{|1-\mu_3\alpha_s|}{1+\mu_3\alpha_s^2}} \tag{6.20}$$

6.6.2 Design of Controller for Coriolis Damper

Similar to the ATMD the fuzzification process of the proposed Coriolis damper involves gaussian membership functions for the input and output variables (see Figures 6.13 and 6.14). Also like previously, the rule base is an "IF-THEN" system and using similar linguistic variables as described in Table 6.1. However, for this system the input variables for the fuzzy control are the relative displacement and velocity of the ATMD w_2 and $\dot{w}_2$ respectively. The output is the control force u_3 to the secondary mass damper. Again, the controller is a Mamdani controller and the rule base is shown in Table 6.3 in the form:

if $\text{Input}_1 = XX$ and $\text{Input}_2 = XX$ then $\text{Output} = XX$

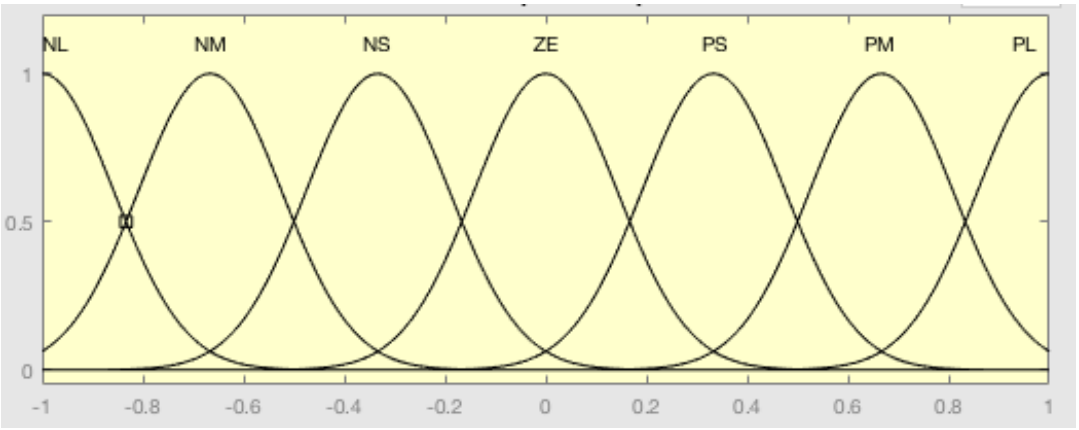

FIGURE 6.13: Fuzzy membership functions for input for Coriolis damper

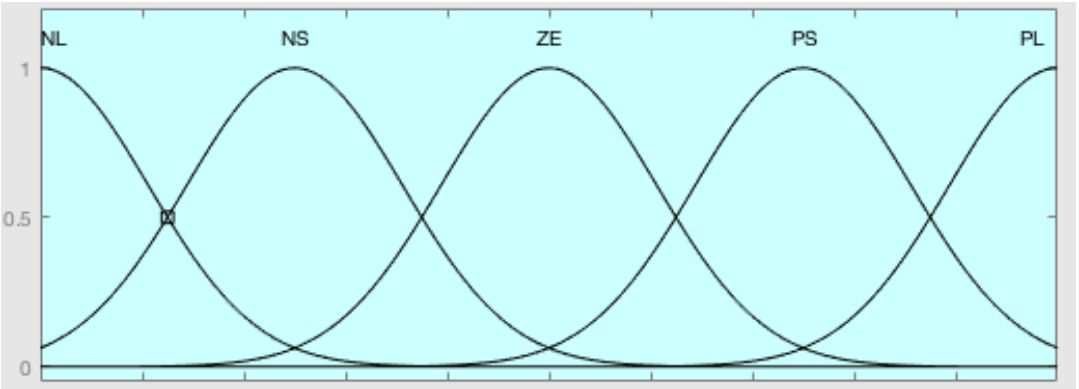

FIGURE 6.14: Fuzzy membership functions for output for Coriolis damper

TABLE 6.3: Fuzzy rules

Velocity $\dot{w}_2$	Displacement w_2						
	NL	NM	NS	ZE	PS	NM	PL
NL	PL	PL	PS	ZE	PS	PL	PL
NM	PL	PS	PS	ZE	PS	PS	PL
NS	PS	ZE	ZE	ZE	ZE	ZE	PS
ZE	ZE	ZE	ZE	ZE	ZE	ZE	ZE
PS	NS	ZE	ZE	ZE	ZE	ZE	NS
PM	NL	NS	NS	ZE	NS	NS	NL
PL	NL	NL	NS	ZE	NS	NL	NL

6.7 Results and Discussion

In this section the results for the hybrid enhanced Coriolis damper are presented. The benchmark model used in the previous investigations will be used with similar parameters and the system will once again be excited by the Loma Prieta earthquake as before to analyse the robustness and effectiveness of the damping system under seismic excitation. Furthermore the system will also be tested under free response. The combination of the hybrid dampers will be 5% of the primary structure, however their ratio to each other will be changed to analyse the effect of their ratio to the effectiveness of the system. The ratio of the hybrid dampers will be 1:4, 2:3, 1:1, 3:2 and 4:1. Their parameters were found using the design techniques mentioned above. For this investigation, the neutral position of the Coriolis mass is $y_3(s_0) = 229.5$ m. Additionally, the results were compared to the case of the standalone ATMD in order to quantitatively assess the contribution solely due to the longitudinal motion of the moving mass.

6.7.1 Seismic Excitation

1:4 Mass Ratio

First, the system with mass ratio 1:4. That is mass of ATMD m_2 and mass of Coriolis damper m_3 are 1% and 4% respectively of the primary structure. The time history of the response of the system is shown in Figures 6.15 - 6.16.

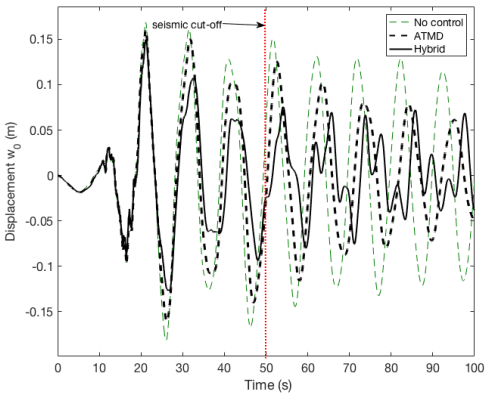

(A) Dynamic response of 2nd floor

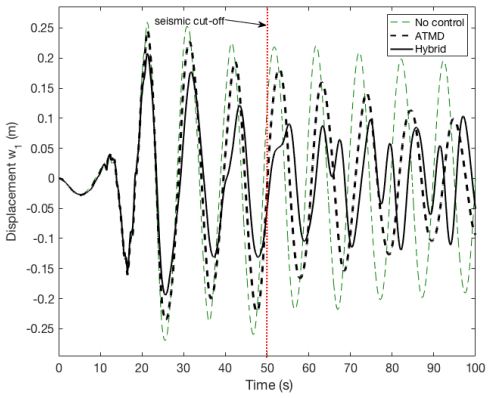

(B) Dynamic response of top floor

FIGURE 6.15: Dynamic response of system with the 1:4 ratio of m_2:m_3 under seismic excitation

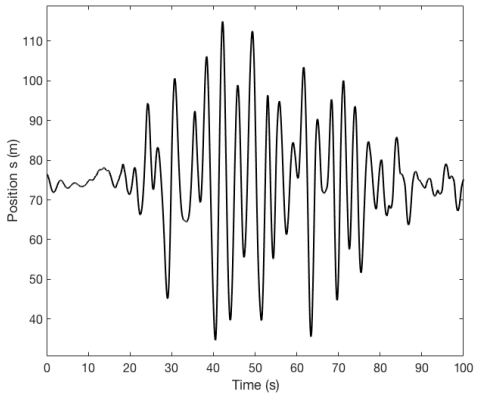

(A) Dynamic response of Coriolis damper along the angular fixture for 1:4 mass ratio

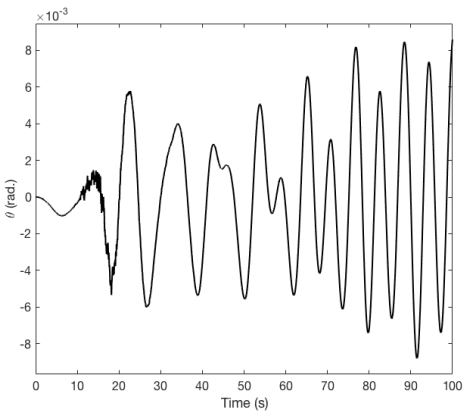

(B) Angular displacement of fixture

FIGURE 6.16: Dynamic response of Coriolis mass damper for 1:4 mass ratio

The results for the hybrid damper with mass ratio of 1:4 showed evident reduction of the dynamic response of the primary structure with the coupled longitudinal moving mass compared to a standalone ATMD at the top. The moving mass provided a 7.2% reduction in maximum response of the 2nd floor and a 15.3% reduction in maximum response of the top floor. Figure 6.17 illustrates the root mean square (RMS) values of the displacement of the 2nd and top floor of the primary structure over the time of the analysis. These results give a clear indication as to the overall performance of the damping system.

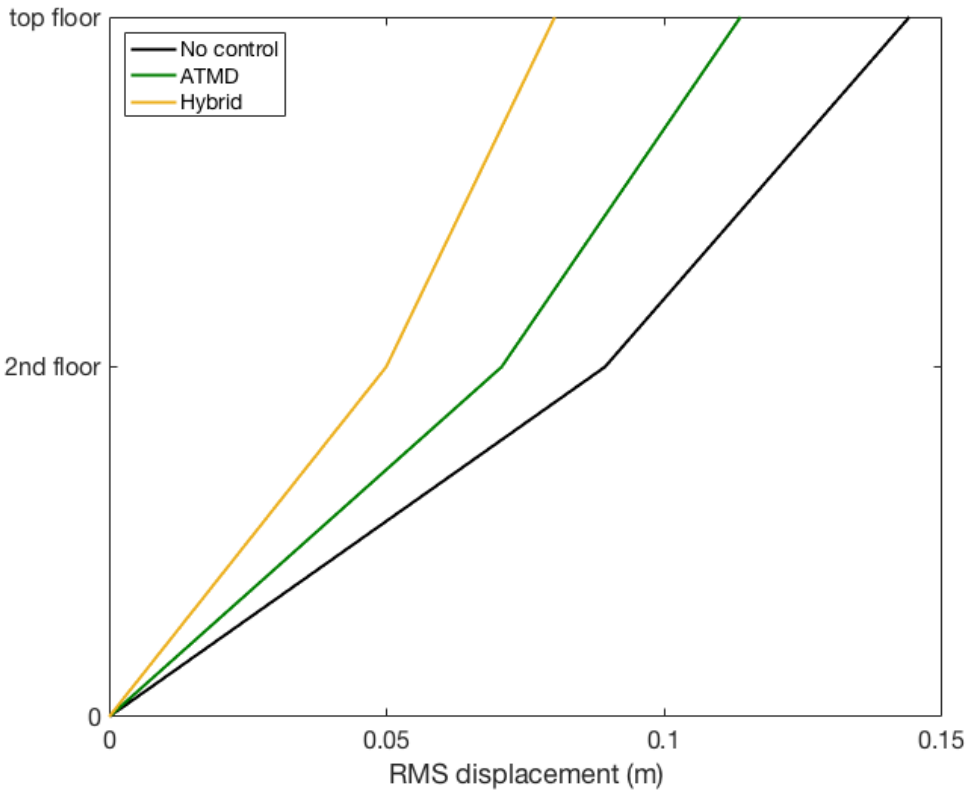

FIGURE 6.17: Dynamic responses without control, with an ATMD and with the coupled hybrid system for ATMD to hybrid mass ratio of 1:4

From the results the longitudinal motion significantly improved the overall performance of the system. We can clearly see a reduction in the RMS values of the 2nd floor (29.4% reduction) and top floor (29.4% reduction) with the coupled system versus the standalone ATMD. It should be noted that these results were obtained from a very small amplitude response of the primary structure. Yet even so, from the results presented above, because of the coupling of the Coriolis damper and the ATMD the system was still able to have sufficient effect.

2:3 Mass Ratio

Second is the mass ratio of m_2 and m_3, 2% and 3% respectively of the primary structure. Figure 6.18 shows the time history of the response of the floors of the primary structure. Figure 6.19 shows the motion of the Coriolis damping system.

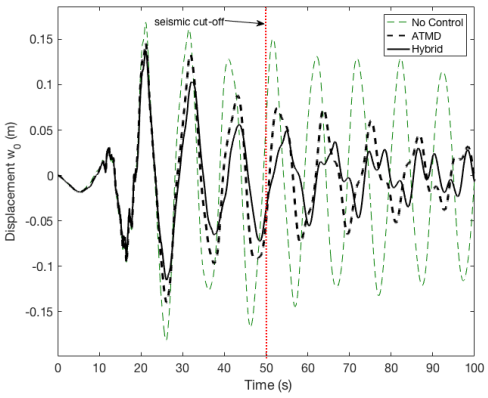

(A) Dynamic response of 2nd floor

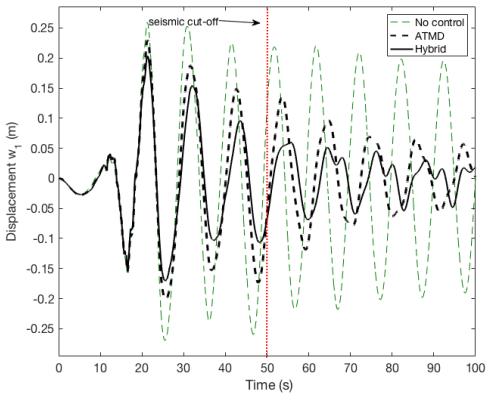

(B) Dynamic response of top floor

FIGURE 6.18: Dynamic response of system with the 2:3 ratio of m_2:m_3 under seismic excitation

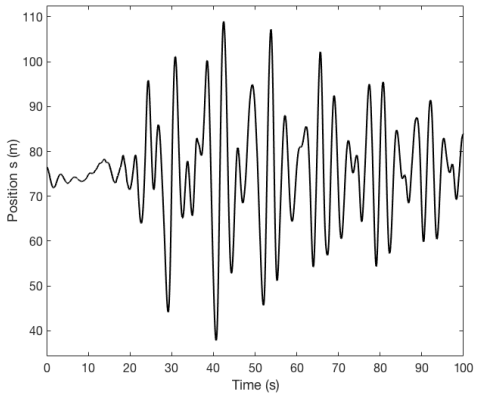

(A) Dynamic response of Coriolis damper along the angular fixture for 2:3 mass ratio

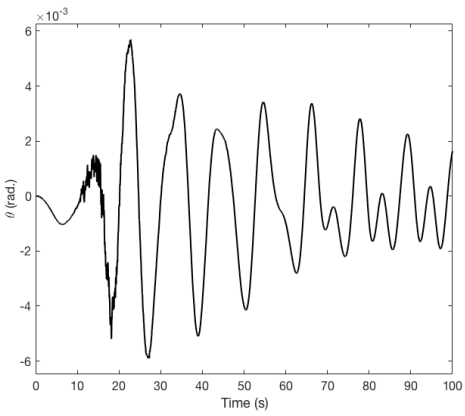

(B) Angular displacement of fixture

FIGURE 6.19: Dynamic response of Coriolis mass damper for 2:3 mass ratio

According to these figures, the motion of the longitudinal moving mass provides attenuating effect to both floors. For the 2nd floor there was an 8.2% reduction in maximum response when the ATMD is coupled with the secondary mass compared to the standalone ATMD system and for the top floor there was an 11.4% reduction. Illustration of the overall performance of the system is shown in the overall RMS response of the primary structure (See Figure 6.20).

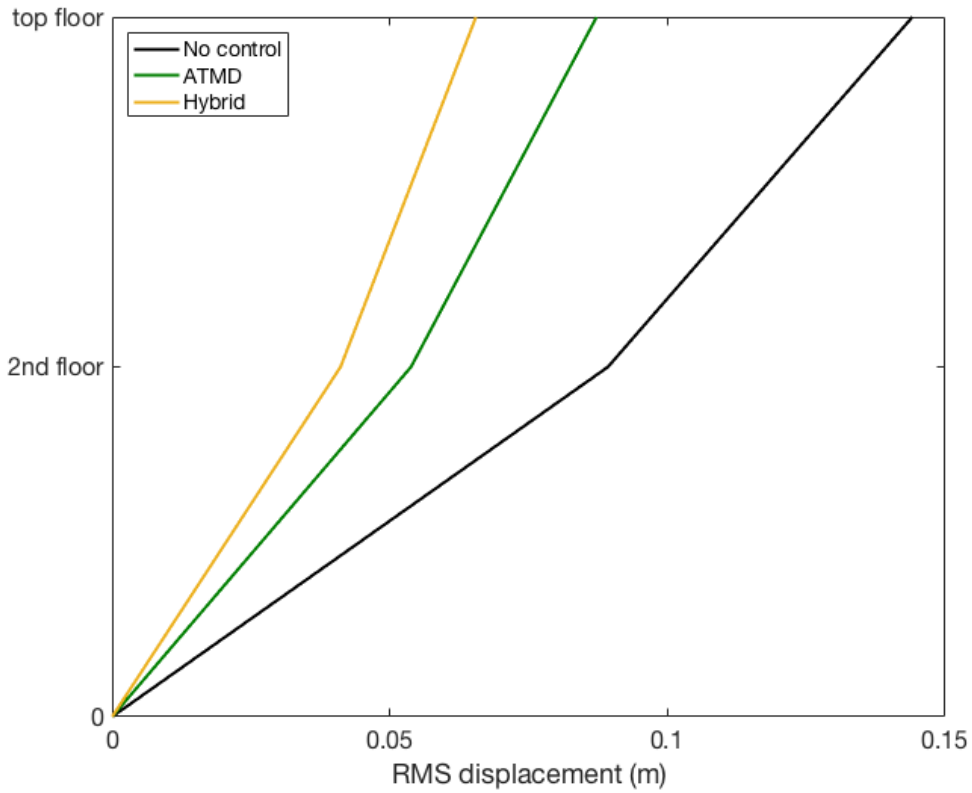

FIGURE 6.20: Dynamic responses without control, with an ATMD and with the coupled hybrid system for ATMD to hybrid mass ratio of 2:3

From the results it is evident there was an improvement in the overall performance of the system. On the other hand, with a 23.3% and 24.9% reduction in the overall RMS displacement of the 2nd and top floor respectively from the comparison of with the ATMD and with the coupled system, we see a decrease in the ratio of reduction.

1:1 Mass Ratio

The mass ratio of m_2 to m_3 of 1:1 with a combined mass ratio of 5% of the primary structure was studied and the results for this are shown in Figures 6.21 and 6.22.

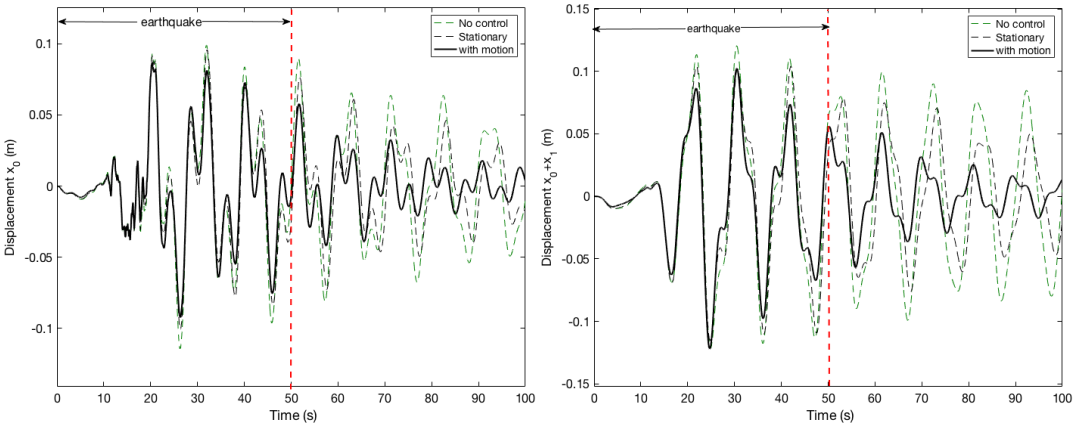

(A) Dynamic response of 2nd floor (B) Dynamic response of top floor

FIGURE 6.21: Dynamic response of system with the 1:1 ratio hybrid enhanced Coriolis damper under seismic excitation

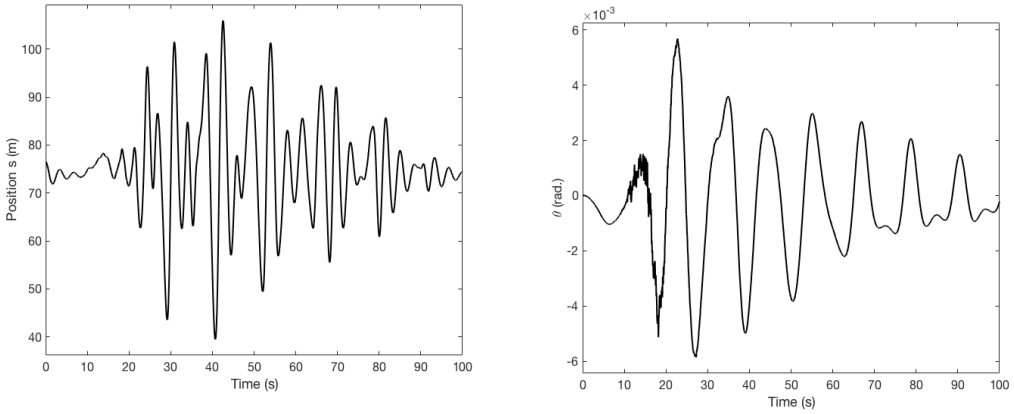

(A) Dynamic response of Coriolis damper along the angular fixture for 1:1 mass ratio

(B) Angular displacement of fixture

FIGURE 6.22: Dynamic response of Coriolis mass damper for 1:1 mass ratio

At a ratio of 1:1, we continue to see from the results a reduction in the maximum response of the 2nd floor and top floor of the primary structure with the coupled system versus with the ATMD. And with a 4.8% and 9.4% reduction respectively, we continue to see a decrease in the percentage of reduction. This is further supported in Figure 6.23 with a 20.1% and 20.2% reduction in overall RMS of the 2nd and top floor respectively. Also the results show an improvement in the overall performance of the system. This trend is explained by the increase in the mass of the ATMD which adds inertial effect to the attenuation of the primary structure and as such the inertial effect adds more to the reduction compared with the Coriolis effect. The decrease in the reduction is explained by the decrease in the Coriolis mass. This trend continues for the other mass ratios (For 3:2 mass ratio - see Figures 6.24 - 6.26 and for 4:1 mass ratio - see Figures 6.27 - 6.29).

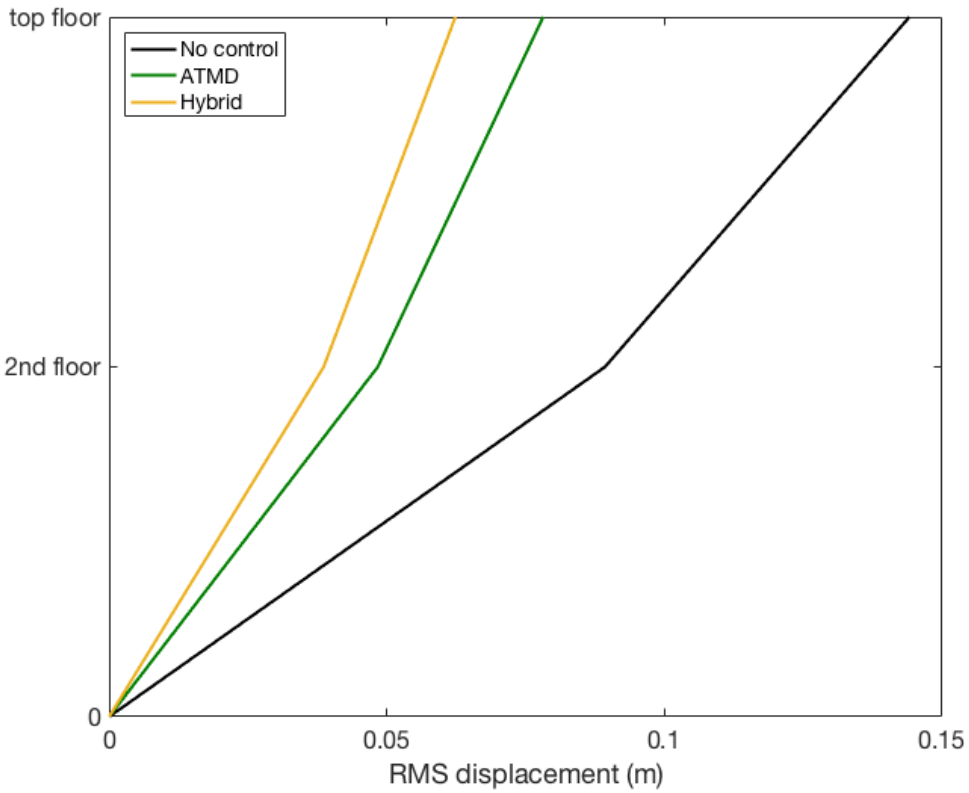

FIGURE 6.23: Dynamic responses without control, with an ATMD and with the coupled hybrid system for ATMD to hybrid mass ratio of 1:1

3:2 Mass Ratio

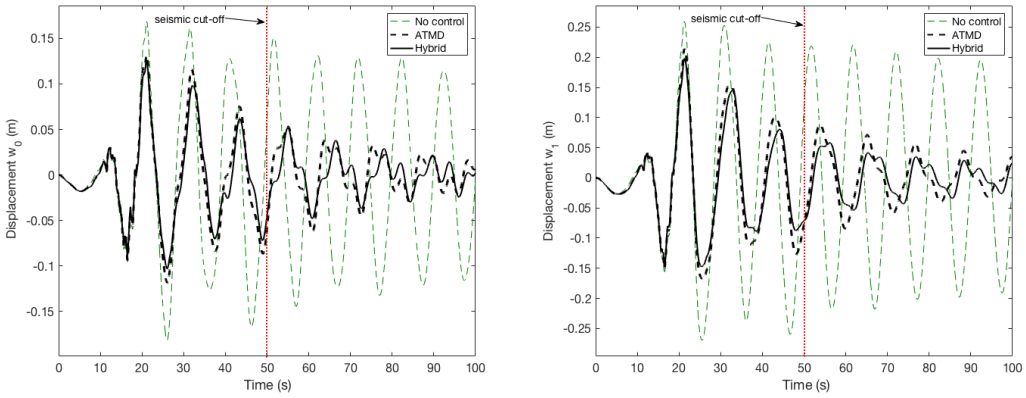

(A) Dynamic response of the 2nd floor (B) Dynamic response of the top floor

FIGURE 6.24: Dynamic response of system with the 3:2 ratio hybrid enhanced Coriolis damper under seismic excitation

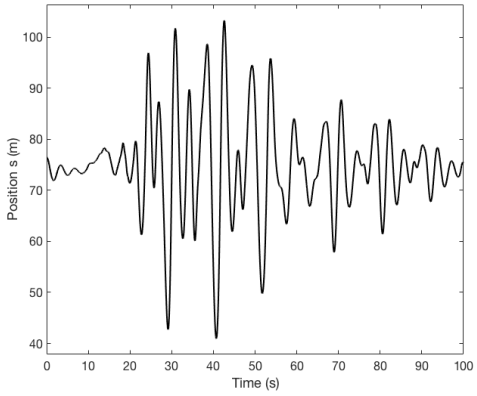

(A) Dynamic response of Coriolis damper along the angular fixture for 3:2 mass ratio

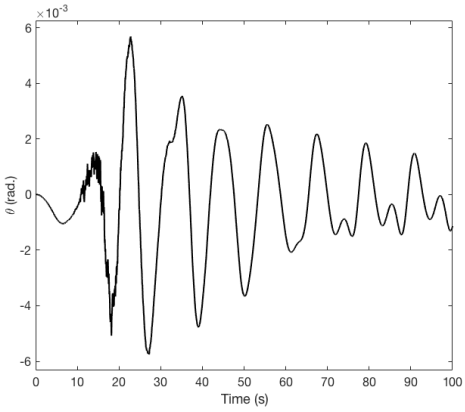

(B) Angular displacement of fixture

FIGURE 6.25: Dynamic response of Coriolis mass damper for 3:2 mass ratio

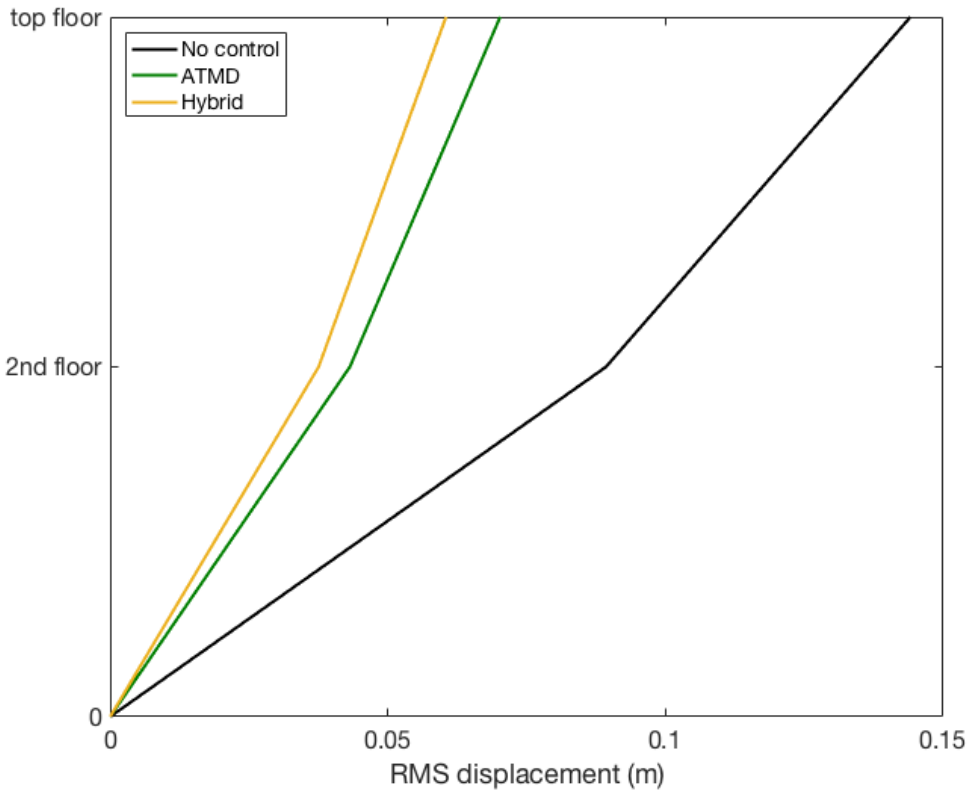

FIGURE 6.26: Dynamic responses without control, with an ATMD and with the coupled hybrid system for ATMD to hybrid mass ratio of 3:2

4:1 Mass Ratio

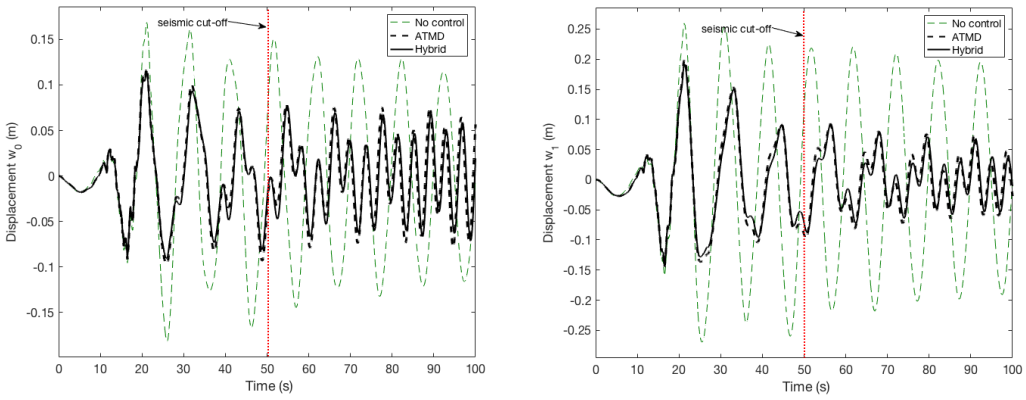

(A) Dynamic response of the 2nd floor (B) Dynamic response of the top floor

FIGURE 6.27: Dynamic response of system with the 4:1 ratio hybrid enhanced Coriolis damper to seismic excitation

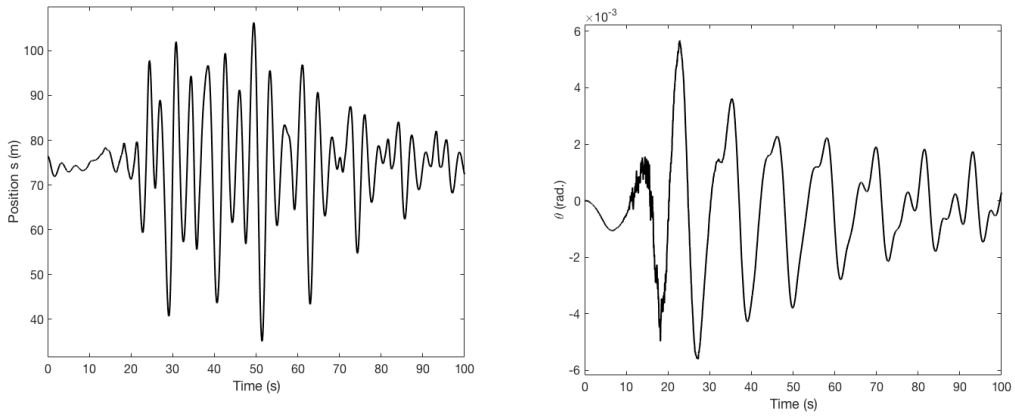

(A) Dynamic response of Coriolis damper along the angular fixture for 4:1 mass ratio

(B) Angular displacement of fixture

FIGURE 6.28: Dynamic response of Coriolis mass damper for 4:1 mass ratio

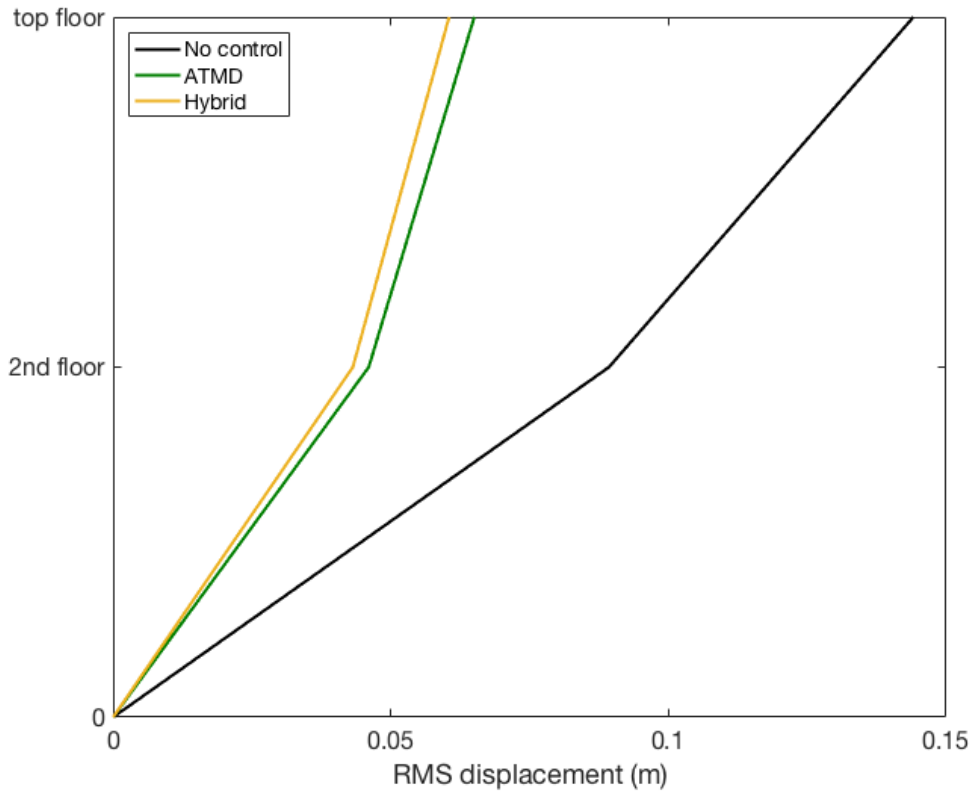

FIGURE 6.29: Dynamic responses without control, with an ATMD and with the coupled hybrid system for ATMD to hybrid mass ratio of 4:1

6.7.2 Effects of mass and velocity

As mentioned in the earlier chapters, the Coriolis effect is influenced by the mass, velocity and angular motion. For better design of control parameters for the proposed system, insights into how these parameters affect the performance is necessary.

To assess the impact the velocity has on the performance of the system, a series of simulations were conducted keeping the mass ratio of the system constant and only varying the control input since the force is directly proportional to the acceleration which is directly proportional to the velocity. In doing so the overall RMS of the velocity of the Coriolis mass changes for various control input. A comparison of these changes and the effect on the overall RMS displacement of the floors are shown in Figure 6.30. The mass ratio used for this was m_2 and m_3 respectively, 1:1.

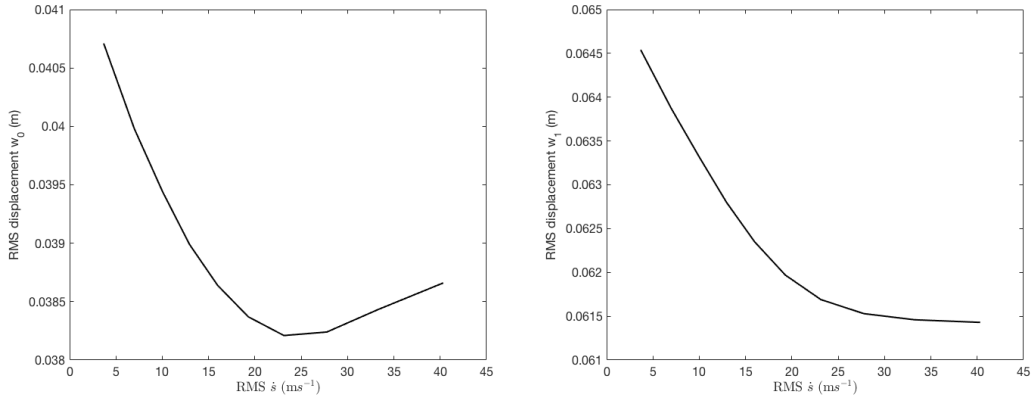

(A) A comparison of how the velocity of moving mass affects the response of the 2nd floor

(B) A comparison of how the velocity of moving mass affects the response of the top floor

FIGURE 6.30: The impact of the velocity of the moving mass on the response of the primary structure

A regression analysis was conducted on the system to determine which parameter provides the larger influence to minimise the response of the primary structure. Figure 6.31 illustrate these results.

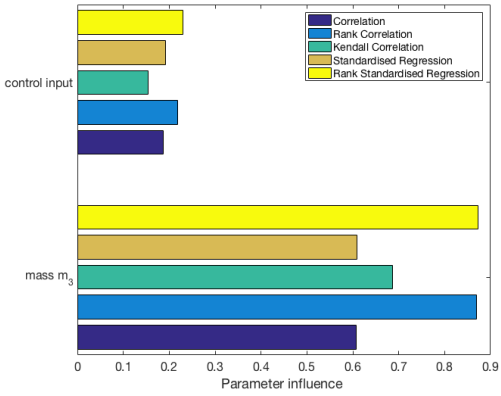

(A) Influence on the overall response of the 2nd floor of the primary structure

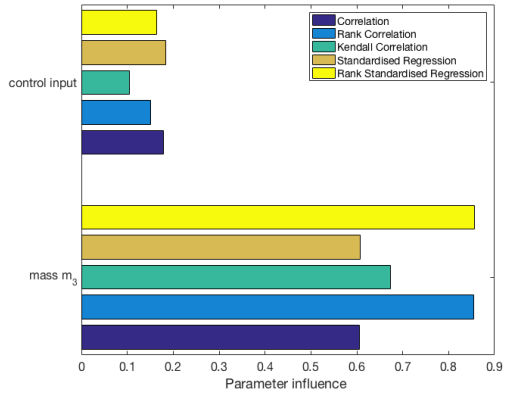

(B) Influence on the overall response of the top floor of the primary structure

centering

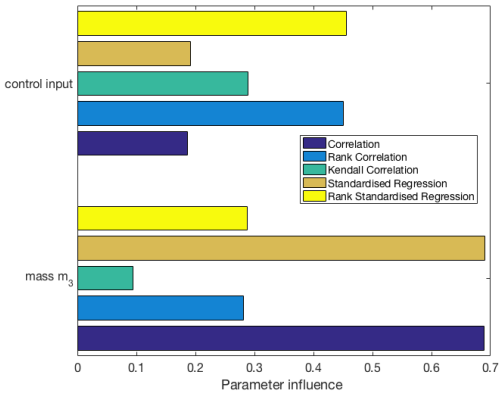

(C) Influence on the maximum response of the 2nd floor of the primary structure

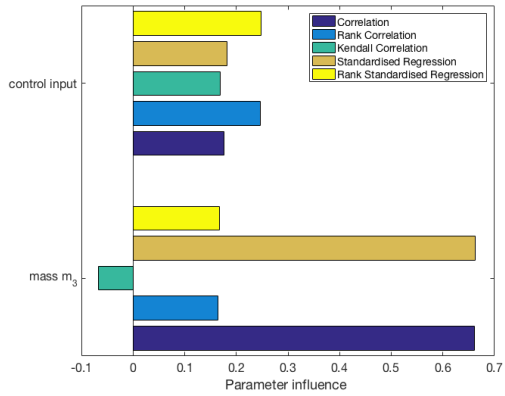

(D) Influence on the maximum response of the top floor of the primary structure

FIGURE 6.31: Regression analysis of the influence of the moving mass and the control input on the response of the primary structure

From the regression analysis conducted it is evident the parameter with the larger influence to minimise the response of the primary structure is mass of the longitudinal damper.

6.7.3 Stability of Hybrid Fuzzy Logic Controller

The stability of a nonlinear fuzzy logic controller can be analysed graphically using phase plane trajectory method (Ibrahim, 2004). A two-dimensional plane called the phase plane is generated of the motion trajectories given various initial conditions which highlights qualitatively the characteristics of the system and from this stability conditions as well as other motion patterns can be obtained (Slotine and Li, 1991). The stability of the system is checked by the systems ability to return at rest after experiencing initial conditions given by an external disturbance (Casciati, 1997; Samali et al., 2004).

The phase plane trajectory of the hybrid system given initial disturbance and allowed free response is illustrated in Figures 6.32 - 6.33

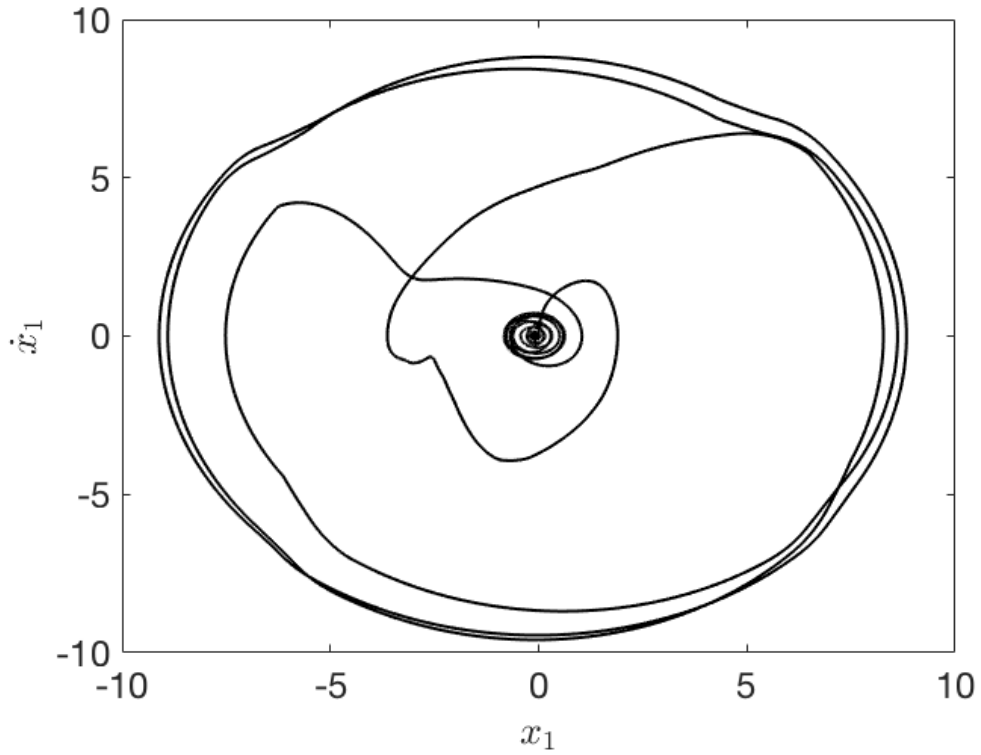

FIGURE 6.32: Plane phase trajectory of the ATMD

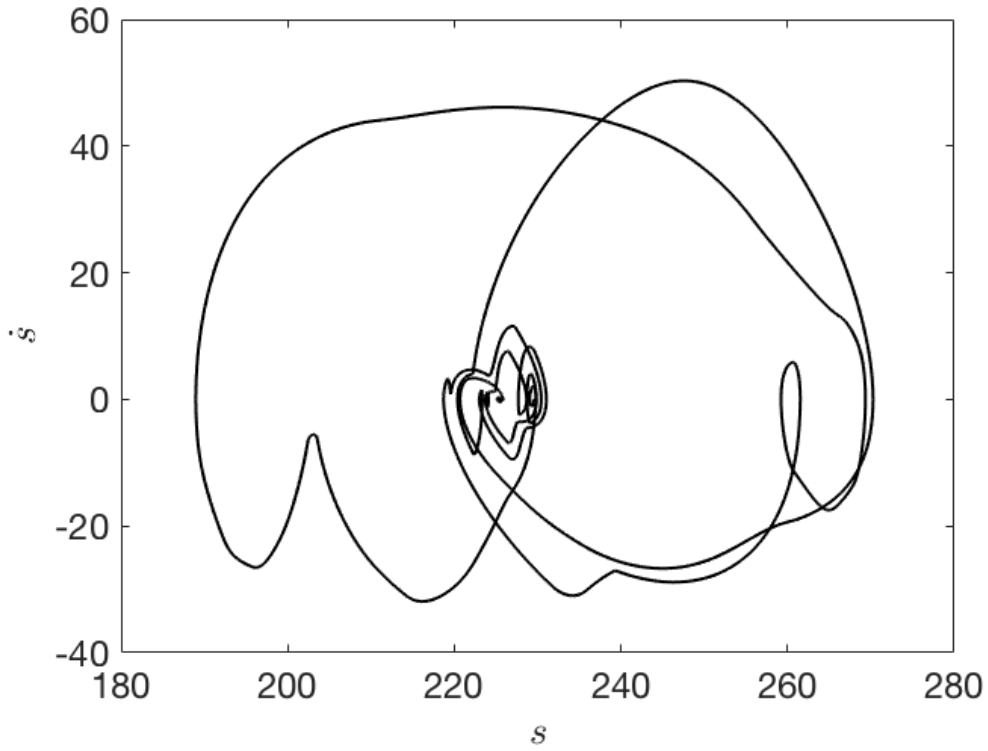

FIGURE 6.33: Plane phase trajectory of the Coriolis damper

From the figures we see the stability of the hybrid system is verified as the phase trajectories converges to zero which proves the system return at rest after given external disturbance.

6.8 Summary

This chapter proposed and investigated the concept of using a hybrid enhanced Coriolis damping system to reduce the dynamic response of a benchmark super tall building subjected to both seismic excitations and free response. The proposed system uses a multi-degree-of-freedom system by coupling an active tuned mass damper with the earlier proposed Coriolis damper in order to enhance the effect. As a result, the proposed system has 3 DOF with horizontal translation of the ATMD, angular motion of the coupled fixture and translation of the secondary mass along the angular fixture. The system was designed first by designing an optimal tuned mass damper based on Hartog's optimal theory. After which, a fuzzy logic controller was proposed for the tuned mass damper. Finally, a fuzzy logic controller was designed for the control of the translating secondary mass along the fixture with angular motion. Numerical simulations were conducted varying the ratio of the two masses of the hybrid system to the mass of the primary structure and compared to the previously designed TMD and ATMD systems to quantitatively assess the effect of the moving mass. The results showed the

hybrid system to perform well for the case of seismic excitation and in particular when the ATMD has the larger mass ratio. Regression analysis on the system to determine the most influential parameter for the minimisation of the response of the primary structure revealed the moving mass to be the most influential parameter. Finally, the stability of the fuzzy controller for both the ATMD and the Coriolis damper were verified based on Lyapunov's direct method and plane phase trajectory method respectively. The next step of this investigation is to carry out small-scale experimental analysis of the proposed system.

Chapter 7

Conclusions

7.1 Summary And Conclusions

The reduction in the response of engineering structures when excited to prevent damage as well as reduce discomfort for their occupants is an important topic for researchers. There are several measures in place to protect structures against excessive vibrations, one of which is through the use of mass dampers. This study focuses on the attenuation of tall flexible and rolling long-period structures. When vibration occur in these structures generally there is some degree of rotational motion and if a mass moves in the longitudinal or radial direction this coupled effect creates Coriolis effect. The effect of this used as a method for attenuation was studied using tall building structures as examples of tall flexible structures and ship as an example of rolling structures.

The main contribution of this study was to propose and verify the idea to mitigate tall building structures by moving a mass along the longitudinal axis and to further apply this concept to other structures such as for ship rolling. This novel approach to structural control has been investigated for several cases and the effect as well as feasibility of such an idea was assessed.

For the first analysis, a tall building structure was modelled as a beam structure and analysed using Finite Element Method (FEM). The moving mass was modelled using the Moving Finite Element Method to easily take into consideration all the nonlinearities and internal forces acting on the system due to the interaction of the vibrating beam and the moving mass. These results were also verified using an analytical approximation of the damping effect. The following are summaries of the results from this study:

1. The interaction of the vibrating structure and the moving mass does influence the motion of the primary structure and with careful analysis of the Coriolis effect a prescribed motion for the moving mass can be obtained to generate mitigating effects. This analysis found that the moving mass dissipates energy when moving away from the pivot and accumulates energy when moving towards. Therefore the moving mass should move away from the pivot when angular velocity is close to maximum and towards the pivot when angular velocity is close to zero which occurs twice in one oscillation of the primary structure and so should move with twice the frequency.

2. Energy considerations can be used to approximate the damping effect of the system given there is a specific prescribed motion of the moving mass. Additionally this gives insights into the design of a proper control law.

3. The motion of the mass over the beam structure constantly changes the natural frequency of the structure and as such the natural period at the end of a cycle is different to the previous one. If the motion of the moving mass remains fixed this creates a phase shift between the structure and the mass and should this shift exceed $\pi/2$ the system will no longer experience attenuation. The phase shift is enhanced by larger mass and velocity and highlights the importance of carefully controlling the motion of the mass to keep the phase shift as close to zero as possible.

4. Due to the small amplitude displacement the damping effect was small added to the large mass of a building which therefore requires a large mass for effect. However this effect can be enhanced by increasing the degree of angular motion of the moving mass or by having the mass moving away from the pivot for as long as possible. This concept is particularly attractive for structures with low inherent damping and limited lateral space, and can be applied to a wide variety of flexible-type, pendulum-type and rolling-type structures. As a standalone method, at the present moment this would be more feasible for lighter flexible structures.

For the second analysis, the rolling of a ship was studied. Drawn from the conclusions of the previous study, the idea of using a constant motion away from the pivot was considered. This was achieved through the use of a constant positive water-flow since ships have easy access to water. The system was investigated under free roll decay and under excited motion from beam waves. The system was analysed numerically using the 4th Order Runge-Kutta Method and these results were verified using approximated analytical results. The results from the investigation are summarised as follow:

1. The idea of using a constant positive water-flow requires no complicated control, creates no hydrodynamic drag effect, operates at zero forward speed, provides no weight and stability issues and could be a very effective method for mitigating the parametric roll of ships.

2. The damping ratio and the response reduction has substantially increased due to the constant positive velocity, removing any amplification effect, and this only increases with the volume of water-flow and the velocity of water-flow.

3. The system performs as well as the maximum capacity of pumping a certain volume of water at a certain velocity. As such, at present this is a very attractive concept for roll reduction, in particular for smaller vessels as they would require smaller pump capacities and this concept could easily be implemented alongside other stabilising system.

For the final analysis, drawn from the conclusions of the first analysis, a new hybrid system was proposed for the case of a super tall structure. The hybrid system involved manipulating the angular displacement of the longitudinal mass by coupling it with a moving mass at the top of the structure. First, a TMD was optimally designed using Hartog's method. To improve the performance of the TMD, a fuzzy logic controller was proposed. Then the newly proposed ATMD was then coupled with a longitudinal moving mass for which also a fuzzy logic controller was proposed. The performance of the system and its effect were analysed. The results are summarised as follow:

1. The coupled enhanced Coriolis system has improved performance over the standalone Coriolis damper and has the advantage of attenuating the primary structure through both the inertial effects of the mass damper at the top as well as the coupled effect due to the longitudinal motion of the moving mass.

2. The influence in the reduction due to the Coriolis effect decreases when the longitudinal mass decreases however the overall performance of the system increases as the mass of the ATMD increases. This is explained by the much larger influence of the inertial effect of the ATMD compared to the Coriolis effect.

3. From previous investigations it is established that the Coriolis effect is proportional to the mass, velocity and angular velocity. But from analysis of the proposed system, the parameter from the Coriolis system that has the largest influence in minimising the response of the primary structure was found to be the mass of the damper.

7.2 Future Recommendations

The following are suggestions for the possible direction of this research topic:

- Optimisation of the parameters of the Coriolis damping system, in particular the previously proposed coupled system should be further investigated. Considering the FLC, promising research concerning optimisation of a FLC system using genetic algorithm has yielded positive results.

- The performance of the damping system should be further analysed under wider range of excitations, frequencies and accelerations.

- Investigation into the implementation of the concept as well as experimentation of the concept should be done.

Bibliography

Akin, John E. and Massood Mofid (1989). "Numerical Solution for Response of Beams with Moving Mass". In: *Journal of Structural Engineering* 115.1, pp. 120 –131. DOI: https://doi.org/10.1061/(ASCE)0733-9445(1989)115:1(120). URL: http://ascelibrary.org/doi/pdf/10.1061/\%28ASCE\%290733-9445\%281989\%29115\%3A1\%28120\%29.

Ali, Mir M. and Kyoung Sun Moon (2007). "Structural Developments in Tall Buildings: Current Trends and Future Prospects". In: *Architectural Science Review* 50.3, pp. 205–223. DOI: 10.3763/asre.2007.5027. eprint: http://www.tandfonline.com/doi/pdf/10.3763/asre.2007.5027. URL: http://www.tandfonline.com/doi/abs/10.3763/asre.2007.5027.

Ang, Kiam Heong, G. Chong, and Yun Li (2005). "PID control system analysis, design, and technology". In: *IEEE Transactions on Control Systems Technology* 13.4, pp. 559–576. ISSN: 1063-6536. DOI: 10.1109/TCST.2005.847331.

Bobál, V. et al. (2009). *Digital Self-tuning Controllers: Algorithms, Implementation and Applications*. Advanced Textbooks in Control and Signal Processing. Springer London. ISBN: 9781848008793. URL: https://books.google.co.jp/books?id=WEAqjgEACAAJ.

Bullo, F. and A.D. Lewis (2004). *Geometric Control of Mechanical Systems*. Texts in Applied Mathematics. Springer New York. ISBN: 9780387221953. URL: https://books.google.co.jp/books?id=TU7sgJ-kh70C.

Casciati, Fabio (1997). "Checking the Stability of a Fuzzy Controller for Nonlinear Structures". In: *Microcomputers in Civil Engineering* 12.3, pp. 205 – 215. DOI: 10.1111/0885-9507.00057. URL: http://onlinelibrary.wiley.com/doi/10.1111/0885-9507.00057/epdf.

Cifuentes, Arturo O. (1989). "Dynamic response of a beam excited by a moving mass". In: *Finite Elements in Analysis and Design* 5.3, pp. 237 –246. ISSN: 0168-874X. DOI: https://doi.org/10.1016/0168-874X(89)90046-2. URL: http://www.sciencedirect.com/science/article/pii/0168874X89900462.

Clough, R.W. and J. Penzien (2003). *Dynamics of Structures*. Computers and Structures, Incorporated. ISBN: 9780923907501. URL: https://books.google.co.jp/books?id=TcxyAAAACAAJ.

Connor, J.J. (2003). *Introduction to Structural Motion Control*. MIT-Prentice Hall series on civil, environmental, and systems engineering. Prentice Hall Pearson Education, Incorporated. ISBN: 9780130091383. URL: https://books.google.co.jp/books?id=FNNRAAAAMAAJ.

Coriolis, Gaspan-Gustave (1835). "Sur les équations du mouvement relatif des systémes de corps". In: *J. De l'Ecole royale polytechnique* 15, pp. 144 – 154.

Craig, R.R. and A.J. Kurdila (2006). *Fundamentals of Structural Dynamics*. Wiley. ISBN: 9780471430445. URL: https://books.google.co.jp/books?id=iP1Er7ULtWwC.

Curry, Stephen M. (1976). "How Children Swing". In: *American Journal of Physics* 44.10, pp. 924 –926. DOI: https://doi.org/10.1119/1.10230. URL: http://aapt.scitation.org/doi/pdf/10.1119/1.10230.

Den Hartog, J.P. (1985). *Mechanical Vibrations*. Civil, Mechanical and Other Engineering Series. Dover Publications. ISBN: 9780486647852. URL: https://books.google.co.jp/books?id=-Pu5YlgY4QsC.

Elkhatib, Mohamed m. and John J. Soraghan (2008). *Fuzzy Stabilization of Fuzzy Control Systems, New Approaches in Automation and Robotics*. I-Tech Education and Publishing. ISBN: 978-3-902613-26-4. URL: http://cdn.intechopen.com/pdfs/794.pdf.

Feng, Gang (2006). "A Survey on Analysis and Design of Model-Based Fuzzy Control Systems". In: *IEEE Transactions on Fuzzy Systems* 14.5, pp. 676 – 697. ISSN: 1063-6706. DOI: https://doi.org/10.1109/TFUZZ.2006.883415. URL: http://ieeexplore.ieee.org/document/1707754/.

Frỳba, L. (1972). *Vibration of Solids and Structures Under Moving Loads*. Mechanics of structural systems. Academia. ISBN: 9789001324209. URL: https://books.google.co.jp/books?id=PV7aAAAAIAAJ.

Himeno, Yuji (1981). *Prediction of Ship Roll Damping - A State of the Art*. Naval Architecture & Marine Engineering. University of Michigan. URL: http://deepblue.lib.umich.edu/bitstream/2027.42/91699/1/Publication_No_239.pdf.

Hori, Yusuke, Haruhiko Kurino, and Yasushi Kurokawa (2016). "Development of Large Tuned Mass Damper with Stroke Control System for Seismic Upgrading of Existing High-Rise Building". In: *International Journal of High-Rise Buildings* 5.3, pp. 167–176. URL: http://global.ctbuh.org/paper/2852.

Ibrahim, A.M. (2004). *Fuzzy logic for embedded systems applications*. Embedded technology series. Newnes. ISBN: 9780750676052. URL: https://books.google.co.jp/books?id=oo9TAAAAMAAJ.

Kareem, Ahsan, Tracy Kijewski, and Yukio Tamura (1991). "Mitigation of motions of tall buildings with specific examples of recent applications". In: *Wind and Structures* 2.3, pp. 201–251. DOI: http://www.techno-press.org/?page=container&journal=was&volume=2&num=3#.

Kickert, W.J.M. and E.H. Mamdani (1978). "Analysis of a fuzzy logic controller". In: *Fuzzy Sets and Systems* 1.1, pp. 29 –44. ISSN: 0165-0114. DOI: https://doi.org/10.1016/0165-0114(78)90030-1. URL: http://www.sciencedirect.com/science/article/pii/0165011478900301.

Korkmaz, Sinan (2011). "A review of active structural control: challenges for engineering informatics". In: *Computers & Structures* 89.23, pp. 2113 –2132. ISSN: 0045-7949. DOI: https://doi.org/10.1016/j.compstruc.2011.07.010. URL: http://www.sciencedirect.com/science/article/pii/S0045794911002070.

Kozak, S. (2016). "From PID to MPC: Control engineering methods development and applications". In: *2016 Cybernetics Informatics (K I)*. Levoca: IEEE, pp. 1–7.

Lee, C. C. (1990). "Fuzzy logic in control systems: fuzzy logic controller. I". In: *IEEE Transactions on Systems, Man, and Cybernetics* 20.2, pp. 404 –418. ISSN: 0018-9472. DOI: https://doi.org/10.1109/21.52551. URL: http://ieeexplore.ieee.org/document/52551/#full-text-section.

Lewis, E. V. (1989). *Principles of naval architecture*. Principles of Naval Architecture. Society of Naval Architects and Marine Engineers. URL: https://books.google.co.jp/books?id=bWwZAQAAIAAJ.

Liang, Z. et al. (2011). *Structural Damping: Applications in Seismic Response Modification*. Advances in Earthquake Engineering. Taylor & Francis. ISBN: 9781439815823. URL: https://books.google.co.jp/books?id=vWuPQQAACAAJ.

Lloyd, A.R.J.M. (1998). *Seakeeping: Ship Behaviour in Rough Weather*. Ellis Horwood series in marine technology. A.R.J.M. Lloyd. ISBN: 9780953263400. URL: https://books.google.co.jp/books?id=NHQqGwAACAAJ.

Mahajan, Nitendra G. and D. B. Raijiwala (2011). "Seismic Response Control of a Building Installed with Passive Dampers". In: *International Journal of Advanced Engineering Technology* 2.3, pp. 246–256. ISSN: 0976-3945. URL: http://www.technicaljournalsonline.com/ijeat/VOL\%20II/IJAET\%20VOL\%20II\%20ISSUE\%20III\%20JULY\%20SEPTEMBER\%202011/ARTICLE\%2047\%20IJAET\%20VOLII\%20ISSUE\%20III\%20JULY\%20SEPT\%202011.pdf.

Matsuhisa, Hiroshi et al. (1995). "Vibration Control of a Ropeway Carrier by Passive Dynamic Vibration Absorbers". In: *JSME international journal. Ser. C, Dynamics, control, robotics, design and manufacturing* 38.4, pp. 657–662. DOI: 10.1299/jsmec1993.38.657.

Michaltsos, G., D. Sophianopoulos, and A.N. Kounadis (1996). "THE EFFECT OF A MOVING MASS AND OTHER PARAMETERS ON THE DYNAMIC RESPONSE OF A SIMPLY SUPPORTED BEAM". In: *Journal of Sound and Vibration* 191.3, pp. 357 –362. ISSN: 0022-460X. DOI: https://doi.org/10.1006/jsvi.1996.0127. URL: http://www.sciencedirect.com/science/article/pii/S0022460X96901273.

Moaleji, Reza and Alistair R. Greig (2007). "On the development of ship anti-roll tanks". In: *Ocean Engineering* 34.1, pp. 103 –121. ISSN: 0029-8018. DOI: https://doi.org/10.1016/j.oceaneng.2005.12.013. URL: http://www.sciencedirect.com/science/article/pii/S0029801806000722.

Monk, K. (1988). "A Warship Roll Criterion". In: *Royal Institution of Naval Architects Transactions* 130. ISSN: 0035-8967.

Nelik, L. (1999). *Centrifugal & Rotary Pumps: Fundamentals With Applications*. CRC Press. ISBN: 9781420049725. URL: https://books.google.co.jp/books?id=OaafH9act5AC.

Nishitani, Akira and Yutaka Inoue (2001). "Overview of the application of active/semiactive control to building structures in Japan". In: *Earthquake Engineering & Structural Dynamics* 30.11, pp. 1565–1574. ISSN: 1096-9845. DOI: 10.1002/eqe.81. URL: http://dx.doi.org/10.1002/eqe.81.

Oguamanam, D.C.D., J.S. Hansen, and G.R. Heppler (1998). "DYNAMIC RESPONSE OF AN OVERHEAD CRANE SYSTEM". In: *Journal of Sound and Vibration* 213.5, pp. 889 –906. ISSN: 0022-460X. DOI: https://doi.org/10.1006/jsvi.1998.1564. URL: http://www.sciencedirect.com/science/article/pii/S0022460X98915644.

Olsson, M. (1991). "On the fundamental moving load problem". In: *Journal of Sound and Vibration* 145.2, pp. 299 –307. ISSN: 0022-460X. DOI: https://doi.org/10.1016/0022-460X(91)90593-9. URL: http://www.sciencedirect.com/science/article/pii/0022460X91905939.

Perez, Tristan (2010). *Ship Motion Control: Course Keeping and Roll Stabilisation Using Rudder and Fins*. 1st. Springer Publishing Company, Incorporated. ISBN: 1849969787, 9781849969789. DOI: https://dx.doi.org/10.1007/1-84628-157-1. URL: http://www.bookmetrix.com/detail/book/79ab04b3-84f5-46cd-bdd0-a5b17ec8028d#downloads.

Perez, Tristan and Mogens Blanke (2012). "Ship roll damping control". In: *Annual Reviews in Control* 36.1, pp. 129 –147. ISSN: 1367-5788. DOI: https://doi.org/10.1016/j.arcontrol.2012.03.010. URL: http://www.sciencedirect.com/science/article/pii/S1367578812000119.

Piccoli, B. and J. Kulkarni (2005). "Pumping a swing by standing and squatting: do children pump time optimally?" In: *IEEE Control Systems* 25.4, pp. 48–56. ISSN: 1066-033X. DOI: 10.1109/MCS.2005.1499390.

Rajasekaran, S. (2009). *Structural Dynamics of Earthquake Engineering: Theory and Application using Mathematica and Matlab*. Woodhead Publishing. ISBN: 9781439801321. URL: https://books.google.co.jp/books?id=Vm5iOgAACAAJ.

Rao, S.S. (2011). *Mechanical Vibrations*. Mechanical Vibrations. Prentice Hall. ISBN: 9780132128193. URL: https://books.google.co.jp/books?id=7Pd3SQAACAAJ.

Samali, Bijan et al. (2004). "Active Control of Cross Wind Response of 76-Story Tall Building Using a Fuzzy Controller". In: *Journal of Engineering Mechanics* 130.4, pp. 492–498. DOI: 10.1061/(ASCE)0733-9399(2004)130:4(492).

Sellars, Frank H. and John P. Martin (1992). "Selection and Evaluation of Ship Roll Stabilization Systems". In: *Marine Technology* 29.2, pp. 84 –101.

Slotine, J.J.E. and W. Li (1991). *Applied Nonlinear Control*. Prentice Hall. ISBN: 9780130408907. URL: https://books.google.co.jp/books?id=cwpRAAAAMAAJ.

Smith, Rob J. and Michael R. Willford (2007). "The damped outrigger concept for tall buildings". In: *The Structural Design of Tall and Special Buildings* 16.4, pp. 501–517. ISSN: 1541-7808. DOI: 10.1002/tal.413. URL: http://dx.doi.org/10.1002/tal.413.

Söder, Carl-Johan et al. (2013). "Parametric roll mitigation using rudder control". In: *Journal of Marine Science and Technology* 18.3, pp. 395–403. ISSN: 1437-8213. DOI: 10.1007/s00773-013-0216-3. URL: https://doi.org/10.1007/s00773-013-0216-3.

Suhardjo, J., B.F. Spencer, and M.K. Sain (1990). "Feedback-feedforward control of structures under seismic excitation". In: *Structural Safety* 8.1, pp. 69 –89. ISSN: 0167-4730. DOI: https://doi.org/10.1016/0167-4730(90)

90031-J. URL: http://www.sciencedirect.com/science/article/pii/016747309090031J.

Surendran, S. et al. (2005). "Non-linear Roll Dynamics of a Ro-Ro Ship in Waves". In: *Ocean Engineering* 32.14–15, pp. 1818–1828. URL: http://www.sciencedirect.com/science/article/pii/S0029801805000557.

Taylan, M (2000). "The Effect of Nonlinear Damping and Restoring in Ship Rolling". In: *Ocean Engineering* 27.9, pp. 921–932. URL: http://www.sciencedirect.com/science/article/pii/S0029801899000268.

Tea, Peter L. and Harold Falk (1968). "Pumping on a Swing". In: *American Journal of Physics* 36.12, pp. 1165 –1166. DOI: https://doi.org/10.1119/1.1974385. URL: http://aapt.scitation.org/doi/pdf/10.1119/1.1974385.

Townsend, Nicholas, A.J. Murphy, and R. Shenoi (2007). "A new active gyrostabiliser system for ride control of marine vehicles". In: 34, pp. 1607–1617.

Viet, La Duc (2015). "Crane sway reduction using Coriolis force produced by radial spring and damper". In: *Journal of Mechanical Science and Technology* 29.3, pp. 973–979. ISSN: 1976-3824. DOI: 10.1007/s12206-015-0211-1. URL: https://doi.org/10.1007/s12206-015-0211-1.

Viet, L.D., N.D. Anh, and H. Matsuhisa (2011). "The effective damping approach to design a dynamic vibration absorber using Coriolis force". In: *Journal of Sound and Vibration* 330.9, pp. 1904 –1916. ISSN: 0022-460X. DOI: https://doi.org/10.1016/j.jsv.2010.10.040. URL: http://www.sciencedirect.com/science/article/pii/S0022460X10007261.

Wu, Shinq-Jen and Chin-Teng Lin (2000). "Optimal fuzzy controller design: local concept approach". In: *IEEE Transactions on Fuzzy Systems* 8.2, pp. 171 –185. ISSN: 1063-6706. DOI: https://doi.org/10.1109/91.842151. URL: http://ieeexplore.ieee.org/document/842151/.

Yang, Jann N. et al. (2004). "Benchmark Problem for Response Control of Wind-Excited Tall Buildings". In: *Journal of Engineering Mechanics* 130.4. URL: https://doi.org/10.1061/(ASCE)0733-9399(2004)130:4(437).

Ye, Zhuchao and Huaihai Chen (2009). "Vibration analysis of a simply supported beam under moving mass based on moving finite element method". In: *Frontiers of Mechanical Engineering in China* 4.4, pp. 397–400. ISSN: 1673-3592. DOI: 10.1007/s11465-009-0044-7. URL: https://doi.org/10.1007/s11465-009-0044-7.

Zadeh, L.A. (1965). "Fuzzy sets". In: *Information and Control* 8.3, pp. 338 –353. ISSN: 0019-9958. DOI: https://doi.org/10.1016/S0019-9958(65)90241-X. URL: http://www.sciencedirect.com/science/article/pii/S001999586590241X.